In vivo cellular reprogramming as a potential method to rejuvenate the growth arrested lungs seen in BPD patients.

By

Adithya Achuthan Karikandathil Vineeth

Thesis submitted to the University of Ottawa in
partial Fulfillment of the requirements for the
MSc degree in Cellular and Molecular Medicine

Department of Cellular and Molecular Medicine

Faculty of Medicine

University of Ottawa

Abstract

Bronchopulmonary dysplasia (BPD), the chronic lung disease that develops in premature babies following mechanical ventilation and oxygen exposure, is the most common complication of extreme prematurity. Currently, there is no cure for BPD. Increasing evidence indicates early-onset emphysema and pulmonary vascular disease in survivors with BPD (Aukland et al., 2006; Wong et al., 2008), suggesting an irreversible arrest in lung growth and/or premature lung aging resulting in life-long health problems (J. Sucre et al., 2021). Transient *in vivo* cellular reprogramming through the activation of the Yamanaka reprogramming factors Oct4, Sox2, Klf4, c-Myc (OSKM), ameliorate cellular and physiological hallmarks of aging and to promote tissue regeneration and improve organ function after injury. (Chen et al., 2021a; Hishida et al., 2022b; Lu et al., 2020) This thesis focuses on determining if transient *in vivo* cellular reprogramming can regenerate an established lung injury in a BPD mouse model. Two strategies, (a) Adeno-Associated virus (AAV) mediated transient overexpression of the OSK factors and (b) using a transgenic reprogrammable mouse line to overexpress the OSKM factors were employed to test the efficiency of in vivo cellular reprogramming in regenerating the lungs. Both the strategies, under the conditions tested, did not regenerate established lung injury in a BPD mouse model but the feasibility of both these strategies was established here laying a foundation for the next phase of the study.

ABBREVIATIONS

BPD	Bronchopulmonary dysplasia
RDS	respiratory distress syndrome
Fig	Figure
g	gram
FEV1	Forced expiratory volume in 1 second.
FVC	forced vital capacity
FEF50	forced expiratory flows at 50% volume
Vpl	Volume plethysmography
Ppl	Pressure plethysmography
CT	Computerized Tomography
ROS	Reactive oxidative species
SASP	senescence associated secretory phenotype
CDK	Cyclin dependent kinase
COPD	Chronic Obstructive Pulmonary Disease
IPF	Idiopathic pulmonary fibrosis
αSMA	alpha-smooth muscle actin
Mcp1	monocyte chemoattractant protein-1

IL6	interleukin 6
Mmp12	matrix metalloproteinase-12
Tgfβ	transforming growth factor beta
SaβG	Senescence-associated beta-galactosidase
AEC I	alveolar epithelial type I cells
AEC II	alveolar epithelial type II cells
DNA	Deoxyribonucleic acid
mTOR	Mammalian target of rapamycin
IGF	Insulin-like growth factor receptor
PNX	pneumonectomy
HeMR	hyperpolarized helium-3 magnetic resonance
SCNT	Somatic cell nuclear transfer
OSKM	Oct3/4, Sox2, klf4, and C-myc
OSK	Oct3/4, Sox2, klf4
MEF	mouse embryonic fibroblasts
iPSC	Induced pluripotent cells
2D	Two dimensional
3D	Three dimensional

h	Human
DE	Definitive endoderm
BMP	bone morphogenic protein
AFE	anterior foregut epithelium
Ngn3	Neurogenin-3
Pdx1	insulin promoter factor 1
MAFA	MAF BZIP Transcription Factor A
Gata4	GATA Binding Protein 4
Mef2c	Myocyte Enhancer Factor 2C
TBX5	T-Box Transcription Factor 5
hand2	Heart and Neural Crest Derivatives Expressed 2
Ascl1	Achaete-Scute Family BHLH Transcription Factor 1
Brn2	POU Class 3 Homeobox 2
Myt1l	Myelin Transcription Factor 1 Like
i4f	inducible 4 factor
mg	milligram
ml	milliliter
dox	doxycycline

Ink4	Cyclin Dependent Kinase Inhibitor 2A
NFkB	Nuclear factor kappa-light-chain-enhancer of activated B cells
CTX	cardiotoxin
TA	Tibialis anterior
NANOG	Nanog Homeobox
mRNA	Messenger ribonucleic acid
H3K9me3	Histone 3 lysine 9 trimethylation
DNAm	DNA methylation
Cm	cardiomyocytes
°C	Degree Celsius
PCR	polymerase chain reaction
PND	postnatal day
µL	microliter
E	Embryonic day
i.p	intraperitoneal
O_2	oxygen
vg	Vector genomes
AAV	Adeno-associated virus

WPRE	Woodchuck hepatitis virus posttranscriptional regulatory element
PBS	Phosphate-buffered saline
Luc	Luciferase
TLC	total lung capacity
RV	residual volume
C	compliance
E	elastance
PV-loop	Pressure-volume loop
IVIS	in vivo imaging system
SD	standard deviation
p	photons
s	second
cm^2	square centimeter
sr	steradian
MOI	multiplicity of infection
TBST	Tris Buffered Saline + Tween 20
qPCR	Quantitative reverse transcription PCR

TABLE OF CONTENTS

ABSTRACT ..... **II**

ABBREVIATIONS ..... **III**

TABLE OF CONTENTS ..... **VIII**

LIST OF FIGURES ..... **XI**

LIST OF TABLES ..... **XII**

ACKNOWLEDGEMENTS ..... **XIII**

CHAPTER 1. INTRODUCTION **1**

1.1 BRONCHOPULMONARY DYSPLASIA 2

1.1.1 Pathophysiology *2*

1.2 Stages of lung development *2*

1.1.3 Long-term outcomes of BPD *4*

1.2 LUNG SENESCENCE 6

1.2.1 Introduction to cellular senescence *6*

1.2.2 Lung senescence *7*

1.2.3 Senescence in BPD *8*

1.3 LUNG REJUVENATION 9

1.4 CELLULAR REPROGRAMMING 12

1.4.1 Induced pluripotent cells (iPSCs) *12*

1.4.2 iPSC-derived lung cells *13*

1.5 REPROGRAMMING AND REJUVENATION 14

1.6 Senescence and reprogramming 16
1.7 Partial reprogramming 18
1.8 Partial reprogramming to regenerate injured tissues. 20
2. RATIONALE HYPOTHESIS AND OBJECTIVES 23
2.1 Rationale 23
2.2 Hypothesis 23
2.3 Objectives 23
CHAPTER 3. MATERIAL AND METHODS 25
3.1 Mouse housing and care 26
3.2 Mouse genotyping 26
3.3 Neonatal hyperoxia mouse model 27
3.4 Intratracheal delivery of AAV vectors 28
3.5 Doxycycline administration in mice 28
3.6 Lung function analysis 29
3.7 Lung histology 29
3.8 *In vivo* imaging 30
3.9 Cell culture, AAV transduction, and protein isolation 30
3.10 Western blot 31
3.11 *In vitro* luciferase detection 32
3.12 Quantitative Real-time PCR 33
3.13 Statistical analysis 34
CHAPTER 4. RESULTS 35

4.1 Hyperoxia alters lung function and structure in neonatal C57Bl/6 mice..... 35

4.2 Neonatal hyperoxia exposure results in persistent lung injury up until 7 weeks of age. 38

4.3 Senescence markers are upregulated at PND14 in hyperoxia-exposed mice..... 40

4.5 Oct4, Sox2, and Klf4 proteins are expressed in HEK293 cells and in the lungs of C57Bl/6 mice only in the presence of AAV-OSK vector and doxycycline..... 44

4.6 Transient expression of AAV system can be achieved with high accuracy..... 47

4.7 Transient overexpression of the OSK factors did not improve the lung structure and function after hyperoxia-induced injury. 52

4.8 14-day hyperoxia exposure in neonatal i4f-b induces an arrest in lung development phenotype and doxycycline administration triggers expression of the OSK factors in the lungs. 57

4.9 Transient expression of OSKM factors for 4 cycles in the i4f-b mice does not improve lung function after hyperoxia induced lung injury. 62

5. DISCUSSION AND FUTURE DIRECTIONS..... 64

5.1 Discussion 65

5.2 Future directions 69

6. CONCLUSION 71

7. REFERENCES..... 72

LIST OF FIGURES

Figure 1 Graphical representation of the course of lung development.

Figure 2 Graphical representation of a Waddington's plot describing the partial reprogramming.

Figure 3 The 14-day hyperoxia exposure altered lung function and structure in neonatal C57Bl/6 mice.

Figure 4 Neonatal hyperoxia exposure results in persistent lung injury up until 7 weeks of age.

Figure 5 Expression of senescence markers are upregulated at PND14 in hyperoxia-exposed mice.

Figure 6 Luciferase is expressed only in the presence of doxycycline and its expression is localized to the lungs in mice.

Figure 7 Oct4, Sox2, and Klf4 proteins are expressed in HEK293 cells and in the lungs of C57Bl/6 mice only in the presence of AAV-OSK vector and doxycycline.

Figure 8 Transient expression of the developed AAV system can be achieved with high accuracy.

Figure 9 Transient overexpression of the OSK factors did not improve the lung structure and function after hyperoxia-induced injury.

Figure 10 14-day hyperoxia exposure in neonatal i4f-b induces an arrest in lung development phenotype and doxycycline administration triggers expression of the OSK factors in the lungs.

Figure 11 Transient expression of OSKM factors for 4 cycles in the i4f-b mice does not improve lung function after hyperoxia induced lung injury.

List of tables

TABLE 1 LIST OF PRIMERS USED FOR GENOTYPING.

TABLE 2 LIST OF ANTIBODIES USED FOR WESTERN BLOT.

TABLE 3 LIST OF QPCR PRIMERS.

ACKNOWLEDGEMENTS

First and foremost, I would like to thank my supervisor, Dr. Bernard Thébaud for giving me the opportunity to pursue an MSc in his lab and for providing invaluable guidance and support throughout the whole process. I would also like to express my appreciation to all the wonderful members of the Thébaud lab: Dr. Arul Vadivel, Celine Fawagreh, Dr. Chanèle Cyr-Depauw, Dr. Ewa Henckel, Dr. Flore Lesage, Kennedy Nangle, Dr. Liqun Xu, Mahnaz Nazari, Dr. Pauline Bardin, Sahar Salari, Shumei Zhong, Dr. Wojciech Durlak for all you help throughout these years. I would also like to extend special acknowledgments to Dr. Liqun Xu for her guidance and training on this project.

I would also like to express my appreciation to Dr. Chanèle Cyr-Depauw and Dr. Wojciech Durlak, and Dr. Bernard Thébaud for the taking time to edit this dissertation. I would also like to acknowledge Dr. Pauline Bardin, Dr. Flore Lesage, Dr. Chanèle Cyr-Depauw, and Dr. Arul Vadivel for their excellent advice and for motivating me throughout.

I wish to acknowledge my thesis advisory committee members, Dr. Michael Rudnicki, and Dr. Andras Nagy for providing direction and feedback on this project. I also wish to thank Dr. Pierre Mattar and Dr. Michael Rudnicki for agreeing to evaluate my thesis and defense.

Finally, and most importantly, I would like to thank my parents for believing in me and for always supporting me.

Chapter 1. Introduction

1.1 Bronchopulmonary dysplasia

1.1.1 Pathophysiology

Bronchopulmonary dysplasia (BPD) is a chronic respiratory disorder of prematurity and the most severe complication of extreme prematurity (birth before 28 weeks of gestational age). "Classic" or "old" BPD was first described by Northway *et al*., in 1967. This condition was reported in newborn infants with severe respiratory distress syndrome (RDS) who were treated with 80% to 100% oxygen [hyperoxia] and mechanical ventilation, which are essential for the survival of a preterm infant, but also cause injury to the preterm lung (Northway Jr. et al., 1967). Classic BPD was seen in relatively mature preterm infants (mean gestational age of 32 weeks). The disease was characterized by severe airway injury along with sites of overinflation and fibrosis as a result of insults to the immature lung. The nature of BPD has changed over the last 50 years due to the progress in perinatal and neonatal care: the improvements in ventilation strategies, and the use of antenatal corticosteroids and exogenous surfactant have increased the survival rates of more immature preterm infants. Lungs in prematurely born infants are very early in their developmental process and as a result, infants who are born extremely preterm are currently at the highest risk of developing the "new" BPD.

1.2 Stages of lung development

The process of lung development is subdivided into 5 major stages (Fig 1). Lung development begins during the embryonic stage where formation of anlage of the left and right lung and the trachea begins. Embryonic stage lasts during 4 to 7 weeks of development. Following this is the pseudoglandular stage where the formation of bronchial tree takes place. Pseudoglandular stage takes place between 5 to 17 weeks of development. This is followed by the canalicular stage of development where formation of distal airways occurs. Canalicular stage of

development takes place during 16 to 26 weeks of development. It's only during the late canalicular stage when gas exchange is possible. This is followed by the saccular stage of development which progresses from 24 to 36 weeks of development. At this period, terminal branches are formed which then integrates with a network of capillaries to form primitive alveoli. The final stage of lung development is the alveolar stage which begins at 36 weeks of development and continues postnatally. During this stage, alveolarization or the formation and maturation of alveoli takes place. (Schittny, 2017)

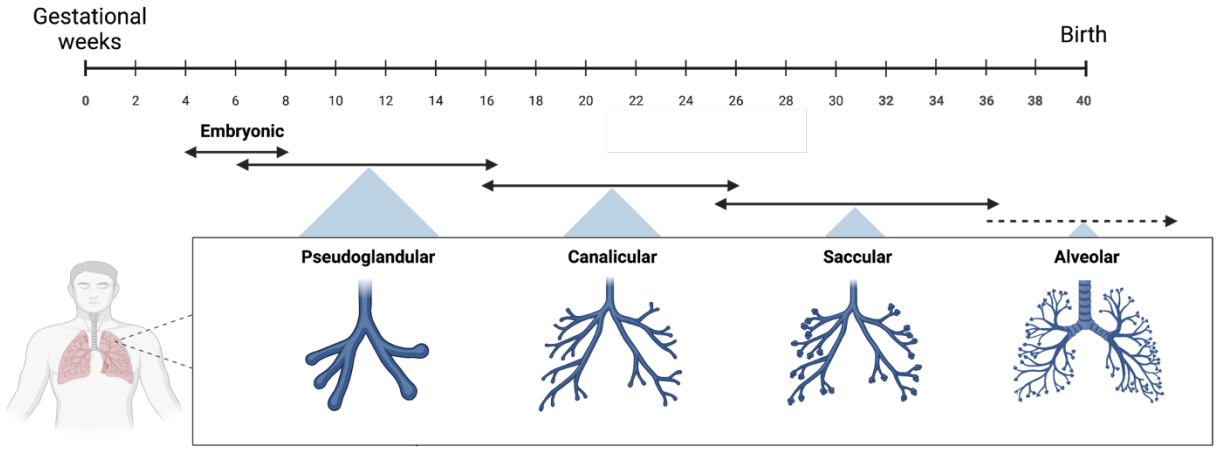

Fig 1. Graphical representation of the course of lung development.

When premature birth happens before 28 weeks of gestation, the lungs are very immature and have just begun the process of alveolarization of the distal saccules along with the expansion of the pulmonary capillary bed (Coalson, 2006; Jobe, 1999). The efficiency of gas exchange is drastically reduced in BPD patients making them more dependent on external respiratory support. Mechanical ventilation and oxygen therapy give rise to a pro-inflammatory response and stunts lung development resulting in larger and fewer alveoli along with impaired pulmonary capillary development (Abman, 2012; Jobe & Bancalari, 2001; Thébaud et al., 2019). This halted pulmonary vascular growth may not just lead to pulmonary hypertension but also to a wide range of other

pulmonary vascular diseases such as systemic to pulmonary collateral vessels and pulmonary vein stenosis. (Mourani & Abman, 2015) Thus, the deteriorated alveolarization along with halted pulmonary vascular growth is responsible for the morbidity and mortality in preterm infants with BPD. (C. D. Baker et al., 2014; Mourani & Abman, 2013)

Despite the measures taken to prevent injury of the preterm lung, BPD is the most common complication of premature pregnancy (infants that are born less than 30 weeks of gestation). In the United States alone, 10,000 to 15,000 infants are diagnosed with BPD annually, moreover, 50% of all the infants who weighed less than 1000g at birth were diagnosed with BPD. (Jensen & Schmidt, 2014)

1.1.3 Long-term outcomes of BPD

School going children who were born preterm in the post-surfactant era and diagnosed with BPD had abnormal lung function indicators such as lower FEV1, FVC, and FEF50 z-scores when compared to children born preterm without BPD even with the use of less invasive ventilation after birth (Doyle et al., 2006, 2017; Fawke et al., 2010; Kotecha et al., 2013; vom Hove et al., 2014). FEV1, FVC, and FEF50 z-scores are parameters of the spirometry test which measures lung function. After a full inspiratory phase, the volume of air forcefully exhaled in the 1st second is the “Forced expiratory volume in 1 second” or FEV1 and the total volume of air that can be forcefully exhaled is the “forced vital capacity” or FVC. FEF50 is the flow of air at 50% timepoint of FVC. Infants who were previously diagnosed with BPD demonstrate more respiratory symptoms such as wheezing, airway reactivity, shortness of breath and cough, and have a higher risk of developing asthma. They also need more respiratory medications compared to the controls. (Lum et al., 2011)

BPD patients present with persistent structural lung abnormalities. (Aukland et al., 2006; Wong et al., 2008) In the study conducted by Auckland and group, 88% of the subjects (adolescents with a history of BPD) had lung parenchymal abnormalities which consequently affected lung function. This is consistent with the data collected by Wong and colleagues wherein the computerized tomography (CT) scans showed structural abnormalities in all their subjects (Aukland et al., 2006; Wong et al., 2008). Emphysema, bronchial wall thickening, gas trapping, and bronchiectasis were the structural abnormalities in survivors of BPD and among which, emphysema was the most commonly observed structural abnormality in BPD patients.

Taken together, these studies indicate a long-term respiratory sequela of infants born extremely preterm which makes them more dependent on long-term medications and is associated with higher rehospitalization rates. These persisting structural and functional abnormalities in BPD survivors indicate a loss of repair capacity and/or early aging.

Development of BPD causes disturbances in many conserved pathways of molecular aging which contributes to premature aging. Exposure to hyperoxia in the neonatal period results in increased levels of reactive oxidation species (ROS) which further induces DNA damage. (Barker et al., 2006; O'Reilly, 2001) Accumulation of DNA damage drives the cells in the lung towards a senescent or an apoptotic state and cause premature aging in the lung. (Meiners & Hilgendorff, 2016) This may be the cause of the various pulmonary abnormalities in young adults who were survivors of BPD as discussed by Wong *et al.* 2008 and Goss *et al*. 2017.

1.2 Lung senescence

1.2.1 Introduction to cellular senescence

Cellular senescence refers to a stable state in which the cell is under an irreversible growth arrest. Senescence is induced by telomere shortening, mitogenic or oncogenic signals and DNA damage. A cell is pushed into the state of senescence due to a variety of damaging stimuli, including ROS and chronic inflammation (López-Otín et al., 2013). Senescent cells undergo various alterations such as taking up a flattened and enlarged morphology, altered gene expression, chromatin rearrangement, secretion of cytokines, and a mix of other proinflammatory factors together called the senescence-associated secretory phenotype (SASP). The various damaging stimuli induce the activation of p53 and Cyclin-dependent kinase inhibitors (CDKIs) such as p16, p21, p15, and p27. In the cell cycle, CDKs play a vital role in promoting G1 to S phase transition. (Bertoli et al., 2013). The inhibition of CDKs leads to a proliferative arrest which is a key component in the implementation of senescence. (Stein et al., 1999) Accumulation of senescent cells promotes aging. The correlation between senescence and aging was discovered based on the observation of a higher number of senescent cells in aged cells (van Deursen, 2014). Senescent cells are arrested at the G1 phase whereas the quiescent cells undergo an arrest at the G0 phase. Senescent cells unlike quiescent cells cannot re-enter the cell cycle even with optimal growth conditions. Senescent cells accumulate over time and contribute to the age-related phenotypes in mice including infertility, cataracts, sarcopenia, cardiac arrhythmias, fat loss, arterial wall stiffening, impaired wound healing, dermal thinning and lordokyphosis (curvature of the spinal column). (D. J. Baker et al., 2011)

1.2.2 Lung senescence

Cellular senescence has now been implicated as an imperative cause in the pathogenesis of chronic lung diseases such as chronic obstructive pulmonary disease (COPD) and pertaining to accelerated aging in the lung. A decrease of telomere length was shown in pulmonary vascular endothelial cells (from COPD patients) in culture and in the lung tissue of COPD patients. Senescence has been suggested to occur in alveolar epithelial and endothelial cells of COPD patients as higher percentages of p21 and p16 positive-alveolar epithelial type II (ATII) cells and a higher percentage of p16-positive endothelial cells were observed compared to healthy control. These findings may explain the loss of alveolar epithelial cells, endothelial cells and fibroblasts seen in COPD patients. (Amsellem et al., 2012; Tsuji et al., 2010, 2012)

Schafer *et al.* describes the involvement of senescence and in turn SASP in the pathology of fibrotic lung disease. Patients with idiopathic pulmonary fibrosis (IPF) have increased molecular markers of senescence-related DNA damage when compared to healthy controls. In the lungs of humans and mice with IPF, fibroblasts and epithelial cells undergo senescence and the resulting SASP causes the pathological effects of this lung disease. This mediation was proved by treating naïve normal human fetal lung fibroblasts with the conditioned medium collected from senescent cells (SASP-conditioned medium). Following treatment with the SASP-conditioned medium, 62% of the fibroblasts tested positive for alpha-smooth muscle actin (αSMA) protein which is an indicator of fibrotic activation. These cells also expressed higher levels of *COL1A1*, *COL1A2*, *actin-a-2*, and *fibronectin 1* (fibrosis related genes) relative to controls (Schafer et al., 2017).

In a mouse model of fibrotic lung disease, elimination of senescent cells with senolytic drugs results in a significant reduction in p16 expression, decrease in the levels of SASP factors

such as monocyte chemoattractant protein-1 (Mcp1), interleukin 6 (IL6), matrix metalloproteinase-12 (Mmp12) and transforming growth factor beta (Tgfβ) and attenuates the increase in inflammatory response thus improving the overall lung function but lung fibrosis remained unaltered. Senolytic drug administration in humans was also seen to be feasible and ameliorate certain aspects of IPF (Justice et al., 2019; Schafer et al., 2017).

1.2.3 Senescence in BPD

Evidence for lung senescence in BPD first emerged in neonatal murine lungs exposed to hyperoxia and resulted in an increased expression of p21 mediated through a p53-dependent pathway (McGrath, 1998). Increased p21 expression promotes cell cycle arrest in senescent cells. Londhe and coworkers demonstrated that hyperoxia-exposure induces increased expression of p21 and p53 in lungs of neonatal mice (Londhe et al., 2011). Exposure of human fetal lung fibroblasts derived from the canalicular phase of development to 40% oxygen (moderate hyperoxia) for 7 days resulted in wide flattened cells characteristic of senescence. Further, there was an increase in Senescence-associated beta-galactosidase (SaβG) $^{+}$ cells and also overexpression of p21 and p53. Data collected from flow cytometry experiments led to the conclusion that hyperoxia exposure activates senescence and hyperoxia-exposed cells get arrested at the G2/M phase instead of the G1 phase. (You et al., 2019)

Further evidence of senescence playing a role in BPD came from exploring the Wnt/β-catenin signaling pathway which is crucial for normal lung development. The Wnt/β-catenin signaling reaches its maximum at the end of the pseudoglandular phase of the lung development which is then followed by minimum Wnt/β-catenin signaling from the canalicular phase. In contrast, pre-term birth and BPD cause the continuous activation of Wnt/β-catenin signaling pathway during the canalicular phase which disturbs normal pulmonary development. Dasgupta *et*

al. first provided evidence of activation of TGF- β and Wnt/β-catenin signaling in neonatal mice exposed to hyperoxia. They found that continuous Wnt/β-catenin signaling activation induces senescence in alveolar epithelial type II cells (AT II), which may explain some of the various pathological effects of BPD. (Dasgupta et al., 2009; Lecarpentier et al., 2019; Lehmann et al., 2020; J. M. S. Sucre et al., 2018)

Hyperoxia-induced cellular senescence and chronic Wnt/β-catenin signaling may thus contribute to accelerated aging in the lung and in turn, contribute to the long-term consequences of BPD (J. Sucre et al., 2021). Reversal of senescence and premature aging that the lung tissues underwent can help overcome the symptoms of the disease and even help in tissue repair and rejuvenation. In recent years, promising strategies have been developed to rejuvenate injured/aged cells, tissues, and organs. These rejuvenation strategies will be discussed in the next chapter.

1.3 Lung Rejuvenation

Rejuvenation is the process of restoring the lost function of tissues into their healthier initial state. Loss of function could be the result of aging, damage, or disease. Aging, once considered irreversible, may now be reversed as evidenced by rejuvenation of old cells in various model systems. The various hallmarks of aging are telomere shortening, DNA damage, epigenetic alterations, mitochondrial dysfunction, cellular senescence, loss of proteostasis, deregulated nutrient sensing, stem cell exhaustion, and altered intracellular communication (López-Otín et al., 2013). Rejuvenation strategies targeting these hallmarks have shown to be effective in delaying and possibly reversing the process of aging. These strategies can be characterized into the four following categories: 1) systemic factors-induced rejuvenation, 2) metabolic manipulation-

induced rejuvenation, 3) rejuvenation due to ablation of senescent cells, and 4) rejuvenation due to cellular reprogramming (Mahmoudi et al., 2019).

Systemic factors induced rejuvenation was first reported by Conboy *et al.* in 2005. They studied the influence of systemic factors on aged stem cells by exposing old mice to young serum. Their observations indicate that decreased stem cell activity due to aging can be rejuvenated using young systemic factors (Conboy et al., 2005). No specific factor was identified, but the Notch signaling activity, which usually reduces with age, was seen to be restored with heterochronic parabiosis.

Rejuvenation due to metabolic manipulation can be induced by following a strict diet regimen. Aging is modulated in this case by nutrient-sensing pathways such as mTOR and insulin-IGF signaling (Mahmoudi et al., 2019).

Eliminating senescent cells is another promising strategy in delaying aging and rejuvenation. Senescence pushes the cell into a permanent cell cycle arrest. These senescent cells produce SASP factors which is responsible for stem cell exhaustion and transmit the senescent characters to its neighboring cells. Thus, removing senescent cells can help restore stem cell function (Chang et al., 2016).

Cellular reprogramming leads to epigenetic remodeling and histone modifications which is responsible for increased regenerative capacity and stem cell function resulting in rejuvenation (Ocampo et al., 2016).

In humans, tissue regeneration capacity is highest at the early stages of life. This capacity decreases with age and only a few organs namely the liver and skin have the capability of scar-free tissue regeneration after an injury. Lung diseases such as BPD, emphysema, pulmonary

fibrosis, and some others have no cure. The regenerative capacity of the lung was previously thought to be low, but in certain cases, a high capacity of tissue regeneration was seen in the lung after an injury (Kotton & Morrisey, 2014). Partial pneumonectomy (PNX) considerably decreases the lung diffusion capacity due to the reduced number of alveoli available for gas exchange. Compensatory growth post-PNX to restore lung mass is well documented in dogs, rabbits, ferrets, and mice. Induction of cell proliferation in the residual tissue helps in restoring the lung mass following PNX (Brown et al., 2001). Evidence for compensatory adult lung growth in humans was shown by Butler and colleagues in a 33-year-old woman who had undergone a right-sided PNX. In a span of 15 years after the procedure, a 77% increase in volume was seen along with a 64% increase in alveoli number. Those progenitors or stem cells that are involved in the regenerative process can be the major link to developing an efficient clinical therapy for various lung disorders. Observations from data collected from cell lineage tracing have shown that the majority of the epithelial cells in the lung, except airway-ciliated cells, are seen to undergo proliferation after injury. One can infer that lung tissue is highly plastic and a variety of dormant cells in the lung can proliferate, dedifferentiate, and change phenotype to repair an injury.

There is also some evidence of catch-up growth in preterm infants as seen from alveolarization continuing through adulthood (Narayanan et al., 2013). A non-invasive technique hyperpolarized helium-3 magnetic resonance (HeMR) was used to assess the alveolar dimensions in young adults who were born preterm. The alveolar dimensions measured for school-age survivors of extreme prematurity were similar to term-born and mild preterm children. This suggests a compensatory development during the first decade of life in the survivors. Re-igniting the repair potential in young infants may be very beneficial in overcoming the abnormalities in the

lungs due to a developmental arrest seen in infants with BPD over treating fibrotic lung in an elderly patient.

Tissue rejuvenation through cellular reprogramming holds great potential in repairing damaged tissue and organs. The process of cellular reprogramming and how it can be used therapeutically will be discussed in the following chapters.

1.4 Cellular Reprogramming

Cellular reprogramming is the process of converting one cell fate to the other by using a set of defined factors. The first evidence of cellular reprogramming, starting from a somatic state to an embryonic state, was shown by Sir John Gurdon in 1962 using the technique of Somatic cell nuclear transfer (SCNT) (J. Gurdon et al., n.d.; J. B. Gurdon, 1962). In this technique, an embryo that is genetically identical to the donor somatic cell is generated by implanting the nucleus from the donor somatic cell into an enucleated egg cell. The genetic material remains unaffected during differentiation. In 1981, mouse embryonic stem cells were derived, and their cell lines were established. These cell lines are pluripotent which means that they can differentiate into all cell types in the body. (Evans & Kaufman, 1981; Martin, 1981) In 1997, Wilmut *et al.* reported the birth of a live lamb, Dolly, born after nuclear transfer from the mammary gland. This is the first reported case of a mammal developing from an adult cell providing proof of concept for cellular reprogramming. (Wilmut et al., 1997) Cellular reprogramming by forced expression of transcription factors was first shown by Harold Weintraub and group where MyoD was used to reprogram fibroblasts into myoblasts. (Davis et al., 1987)

1.4.1 Induced pluripotent cells (iPSCs)

The most important breakthrough in the field of reprogramming was in the year 2006 by Yamanaka and Takahashi, who showed that reprogramming of differentiated mouse fibroblasts

into an embryonic-like state is possible by ectopic expression of just four transcription factors, Oct3/4, Sox2, klf4, and C-myc (OSKM). These reprogrammed pluripotent cells were named iPSCs. Reprogramming was first reported in mouse embryonic fibroblasts (MEF) by introducing carefully selected candidates that were identified as potential reprogramming factors. A retroviral transduction system which was developed by Toshio Kitamura of the University of Tokyo was used as the delivery mechanism used. After a successful generation of mouse iPSCs, similar studies were conducted in generating human iPSCs using the same factors (OSKM) (Takahashi et al., 2007; Yamanaka & Takahashi, 2006). The transition in the state of the cell to induced pluripotent stem cells was due to epigenetic remodeling involving a change in the epigenetic and transcriptomic profiles. Since the discovery of iPSCs in 2007, this technology has rapidly developed and has played a significant role in shaping the future of disease modeling and drug discovery. Disease modeling using iPSCs started as a conventional 2D monolayer of differentiated cells. As this method did not portray the real cell working environment it evolved into sophisticated 3D organoids and *in vivo* chimeras that better mimic the working ecosystems in complex tissues.

1.4.2 iPSC-derived lung cells

Derivation of patient-specific iPSCs holds promise to study and treat a variety of human diseases through regenerative medicine. iPSCs can play a vital role in generating a source of patient-specific cells that may be used for lung-related cell therapies. Directed differentiation of human (h)iPSCs towards lung progenitor cells was described by Green and colleagues. Definitive endoderm (DE) was induced by activin A which when followed by dual inhibition of TGF-β and bone morphogenic protein (BMP) led to the formation of anterior foregut epithelium (AFE). To differentiate AFE into a lung cell fate, treatment with a combination of different factors such as *WNT3a*, *FGF10*, *KGF*, *BMP4*, and *EGF* was used. A lung cell fate confirmed by the expression

of *NKX2.1, NKX2.5,* and *PAX1*. Another study by Ghaedi *et al.* in 2013 showed evidence of derivation of AEC II and type I (AEC I) cells from human iPSCs. A similar protocol as described above was used to generate ATII and ATI. iPSC derived ATII cells behaved similarly to isolated ATII cells from human lung tissue and seeded into a decellularized rat or human lung sections under appropriate culture conditions (Ghaedi et al., 2013).

iPSCs are an excellent source of cells as they can be expanded limitlessly and can be differentiated into any cell type for therapeutic applications. However, there are certain drawbacks and obstacles such as the risk of tumorigenicity, strong immune response and a lengthy differentiation process that hinder translation into the clinic. Inducing reprogramming *in vivo* aids to overcome these drawbacks.

1.5 Reprogramming and rejuvenation

Direct *in vivo* reprogramming to replenish damaged cells in a tissue represents an exceptional candidate for therapy in the field of regenerative medicine. This strategy would eliminate immune rejection, which is the main drawback of transplantation. A study by Zhou *et al.* in 2008 laid groundwork in establishing direct *in vivo* reprogramming as a strategy to revive injured and damaged cells in the pancreas. In their study, the authors focused on converting fully differentiated exocrine cells to functional β cells *in vivo* using a diabetic mouse model. Substantial improvement in the fasting blood glucose levels was observed in mice overexpressing the three transcription factors, *Ngn3*, *Pdx1*, and *Mafa* compared to the control mice, suggesting derivation of functional β cells (Zhou et al., 2008). Reprograming cardiac fibroblasts into cardiomyocytes was first shown by Qian *et al*. Retroviral vectors were used for the delivery of *Gata4*, *Mef2c*, and *Tbx5* to the damaged heart which resulted in cardiac reprogramming and rejuvenation as seen from the significant improvement of the total cardiac output in the GMT-infected mice (Gata4, Mef2c

and Tbx5). Another interesting finding was that due to the factors present in their native microenvironment, the *in vivo*-induced cardiomyocytes resembled more closely the endogenous cardiomyocytes than the ones induced *in vitro* as they were more fully reprogrammed (Qian et al., 2012). Song *et al.* showed similar results where reprogramming non-cardiomyocytes into induced cardiomyocytes was achievable by expressing transcription factors such as *Gata4*, *hand2*, *Tbx5* in mice (Song et al., 2012). Reprogramming into a neuronal lineage was first done by Torper *et al*. The *Ascl1*, *Brn2*, and *Myt1l* genes (neural conversion factors) were expressed with the help of a cre inducible lentiviral vector, which when injected into the striatum of mice helped reprogram endogenous mouse astrocytes into induced neurons (Torper et al., 2013).

Reprogramming mature, differentiated, and specialized cells into a pluripotent state by overexpression of a combination of transcription factors such as Oct3/4, Sox2, klf4, and C-myc OSKM) *in vivo* has been shown to cause tissue regeneration in several studies. A study by Abad and group demonstrated that overexpression of OSKM *in vivo* can induce differentiation into pluripotency in different cell types. This study showed evidence of cell reprogramming from the hematopoietic lineage and epithelial cells from the kidney, pancreas, intestines, and stomach (Abad et al., 2013). *In vivo* reprogramming caused teratoma formation in several organs. Formation of teratomas was also reported by Ohnishi *et al.* due to continuous *in vivo* reprogramming. The presence of these teratomas proved successful reprogramming into full pluripotency, but also raised concerns regarding the safety of this approach for rejuvenation. Both these studies made use of a reprogrammable mouse (i4f-a and i4f-b) which has a copy of doxycycline (dox) inducible polycistronic cassettes encoding the four factors (OSKM). This dox-inducible promoter made it very easy to switch on and off OSKM expression. The association between the period of OSKM expression and tumor formation was established in these reports. A shorter administration period

with a high dose of dox (1mg/ml for 7 days) resulted in lower tumorigenesis and mortality compared to longer administration periods with a low dose of doxycycline (0.25ml/ml for 17 days). Using the same transgenic mouse line, it was observed that mice treated with dox for a period of less than 5 days did not have any dysplastic cells (Ohnishi et al., 2014).

Senescence signals from injured or aged cells have been shown to increase the efficiency of *in vivo* reprogramming (Chiche et al., 2017; Mosteiro et al., 2016, 2018). This aspect could be exploited to reprogram the lungs more efficiently and will be discussed in the following section.

1.6 Senescence and reprogramming

Some studies have shown an interesting upside to senescence which is to promote reprogramming and hence tissue repair. The first report to show evidence of senescence promoting reprogramming was by Mosteiro and group in 2016. In this study, reprogrammable mice (i4f) which had dox-induced OSKM transgene were crossed with mice that were deficient in p53 or Ink4a/Arf to obtain i4f;p53-null and i4f;Ink4a/Arf-null mouse lines. When treated with dox, the trends seen for the efficiency of reprogramming and teratoma formation were i4f;p53-null > i4f > i4f;Ink4a/Arf-null. This suggests that p53 (cell cycle regulator) absence promotes reprogramming and Ink41/Arf (tissues lacking p16INK4a/ARF, which do not undergo senescence) absence reduces the efficiency of reprogramming. Presence of $NANOG^{+}$ cells (fully reprogrammed cells) was also observed in close proximity to SaβG+ when reprogramming was induced and the number of SaβG+ cells was in the order i4f;p53-null > i4f > i4f;Ink4a/Arf-null. These observations prove the coexistence of senescence and reprogramming. There is evidence that cytokine rich microenvironment mediates the crosstalk between senescence and reprogramming as repression of NFkB (which regulates the secretory activity of the senescent cells) resulted in a decreased expression of SASP factors and in turn reduced the extent of *in vivo* reprogramming. Among the

SASP factors, it was found that IL-6 may have a dominant role as it was the most up-regulated factors during OSKM induction, and blockade of IL-6 reduced the efficiency *in vivo* reprogramming significantly. This is consistent with the data generated by Chiche *et al*. which showed that IL-6 released from senescent cells promotes reprogramming.

In vivo reprogramming has been reported in many cell types, but it has been unmanageable for some lineages. An example of such a lineage is the skeletal muscle system. Chiche *et al.* were the first to show that *in vivo* reprogramming was possible in skeletal muscles but only with an acute or chronic injury. To assess the influence of an injury *in vivo* reprogramming, damage in the Tibialis anterior (TA) muscle of i4F-A mice was induced using snake venom cardiotoxin (CTX). Administration of dox for 7 days resulted in easily detectable regeneration in the skeletal muscle examined 10 days post-injury and no evidence of regeneration in the non-injured TA muscles (Chiche et al., 2017).

The lung is another organ in which *in vivo* reprogramming has not been reported in despite OSKM expression. To analyze if senescence would induce reprogramming in the lung, Mosteiro and group used bleomycin (a DNA-damaging agent) to injure the lung of I4f mice, and in turn, induce senescence. The mice subsequently treated with doxycycline revealed an ample number of senescent cells and clusters of $NANOG^{+}$ cells unlike the control i4f mice (not treated with bleomycin), which did not show signs of reprogramming (no NANOG expression). An increase in the mRNA levels of SASP factors including IL-6 was also observed. This study thus provides evidence of the feasibility of reprogramming in the lungs but only enabled by tissue damage (Mosteiro et al., 2016, 2018).

1.7 Partial reprogramming

Continuous OSKM exposure *in vitro* leads to the formation of iPSCs, and continuous OSKM exposure *in vivo* leads to teratoma formation. Sustained reprogramming results in the loss of cellular identity as the cells become pluripotent and when reprogrammed fully, leads to loss of function and hence can be harmful rather than being therapeutic.

To overcome this, partial reprogramming strategies have been identified. Partial reprogramming is the process of reprogramming the cells only to a certain extent where they do not lose their identity and can go back to their initial state when OSKM overexpression is stopped. This process is summarized in Fig 2.

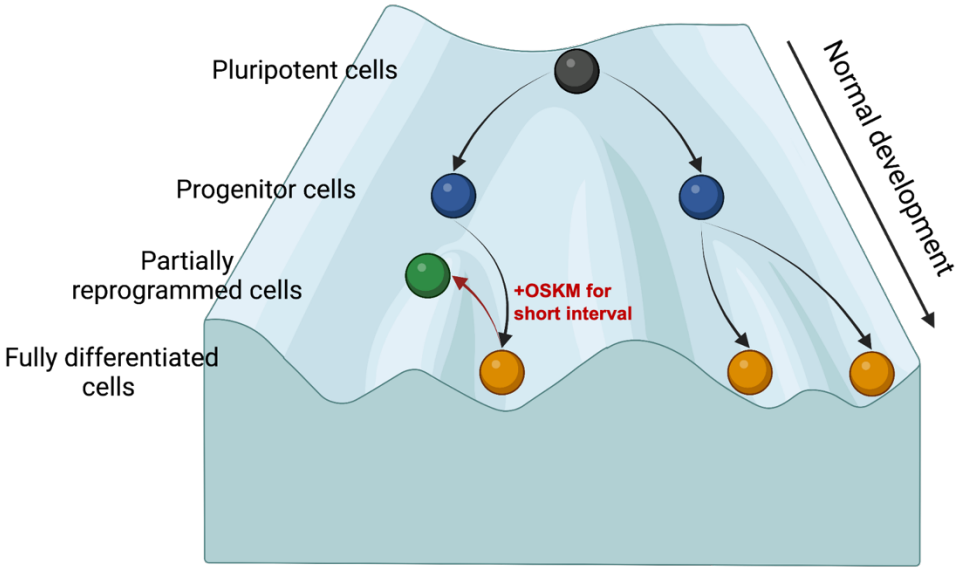

Fig 2. Graphical representation of a Waddington's plot describing the partial reprogramming.

The effects of transient reprogramming were previously studied in fibroblasts (Gill et al., 2022). These cells were reprogrammed by overexpressing OSKM factors for 10 to 17 days, and when taken off OSKM exposure, the cells were returned to their original identity (fibroblasts) rather than going to a pluripotent state. Using single-cell RNA sequencing, it was observed that

the transcriptome of the partially reprogrammed cells was more similar to younger fibroblasts rather than the negative controls (fibroblasts that did not undergo reprogramming). The epigenome of the partially reprogrammed cells was also rejuvenated as demonstrated with the restoration of H3K9me3 levels and reduction of DNA methylation age. This study demonstrates the potential of partial OSKM reprogramming in rejuvenation without having to completely reprogram the cells into iPSCs.

Partial reprogramming *in vivo* was first described by Dr. Belmonte's group using a transgenic mouse line which models progeria (a disorder of accelerated aging) and carries a dox inducible OSKM polycistronic cassette. Partial reprogramming was achieved by employing a cyclical OSKM induction strategy, in which each cycle consisted of 2 days of OSKM activated period followed by 5 days of OSKM deactivated period. Cyclic OSKM activation resulted in extended median lifespan in the accelerated aging mouse model and restoration of various aging hallmarks was observed. Short and cyclical OSKM activation also did not generate any teratomas. Partial *in vivo* reprogramming strategy described in this study opened exciting opportunities to further explore the field of rejuvenation without the concern of teratoma formation.

Partial *in vivo* reprogramming was also shown beneficial in delaying the normal physiological changes associated with aging. This was described by Belmonte's group in a consecutive study where they used in-depth transcriptomic and methylation analysis to decode the effect of partial OSKM reprogramming on molecular aging phenotypes in various tissue types. They observed that long-term partial reprogramming (spanning 7 and 10 months, starting either at 12 or 15 months of age respectively) was better in delaying aging phenotypes rather than short-term partial reprogramming (1 month, starting at 25 months of age). This was because the mice that underwent partial reprogramming acquired a younger transcriptomic and DNA methylation

signature. Not all tissues respond to reprogramming equally and, in their set-up, the authors observed that the skin and kidney were more susceptible to being reprogrammed (Browder et al., 2022). Overexpression of just the OSK (without c-Myc) factors was seen to significantly improve the age of wild type mice. Cyclic OSK treatment was started at 124 weeks of age and continued for the remainder of their lives. The median life of the mice in the OSK treated group was increased by 109% relative to the control mice and the overall health of the treated mice was better. They also observed that the treated animals acquire a younger DNA methylation signature.

Taken together, these results suggest that partial reprogramming using the OSK/OSKM factors work by resetting the epigenome to a younger state which in turn slows down the natural aging process.

Partial reprogramming results in a younger version of the cell. As a consequence, these cells have increased rate of proliferation. This strategy was subsequently exploited by various groups to rejuvenate injured tissues.

1.8 Partial reprogramming to regenerate injured tissues.

In recent years, various groups have had tremendous success in using partial reprogramming using the OSKM or the OSK factors to rejuvenate certain tissues after an injury. In 2020, David Sinclair's group showed that overexpression of the OSK factors in the retinal ganglion cells allowed for regeneration of injured axons. Under normal circumstances, mature retinal ganglion cells lose their ability to regenerate. They observed that ectopic expression of the OSK factors restored the DNA methylation (DNAm) age (otherwise increased due to injury) back to a younger signature which in turn helped in axon regeneration. Using a glaucoma injury model,

they also demonstrated that OSK overexpression for 4 weeks helped the mice to recover from the injury. Similarly, OSK overexpression in old mice restored their transcriptomic signatures to a youthful state and hence restore vision in these mice. (Lu et al., 2020)

Adult cardiomyocytes (cm), much like retinal ganglion cells also have very low regenerative capacity. Braun and colleagues generated transgenic mice capable of cardiomyocyte specific OSKM expression. Using these mice, they showed that cardiomyocyte specific transient OSKM expression pushed them back to a gene expression profile resembling the neonatal period. Cardiomyocytes that underwent partial reprogramming (pretreated) were more proliferative when compared to the ones that were not reprogrammed. They further proved that partially reprogrammed adult mice which underwent an injury (myocardial infarction) were able to better recover functionally and structurally when compared to untreated mice. Mice that underwent partial reprogramming after the injury did not show improvement in cardiac function but had significant reduction in scar size when compared to untreated animals.

The ability to rejuvenate complex tissues in the heart and the eyes by partial reprogramming proves that this is a very promising strategy in regenerating injured tissues.

Other examples of rejuvenation by targeting a specific cell type stem from other work of Belmonte's group. In two consecutive studies, they show that myofiber or hepatocyte specific OSKM reprogramming improved the muscle and liver regeneration capabilities respectively. The improvements in the regenerative capabilities were mediated through different mechanisms, liver rejuvenation was mediated through topoismerase2a and muscle regeneration was mediated through wnt4 downregulation. (Hishida et al., 2022a; Wang et al., 2021).

Cyclic activation of the OSKM factors was proved to be safe in mice (Ocampo et al., 2016) and some groups capitalized on this strategy to improve the process of wound healing (Doeser et al., 2018) and for intervertebral disc rejuvenation (Cheng et al., 2022). Doeser and group using a dox inducible OSKM transgenic mice showed that *in situ* OSKM activation by dox application locally on the wounded region significantly reduced scar formation and hence improved the process of wound healing. In another study, Cheng and group showed that partial reprogramming through cyclical OSKM activation can reverse intervertebral disc degeneration using an induced injury (needle puncture) model and an age-related model.

Not all tissues react to OSKM reprogramming in a similar way. Some tissues such as the skin, liver, and kidney are more susceptible to being reprogrammed whereas other tissues such as the lungs do not reprogram as efficiently. (Browder et al., 2022)

To overcome the issue of lower efficiency of reprogramming in the lung, Waddel and colleagues developed a strategy where the ATII cells isolated from reprogrammable mice were cultured for two weeks without dox and followed by late induction for two weeks. This strategy was termed "interrupted reprogramming" (Guo et al., 2018). Interrupted reprogramming prevented the conversion of the ATII cells into a pluripotent state but rather into an induced progenitor-like (iPL) cells. ATII-iPL had significantly higher clonogenic capacity when compared to those cells that were not reprogrammed. ATII-iPL cells when transplanted into bleomycin injured lung were able to engraft and produce ATII and ATI cells and in turn were able to reduce fibrosis and improve lung function. This is an effective strategy which improves the bleomycin-induced pulmonary fibrosis.

2. Rationale Hypothesis and objectives

2.1 Rationale

BPD is a major complication of premature birth that lacks a safe and effective treatment. BPD results in interrupted lung growth. Increasing evidence indicates early-onset emphysema and pulmonary vascular disease in young adult survivors with BPD, suggesting irreversible arrest in lung growth and/or premature lung aging resulting in life-long health problems. Our lab has so far investigated cell therapies to prevent neonatal lung injury. Here, we propose a new direction by investigating the possibility of reversing established lung injury by adopting a new concept: cellular reprogramming. *In vivo* partial reprogramming via activation of Oct4, Sox2, Klf4, and c-Myc (OSKM) has previously been shown to ameliorate cellular and physiological hallmarks of aging and in turn, promote tissue regeneration and improve organ function after injury but its effect to regenerate an established lung injury is unknown.

2.2 Hypothesis

Based on these findings, I hypothesize that partial reprogramming induced by transient overexpression of the OSKM or the OSK factors regenerates neonatal oxygen-induced lung damage.

2.3 Objectives

My objectives are to i) Characterize long-term mouse neonatal hyperoxia lung injury model (in C57Bl/6 mice). ii) Characterize the AAV vector system developed to overexpress the OSK factors and determine if transient overexpression of the OSK factors improves lung function and structure in a mouse neonatal hyperoxia lung injury model. iii) To develop and characterize mouse neonatal hyperoxia lung injury model in the transgenic i4f-b mouse line. iv) Determine if transient

overexpression of the OSKM factors improves lung function and structure after neonatal hyperoxia-induced lung injury in i4f-b mice.

Chapter 3. Material and Methods

3.1 Mouse housing and care

All mouse experiments conformed to the standards of the Canadian Council on Animal and were approved by the Animal Care Committee of the University of Ottawa (protocol: OHRI-1696). Male and female mice were equally distributed for all experiments. All mice were housed in standard ventilated cages in temperature (23 to 24 °C) and humidity-controlled (30-60% humidity) rooms with a 12-hour light-dark cycle. Food and water were available ad libitum throughout all experiments.

3.2 Mouse genotyping

AccuStart II PCR Genotyping Kit (Quanta bio) was used for genotyping. Briefly, DNA was extracted from ear notches made on postnatal day (PND) 14. For DNA extraction, each ear notch was placed in 60 µL of the extraction buffer and placed on a heating plate at 95^{o}C for 45 minutes. After cooling down the solution to room temperature, 60µL of the stabilization buffer was added. PCR amplification was carried out using as per the manufacturer's instructions. PCR product was analyzed by agarose gel electrophoresis. Primer sequences used are listed below.

Gene	Forward primer	Reverse primer	Amplicon size
ROSA26 WT locus	AAAGTCGCTCTGAGTTGTTAT	GGAGCGGGAGAAATGGATATG	650
ROSA26-rtTA	AAAGTCGCTCTGAGTTGTTAT	GCGAAGAGTTTGTCCTCAACC	300
ORF (lentiviral transgene)	GGATGGAGTGGGACAGAGAA	GTGCCGATCCGTTCACTAAT	300

Table 1 List of primers used for genotyping.

3.3 Neonatal hyperoxia mouse model

Mice are born during the saccular stage of lung development, which corresponds to the stage of lung development during extreme preterm births in humans. Pregnant C57Bl/6 mice (Charles Rivers, Saint Constant, QC, Canada) were delivered on embryonic day 15 (E15). Pups from all litters were randomized on the day of birth (PND 0) and distributed equally to all the dams such that each had 6 pups. Dams along with the pups were exposed to either normoxia (21% oxygen) or hyperoxia (85% oxygen) by placing them in a semi-sealed Plexiglas chamber (BioSpherix, Redfield, New York, USA) for 14 days as previously described (Hurskainen et al., 2021). The oxygen levels were monitored at all times. Hyperoxia and normoxia-exposed dams were switched

every 48 hours to prevent injury to their lungs. Mice pups were euthanized by intraperitoneal (*i.p.*) injections of pentobarbital sodium (Euthanyl, 0.2 mL, 65 mg/mL) upon reaching the endpoint.

3.4 Intratracheal delivery of AAV vectors

The animals received an analgesic (buprenorphine) subcutaneously (*s.c.*) at a dosage of 0.1 mg per kg (Vetergesic) one hour before the surgery. Directly before the procedure, each animal was anesthetized individually with isoflurane (Fresenius Kabi) (anesthesia was induced and maintained with 5% and 3% of isoflurane respectively, in a mixture of 100% O_2 at 1.5 L/min) and received *s.c.* injections of saline solution (Baxter Corp). The thorax region was shaved to the skin to remove any fur covering that area. Tracheotomy was performed while constantly maintaining each animal under anesthesia using isoflurane. 10^{11} vg of both AAV vectors, AAV-Tet3g and AAV-Luc-WPRE or the AAV-OSK-WPRE were diluted with 1X PBS to a total volume of 30 μL. A single intratracheal (*i.t.*) injection of the combination of the vectors was delivered using the 3/10 mL insulin syringe 29 gauge × ½" (Covidien). The incisions were sutured followed by an application of a topical 2% transdermal bupivacaine HCL as monohydrate (Chiron) post-surgery. The pups were allowed to recover in a 37 °C incubator for 1 h post-surgery.

3.5 Doxycycline administration in mice

Doxycycline hyclate (Sigma Aldrich) along with 1% sucrose was diluted at a concentration of 1 mg/ml in Milli-Q water. Standard water bottles from the mouse cages were replaced with darkened bottles containing 1 mg/ml dox water for 2, 3, or 4 days per cycle. Mice were subjected to a course of 4 such cycles per experiment.

3.6 Lung function analysis

Lung function of each mouse at the endpoint was measured using the flexiVent machine (flexiVent, Scireq, Montreal, Canada). Mice were euthanized by *i.p.* injections of pentobarbital sodium (Euthanyl, 0.2 mL, 65 mg/mL). A tracheotomy was performed, and the trachea was connected to a 18-guage cannula attached to the flexiVent. The lungs of each mouse were then inflated gradually in step-by-step increments of applied pressure until a maximum of 30 cmH_2O was reached. This is followed by a gradual deflation in the same manner to obtain the pressure-volume (PV) loops. The PV curves are normalized to the body weights of the respective mice. The values for lung function parameters such as the total lung capacity (TLC), residual volume (RV), compliance (C), and elastance (E) were extracted from the PV loops (Kang et al., 2020).

3.7 Lung histology

The left lungs were inflated and perfused through the trachea using 10% buffered formalin while maintaining a constant pressure of 20cm H_2O. The inflated lungs were kept in 10% buffered formalin for 48 hours and then transferred to 70% ethanol. The lungs were then embedded in paraffin and longitudinal sections of 4 μm thickness were prepared. These serial sections were then stained with hematoxylin and eosin (H&E) by the Louise Pelletier Histology Core Facility of the University of Ottawa (Ottawa, ON). Blinded analysis of alveolar size was performed using a motorized microscope stage by calculating the mean linear intercept (MLI) for each animal (Pierro et al., 2013).

3.8 *In vivo* imaging

Mice on PND 14 were injected *i.t.* with 10^{11} vg of AAV-Tet3g and AAV-Luc as described above. The injected mice were allowed to recover from the surgery for 7 days. Dox was administered in a cyclic manner as mentioned above for 4 weeks starting from PND 21. IVIS images were taken on day 0, day 3, and day 5 of every cycle. D-luciferin (BioVision) was freshly prepared 1 hour before the imaging session at a concentration of 15 mg/mL in 1X PBS. All mice received 150 mg/kg *s.c.* injection of the D-luciferin solution 20 minutes before imaging. Up to 4 mice were imaged at once.

Quantification of the luciferase signal from the region of interest was performed according to the manufacturer's instructions using the Living Image 3.2 software (Caliper Life Sciences, Hopkinton, MA, USA). For each animal, the average radiance (p/s/cm^2/sr), the standard deviation (SD) of radiance, as well as the minimum and maximum radiance were obtained from the thorax (lung) and abdominal regions. All representative images are presented as count measurements which are uncalibrated measurements of photons in a pixel. Radiance (p/s/cm^2/sr) was used to quantify the bioluminescence signal from IVIS figures in this study, which are calibrated measurements of photon emissions. (Kang et al., 2020)

3.9 Cell culture, AAV transduction, and protein isolation

Human embryonic kidney cells (HEK293; ATCC® CRL-1573) were maintained in DMEM/F-12 supplemented with 10% Fetal Bovine Serum (FBS; HyClone; SH30088) and 1% Penicillin Streptomycin (HyClone; SV30010). For transductions, either AAV-Tet3g or AAV-OSK or both together (AAV-Tet3g + AAV-OSK) at a multiplicity of infection (MOI) of 20000 was incubated with the HEK293 cells. Dox was added to the media 24h post-transduction at a final concentration

1 ug/ml. At 72h post-transduction, media was replaced with fresh dox to maintain its activity. The cells were harvested 96 hours post-transduction. The cells were washed with ice-cold 1XPBS twice followed by the addition of cell lysis buffer (CelLytic™ MT Cell Lysis Reagent; Sigma) and protease inhibitors (Sigma). The cells were then scrapped off using a cell scrapper and transferred to a 1.5 ml microcentrifuge tube. They are centrifuged at 16000 g for 20 minutes at 4ºC and the supernatant is collected and stored in -80ºC. Bradford assay using the Quick Start™ Bradford 1x Dye Reagent (Bio-Rad Laboratories) was used to determine the protein concentration of the isolate.

3.10 Western blot

The cell lysates were fractioned on a Mini-PROTEAN® TGX™(Bio-Rad Laboratories) gel at 120V for 60 minutes. The proteins were then transferred to a nitrocellulose membrane using the iBlot™ 2 Gel Transfer Device (Thermo Fisher Scientific). The membrane was blocked with 5% non-fat dairy milk in Tris Buffered Saline + Tween 20 (TBST) for 3 hours at room temperature on a rocker. Membranes were washed 3 times (10 minutes each) with TBST and incubated in the primary antibody overnight at 4ºC. The primary antibody was then removed, and the membrane was washed with TBST 3 times. The membrane was then incubated with the respective secondary antibody at room temperature for 1 hour. The membrane was then washed 3 times (10 minutes each) with TBST. Blots were developed using ECL substrate (Amersham™ ECL™) and Bio-Rad Imager.

Antibody	Species	Dilution	Source	Catalog number
Primary				
Oct4	Rabbit	1:1000	Abcam	ab181557
Sox2	Rabbit	1:1000	Abcam	ab181557
Klf4	Rabbit	1:1000	Abcam	ab214666
Actin	Mouse	1:5000	Cell Signalling technology	3700S
Secondary				
Anti-mouse	Horse	1:5000	Cell Signalling technology	7076S
Anti-rabbit	Goat	1:10000	Cell Signalling technology	7074S

Table 2 List of antibodies used for Western Blot.

3.11 *In vitro* luciferase detection

In vitro luciferase detection was performed at the University of Guelph by Dr. Sarah Wootton's lab. HEK293 cells were transduced with either AAV-TRE-Luc and AAV-CASI-Tet3G at MOI of 10000 or no-AAV vector controls at 24h after seeding the cells. Dox was added into the cells 24h post-transduction at a final concentration 1ug/ml. At 72h post-transduction, media was replaced with fresh dox to maintain its activity. Firefly luciferase activity was measured 96h after the

addition of dox using Promega Luciferase assay kit (Promega) as per the manufacturer's recommendations. The treatments were performed in triplicate wells.

3.12 Quantitative Real-time PCR

The right lung tissues were chopped and stored in RNAlater Solution (Thermo Fisher Scientific). Randomly chosen small pieces of lung (30mg) were used for RNA extraction. The RNeasy Plus mini kit (Qiagen) was used for the extraction of total RNA from the lung tissues. The tissues were homogenized with the TissueLyser II (Qiagen) machine and RNA was isolated subsequently according to the manufacturer's instructions. RNA concentration and quality were assessed by NanoDrop spectrophotometer (Thermo Fisher Scientific). RNA was then reverse transcribed into cDNA using the iScript Reverse Transcription Supermix (BioRad). Quantitative real-time-PCR (qPCR) analysis was performed using CFX96 Touch Real-Time PCR (Bio-Rad). Predesigned PrimeTime™ qPCR Probe Assays (IDT DNA) were used and are listed below.

Gene	Probe	Assay ID
p53	Fam	Mm.PT.58.44013092
p16	Fam	Mm.PT.58.8388138
p21	Hex	Mm.PT.58.17125846
Il6	Hex	Mm.PT.58.10005566
Mmp12	Fam	Mm.PT.58.31615472
Ki67	Hex	Mm.PT.58.7871981
Hprt	Cy5	Mm.PT.39a.22214828

Table 3 List of qPCR primers.

3.13 Statistical analysis

All statistical analysis were performed on GraphPad Prism 9 Version 9.5.0. Unpaired two-tailed Student's t-test or one-way or two-way analysis of variance (ANOVA) for more than two groups were used as appropriate. P values less than 0.05 were considered statistically significant. Significant results are shown as *$P \leq 0.05$, **$P \leq 0.01$, ***$P \leq 0.001$, and ****$P \leq 0.0001$.

Chapter 4. Results

4.1 Hyperoxia alters lung function and structure in neonatal C57Bl/6 mice.

Newborn C57Bl/6 mice were exposed to 85% oxygen (from birth to PND14) (neonatal mice hyperoxic model of BPD) (fig 3a). Age-matched control mice were housed in room air. A significant reduction in lung function in hyperoxia-exposed animals compared to control room air-exposed mice was observed as indicated by an upward shift in the PV loop at PND21 which is a representation of an emphysematous lung (fig 3b). We observed a significant increase in the inspiratory capacity and residual volume. A significant increase in compliance and a significant decrease in elastance were also observed which further confirmed an emphysematous profile (fig 1c)

Examination of fixed lung sections revealed that alveoli were much larger in size and lesser in number in hyperoxia-exposed animals compared to room air control animals at PND21 (fig 1d). This was quantitatively confirmed by the significantly higher MLI in compared to room air control animals (Fig 1e).

Thus, hyperoxia exposure resulted in a lung phenotype that resembles BPD.

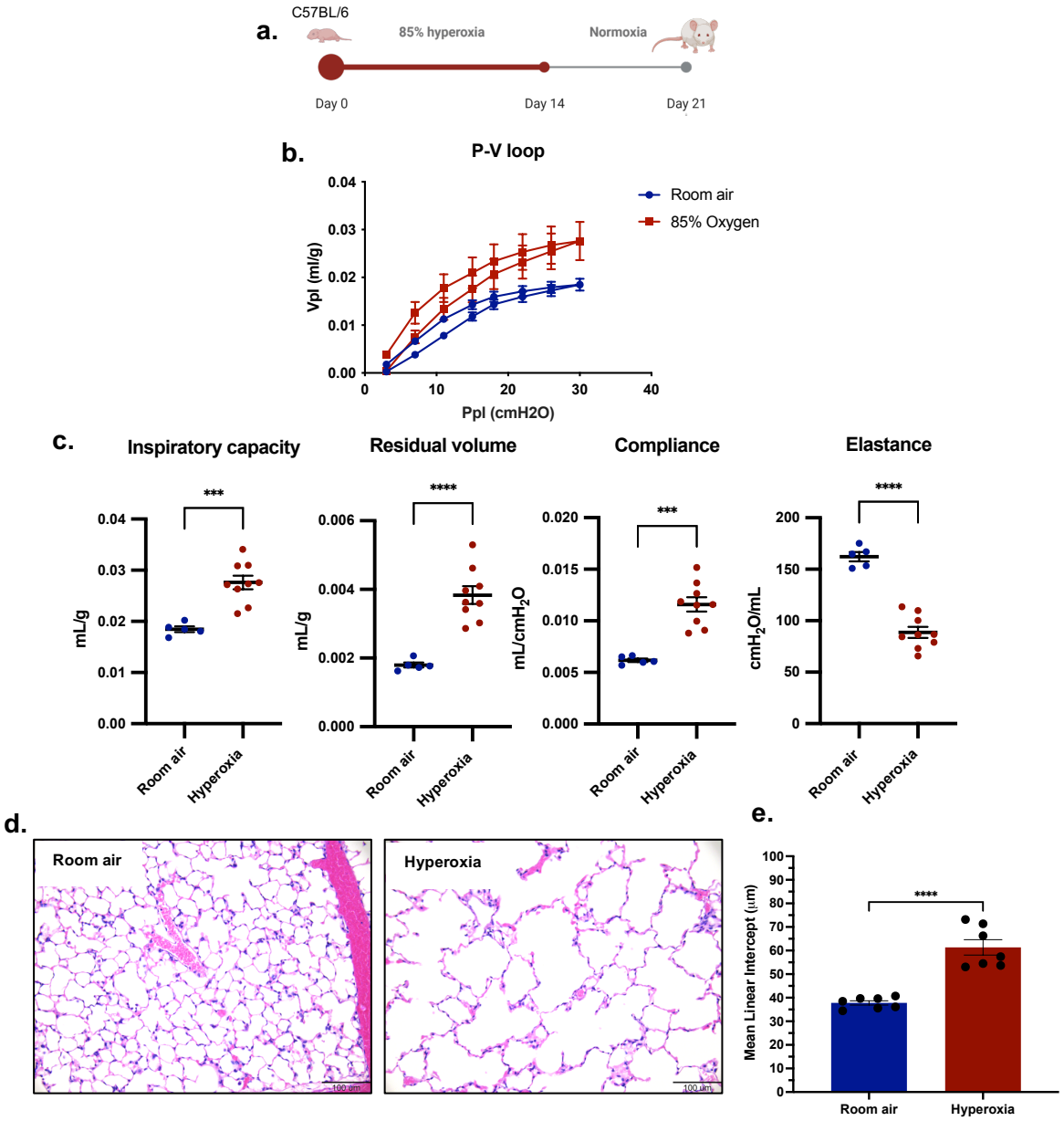

Fig 3. The 14-day hyperoxia exposure altered lung function and structure in neonatal C57Bl/6 mice. A) Schematic representation of hyperoxia-induced lung injury model in neonatal mice. Newborn C57Bl6 mice pups were exposed to continuous hyperoxia (85% O_2) until PND14. Left lung histology and lung function was assessed at PND21. **B)** Body weight adjusted PV-loop. PV-loops are shown as mean volumes of all mice in one group at each set pressure level. (Room air: n= 5; Hyperoxia: n=9) **C)** Respiratory mechanics parameters extracted from PV-loop comparing room air mice vs hyperoxia exposed mice. (Room air: n= 5; Hyperoxia: n=9) **D)** Representative images of left lung histology stained with H&E from room air and hyperoxia exposed animals. **E)** Graph comparing the MLI of room air control mice vs hyperoxia exposed mice. (Room air: n= 5; Hyperoxia: n=7) Values are represented as mean ± SEM. P values were calculated using the student's t-test except in fig B where two-way ANOVA with Tukey's multiple comparisons test was used. Significant results are shown as *P ≤ 0.05, **P ≤ 0.01, ***P ≤ 0.001, and ****P ≤ 0.0001.

4.2 Neonatal hyperoxia exposure results in persistent lung injury up until 7 weeks of age.

This arrest in lung development was also observed in 7-week-old mice exposed to 85% hyperoxia from PND0 to PND14 (fig 4a). The control animals were age-matched mice placed in room air. PV loops generated using the flexiVent machine confirmed the presence of an established lung injury at 7 weeks of age in hyperoxia-exposed mice. The PV loop was significantly shifted upwards in hyperoxia-exposed animals compared to room air control animals (fig 4b). There was also a significant change in lung function parameters such as inspiratory capacity, residual volume, compliance, and elastance. (fig 4c). Similar to the PD21 timepoint, the alveoli appear much larger in size and lower in number (fig 4d). When quantified, the MLI of hyperoxia-exposed mice was significantly higher than room air control animals (fig 4e). These data confirm that there is no catch-up growth in the lungs of hyperoxia-exposed mice, even though the animals are moved into room air conditions after a period of neonatal hyperoxia exposure.

Consequently, the 14-day BPD hyperoxia mouse model represents an excellent platform to test the therapeutic efficiency of partial reprogramming to rejuvenate injured lungs.

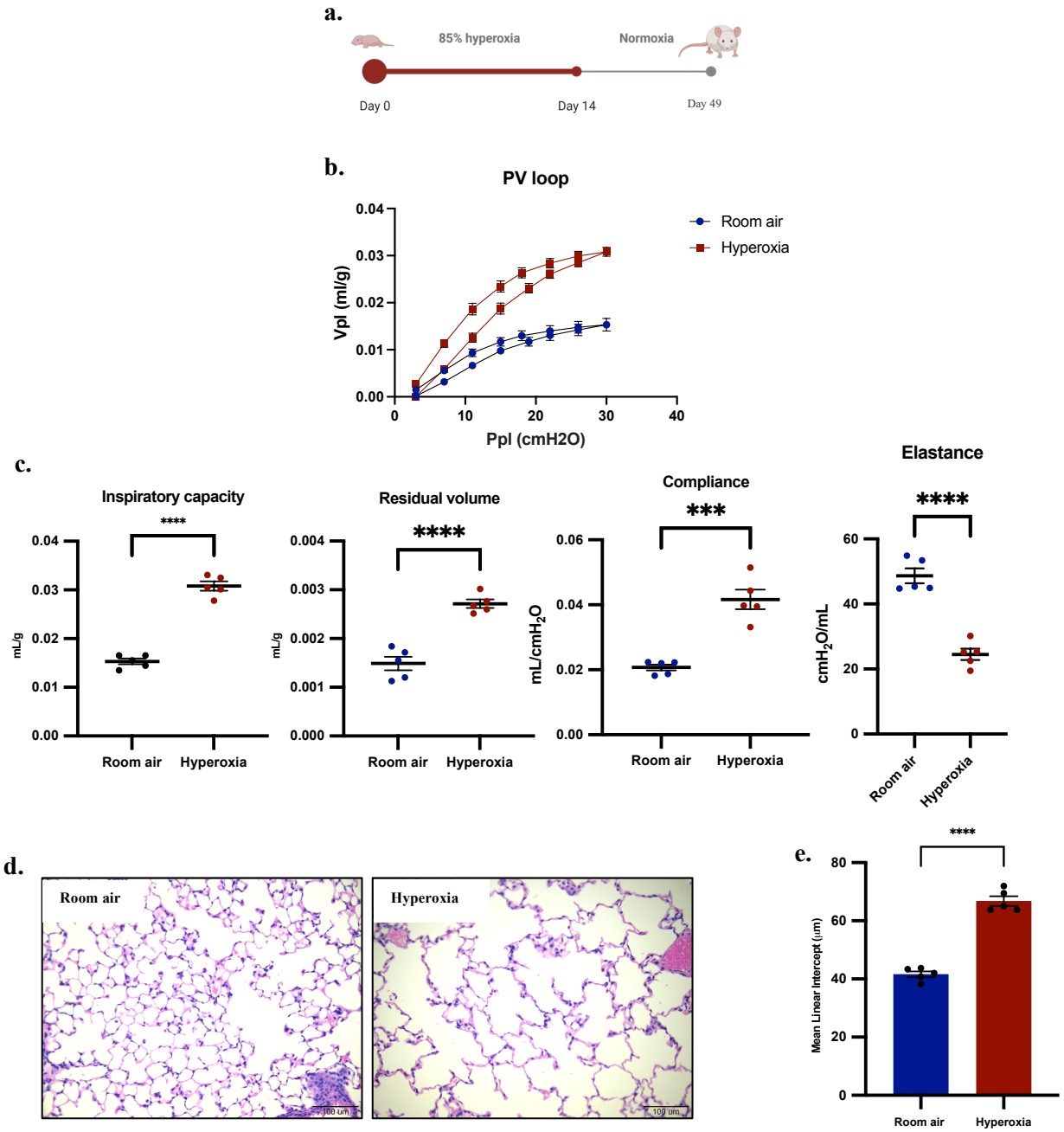

Fig 4. Neonatal hyperoxia exposure results in persistent lung injury up until 7 weeks of age. A) Schematic representation of hyperoxia-induced lung injury model in neonatal mice. Newborn C57Bl6 mice pups were exposed to continuous hyperoxia (85% O_2) until PND14. Left lung histology and lung function was assessed at PND49. **B)** Body weight adjusted PV-loop. PV-loops are shown as mean volumes of all mice in one group at each set pressure level. (Room air: n= 5; Hyperoxia: n=5) **C)** Respiratory mechanics parameters extracted from PV-loop comparing room air mice vs hyperoxia exposed mice. (Room air: n= 5; Hyperoxia: n=5) **D)** Representative images of left lung histology at PND 49 stained with H&E from room air and hyperoxia exposed animals. **E)** Graph comparing the MLI of room air control mice vs hyperoxia exposed mice. (Room air: n= 5; Hyperoxia: n=5) Values are represented as mean ± SEM. P values were calculated using the student's t-test except in PV loop where two-way ANOVA with Tukey's multiple comparisons test was used. Significant results are shown as *P ≤ 0.05, **P ≤ 0.01, ***P ≤ 0.001, and ****P ≤ 0.0001.

4.3 Senescence markers are upregulated at PND14 in hyperoxia-exposed mice.

Previous studies have shown evidence of senescence induction in the lungs following short-term hyperoxia exposure during the neonatal period (Londhe et al., 2011; Yao et al., 2023; You et al., 2019). However, the effect of long-term hyperoxia exposure on senescence markers expression remains unknown. We measured gene expression of some well-established senescence markers (p16 and p21) and SASP factors (Il6 and MMP12) in lung tissue of mice exposed to hyperoxia from PND0 to PND14 at 3 time points: PND14 (fig 5a), PND21 (fig 5b), and PND49 (fig 5c) and compared them to room air controls. There was a significant increase in the expression of p21 after 14 days of hyperoxia exposure which suggests induction of senescence (fig 5a). We also observed increase in the expression of p16 and SASP factors such as Il6 and MM12 at this time point (fig 3a). At later time points (PND21 and PND49), the expression levels of these markers returned to baseline levels (fig 5b, c).

Thus, hyperoxia-exposure from PND0 to PND14 caused an increase in some senescence markers which may suggest an induction of a lung senescent phenotype in this model.

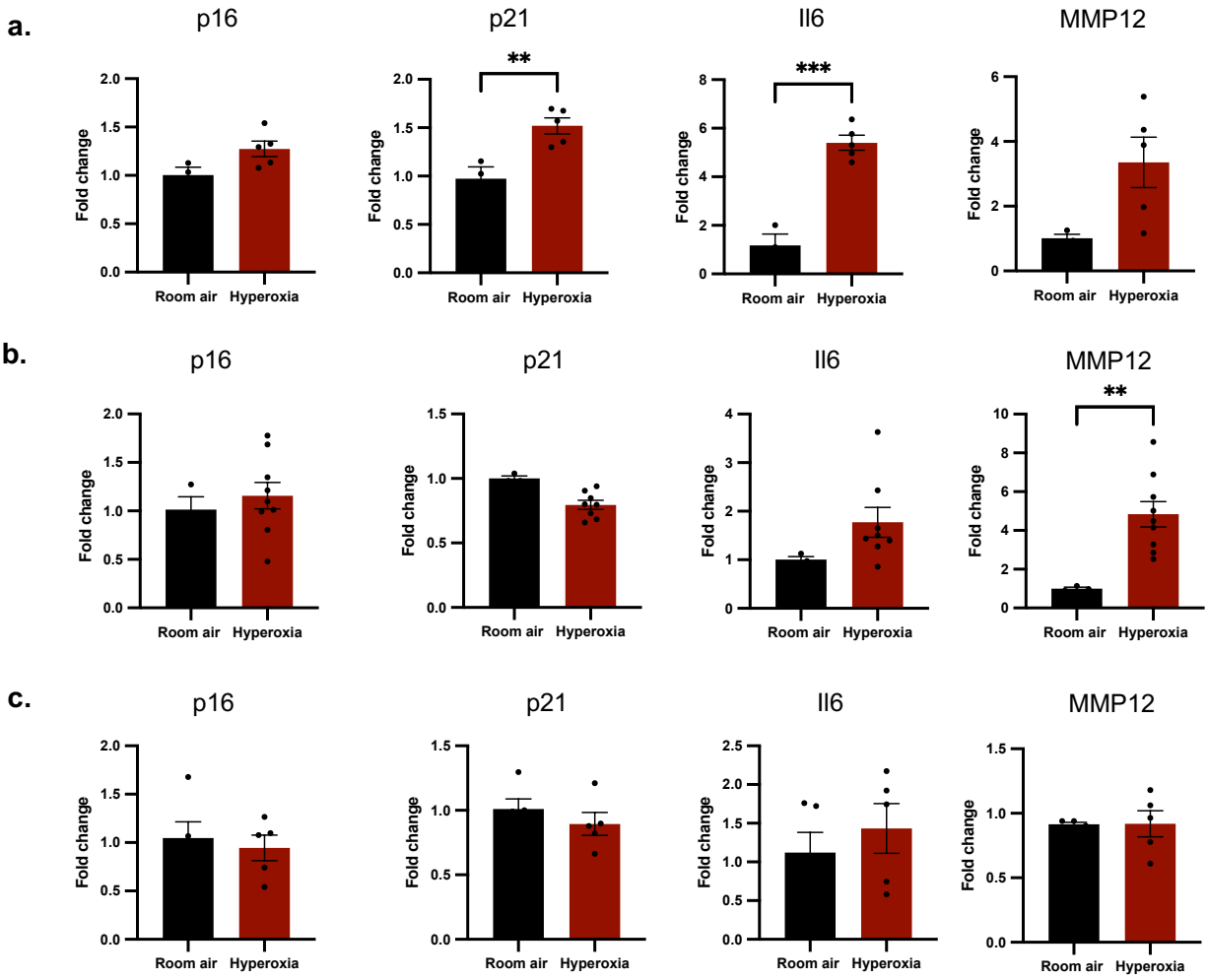

Fig 5. Expression of senescence markers are upregulated at PND14 in hyperoxia-exposed mice. Relative fold change in gene expression of senescence markers at PND14 **(A),** PND21 **(B),** and PND49 **(C)** as quantified from real-time QPCR analysis. Values are represented as mean ± SEM. P values were calculated using the student's t-test. Significant results are shown as *P ≤ 0.05, **P ≤ 0.01, ***P ≤ 0.001, and ****P ≤ 0.0001.

4.4 Luciferase is expressed only in the presence of doxycycline and its expression is localized to the lungs in mice.

Validation of the AAV-luciferase vectors was done both *in vitro* and *in vivo* to confirm the absence of any leak in expression. *In vitro* validation of the Tet-On system was done by measuring the luciferase activity in HEK293 cells transduced with the AAV-Tet and AAV-Luc vectors. Various combinations of the vectors were tested, and we observed that luciferase activity was significantly higher in cells transfected with the AAV-Tet and AAV-Luc vectors and treated with dox (fig 6a). The cells transduced with the vectors responded to a dosage of 1 µg/ml of doxycycline. *In vivo* validation was done by transducing B6 albino mice with the AAV-Tet and AAV-Luc vectors. To obtain localized expression in the lung, the AAV-Tet and AAV-Luc vectors were injected *i.t.* into B6 albino mice. The albino variant is preferred over dark mice as the black/brown pigmentation in the skin absorbs emitted signals and affects the quality of the signal. Using an In vivo imaging system (IVIS), we confirmed that the luciferase was expressed only in mice that received the AAV-Tet and AAV-Luc vectors followed by doxycycline administration for 2 days. The expression was mostly localized to the lungs and was detected as early as 2 days after the start of dox treatment (fig 6b).

Based on these data we conclude that the Tet-On vector system functions well and localized expression in the lung can be achieved by *i.t.* injections.

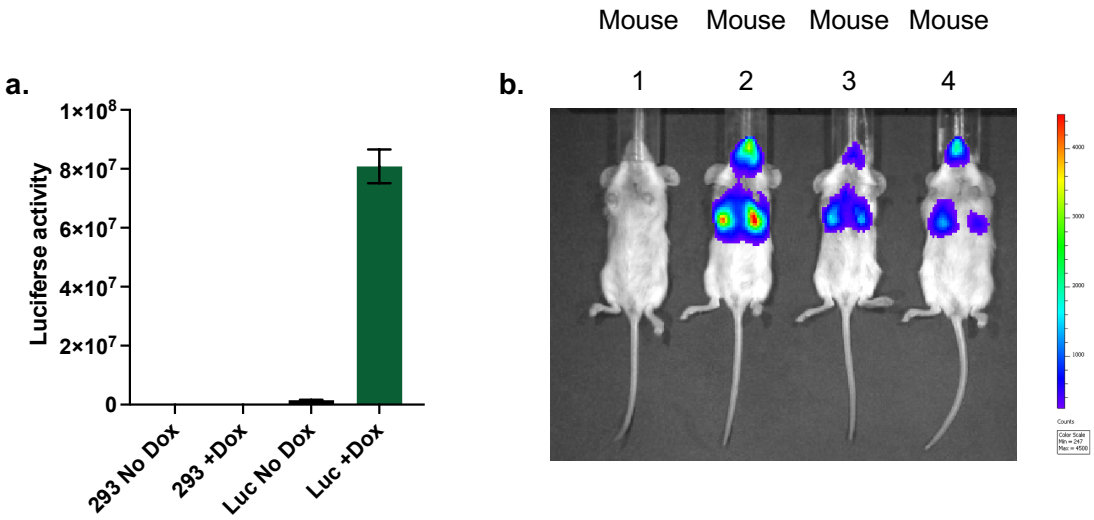

Fig 6. Doxycycline induces luciferase expression *in vitro*, and in mice, the expression is localized to the lungs. A) Expression of luciferase in HEK293 cells that were either transduced with or without AAV-Luc and AAV-Tet (at MOI of 10000) was determined by Promega luciferase activity kit. The treatments performed in triplicate wells. **B)** Bioluminescence detection with IVIS of mice either infected with 10^{11} vg of AAV-Luc and AAV-Tet (Mice 2, 3, and 4) or PBS (Mouse 1).

4.5 Oct4, Sox2, and Klf4 proteins are expressed in HEK293 cells and in the lungs of C57Bl/6 mice only in the presence of AAV-OSK vector and doxycycline.

Any leaky expression from the AAV-OSK vector would lead to deleterious effects. To confirm that AAV-OSK vectors do not results in leaky expression, we transduced HEK293 cells with the AAV-Tet and the AAV-OSK vectors in various combinations: AAV-Tet without dox, AAV-OSK without dox, AAV-Tet + AAV-OSK without dox, AAV-Tet with dox, AAV-OSK with dox and AAV-Tet + AAV-OSK with dox. Oct4 and Klf4 protein expression was seen only in cells that received both the vectors and dox (fig 7 a and b). All other conditions, including transduction with both vectors but without dox and each vector individually with dox did not induce expression of these proteins. As expected, Sox2 expression was seen in all these conditions since HEK293 cell line has endogenous expression of the Sox2 protein.

We then delivered 10^{11} vg of the AAV-Tet and AAV-OSK vectors to C57Bl/6 mice via *i.t.* injections. After 2 days on dox, the lungs were collected, and immunoblotting was performed to detect the expression of the OSK factors. We observed that Oct4 and Sox2 were expressed only in mice that received the AAV vectors and dox. We also observed that all mice expressed Klf4, but the expression was significantly higher in mice that received AAVs and dox. (Fig 7 c and d)

Consequently, we can confirm that the developed AAV-OSK vectors effectively transduce the cells in mouse lungs and express the transgenes only in the presence of dox.

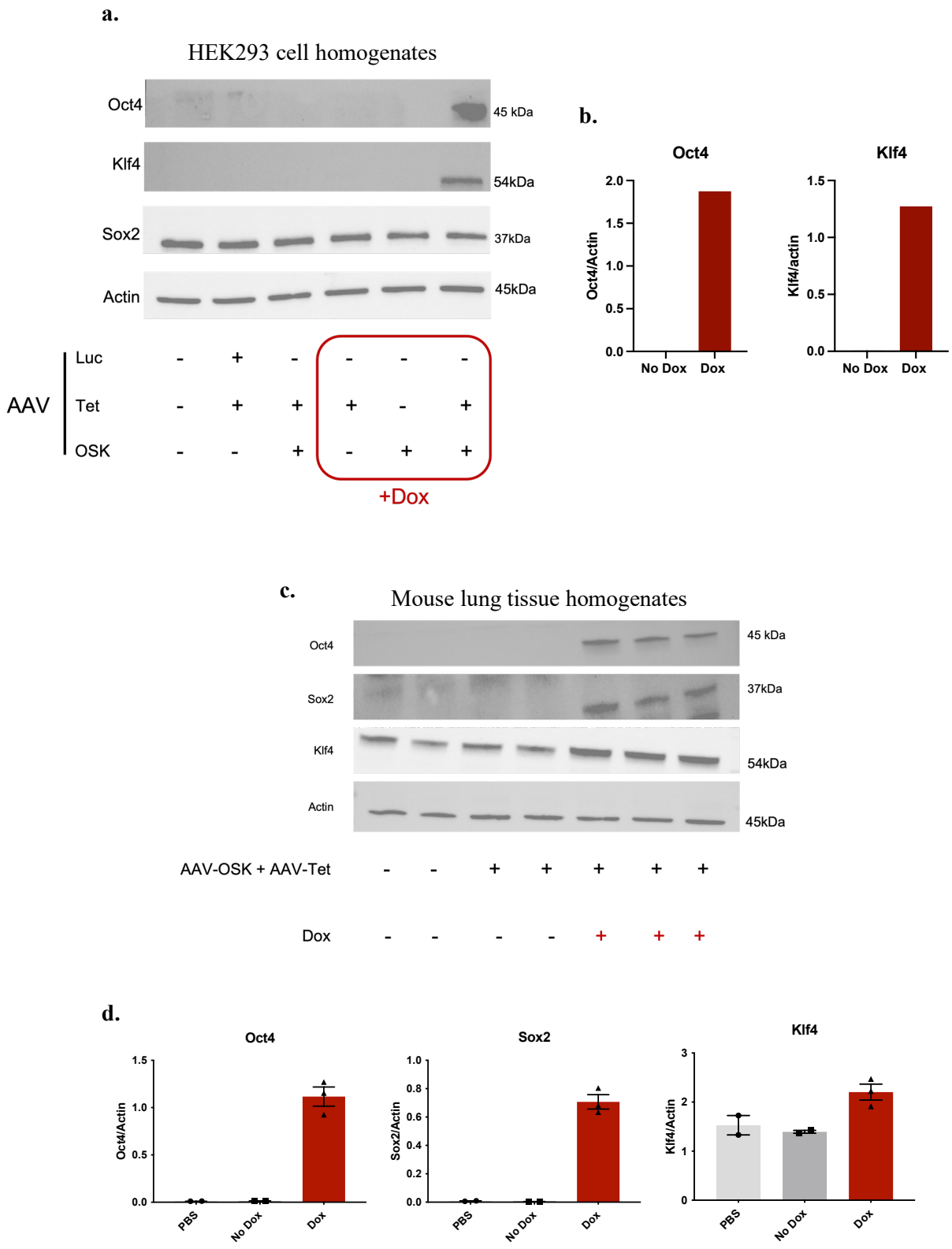
a.
HEK293 cell homogenates
Oct4
45 kDa
Klf4
54kDa
Sox2
37kDa
Actin
45kDa
AAV
Luc
Tet
OSK
+Dox
b.
Oct4
Klf4
Oct4/Actin
Klf4/actin
No Dox
Dox
c.
Mouse lung tissue homogenates
Oct4
45 kDa
Sox2
37kDa
Klf4
54kDa
Actin
45kDa
AAV-OSK + AAV-Tet
Dox
d.
Oct4
Sox2
Klf4
Oct4/Actin
Sox2/Actin
Klf4/Actin
PBS
No Dox
Dox

Fig 7. Oct4, Sox2, and Klf4 proteins are expressed in HEK293 cells and in the lungs of C57Bl/6 mice only in the presence of AAV-OSK vector and doxycycline. A) Protein levels of Oct4, Sox2, and Klf4 in HEK293 cell lysates that were either untouched or transduced with AAV-Tet or AAV-OSK or both vectors together and detected by immunoblotting. **B)** Quantification of the Oct4 and Klf4 protein levels from HEK293 cell lysates normalized to ß-Actin. **C)** Protein levels of Oct4, Sox2, and Klf4 in mouse lung tissue that were transduced with AAV-OSK and AAV-Tet detected by immunoblotting. **D)** Quantification of the Oct4, Sox2, and Klf4 protein levels from mouse lung normalized to ß-Actin. (PBS: n= 2; No dox: n=2; Dox: n=3) Values are represented as mean ± SEM. P values were calculated using the one-way ANOVA. Significant results are shown as *P ≤ 0.05, **P ≤ 0.01, ***P ≤ 0.001, and ****P ≤ 0.0001.

4.6 Transient expression of AAV system can be achieved with high accuracy.

Continuous expression of the OSK factors was previously shown to cause adverse effects in various organs in mice. This organ dysfunction arises because of the loss of normal cell function due to dedifferentiation and teratoma formation (Abad et al., 2013; Ohnishi et al., 2014). Short-term but cyclic OSKM induction (transient) was shown to prevent the loss of cellular identity and hence avoid any adverse effects of *in vivo* reprogramming (Ocampo et al., 2016). The control luciferase vector provides us with the perfect opportunity to test the capability of transient expression in mice longitudinally over the desired amount of time.

To test this, B6 albino mice were injected *i.t.* with the AAV-Tet and AAV-Luc vectors. Mice that received these vectors were subjected to three dox treatments: 1) no dox administration (the control group), 2) dox administration for 2 days only (P21 to P23) (activated once group), and 3) dox administration for 2 days followed by no dox for 5 days (which correspond to 1 cycle) for 4 cycles in total (the transiently activated group). IVIS imaging was performed on day 2, day 4, and day 7 of each cycle (fig 8a). As expected, after 2 days in the first cycle, no luciferase expression was observed in the control group, whereas high luciferase expression was observed in mice from the transiently activated and the activated once group (fig 7b). Upon dox withdrawal, in the transiently activated and the activated once group, a drastic decrease in the luciferase expression was observed at day 4, which was then back to baseline levels by the end of the cycle (fig 8b). The mice in the control group remained without any luciferase expression throughout the course of the experiment. In the subsequent cycles, luciferase expression was seen only in mice in the transiently activated group at day 2 which then went back to baseline levels by the end of each cycle (due to dox withdrawal). Quantification of the luciferase signal in radiance revealed that we could reach consistent levels of luciferase expression each week from mice lungs in the transiently activated

group (fig 8c). In another cohort of mice, long-term longitudinal tracking for over 150 days revealed that without dox administration, luciferase expression remained at low basal levels throughout the experimental timeline (fig 8d).

In summary, these experiments prove that transient expression is possible with the developed AAV system and there is no leaky expression from the vectors over extended periods of time.

a.

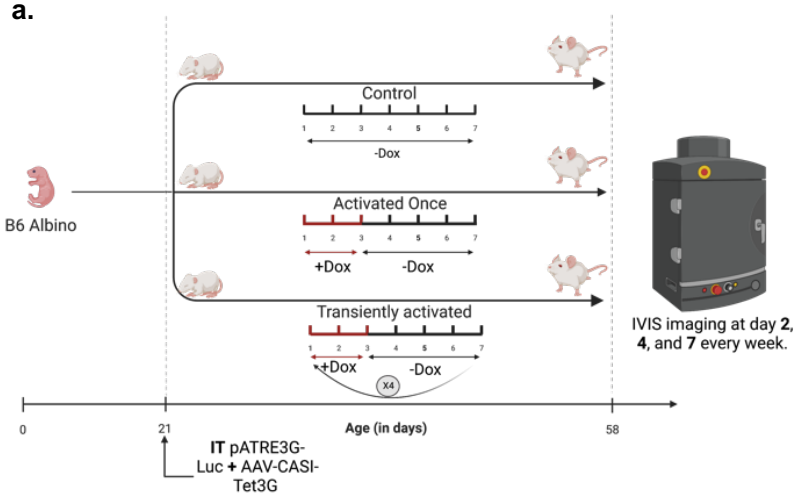
Control
-Dox
B6 Albino
Activated Once
+Dox
-Dox
Transiently activated
+Dox
-Dox
X4
IVIS imaging at day 2, 4, and 7 every week.
0
21
Age (in days)
58
IT pATRE3G-Luc + AAV-CASI-Tet3G

b.

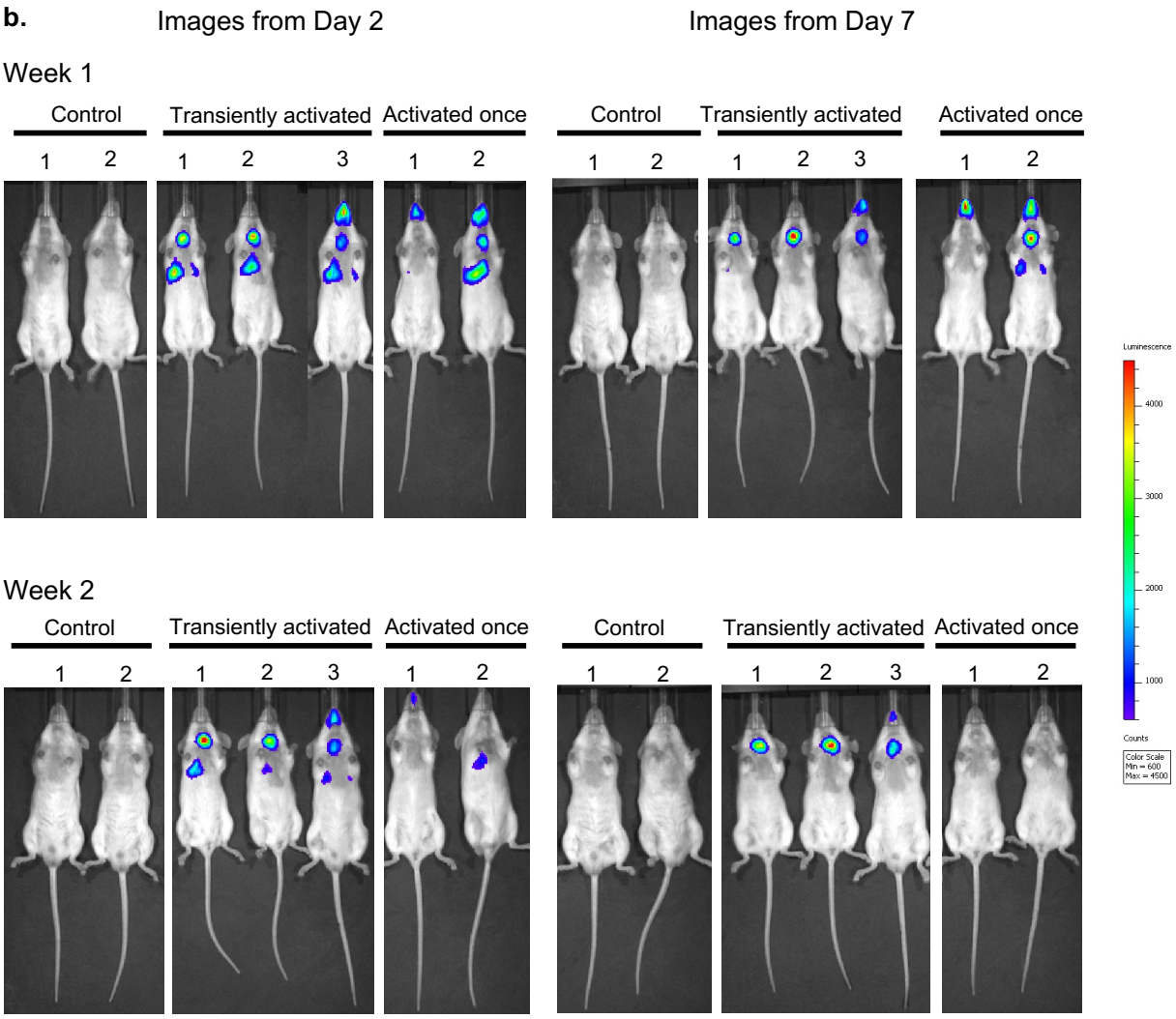
Images from Day 2
Images from Day 7
Week 1
Control
Transiently activated
Activated once
Control
Transiently activated
Activated once
Week 2
Control
Transiently activated
Activated once
Control
Transiently activated
Activated once
Luminescence
4000
3000
2000
1000
Counts
Color Scale
Min = 600
Max = 4500

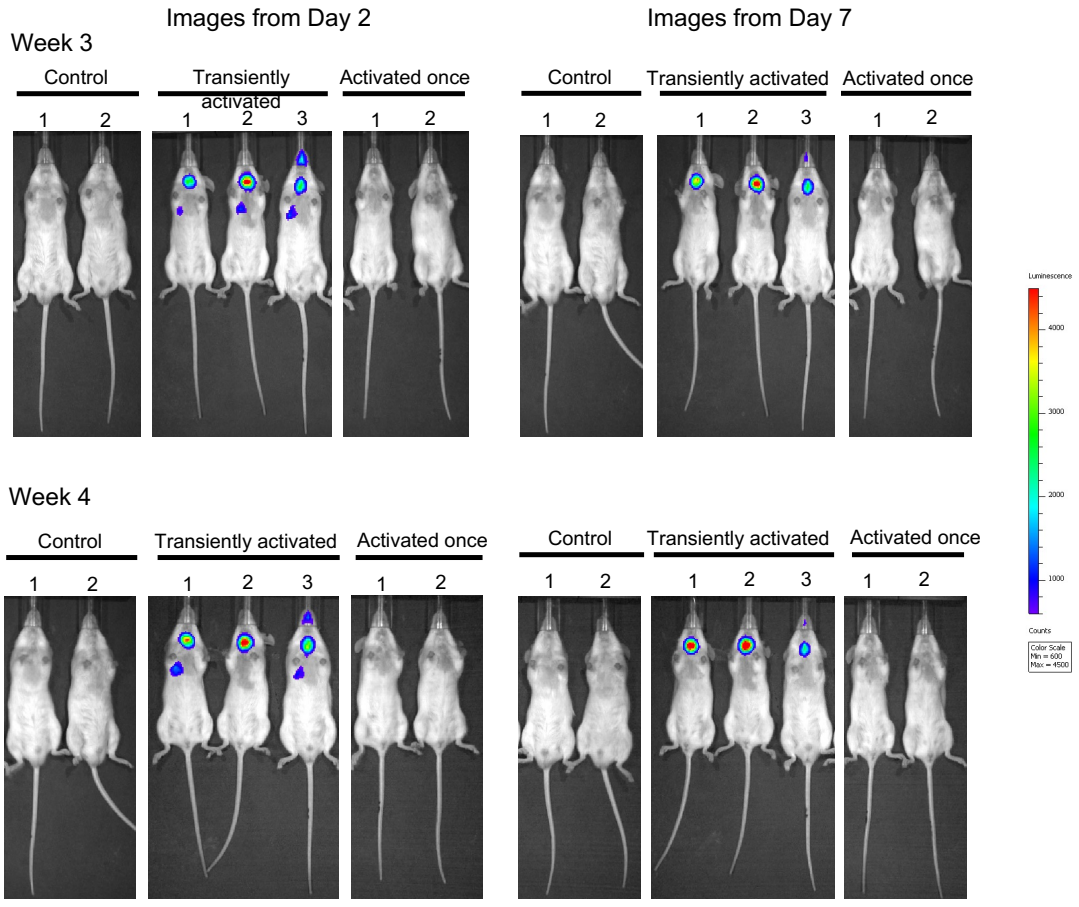
Images from Day 2
Images from Day 7
Week 3
Control
Transiently activated
Activated once
Control
Transiently activated
Activated once
1 2
1 2 3
1 2
1 2
1 2 3
1 2
Week 4
Control
Transiently activated
Activated once
Control
Transiently activated
Activated once
1 2
1 2 3
1 2
1 2
1 2 3
1 2
Luminescence
4000
3000
2000
1000
Counts
Color Scale
Min = 600
Max = 4500

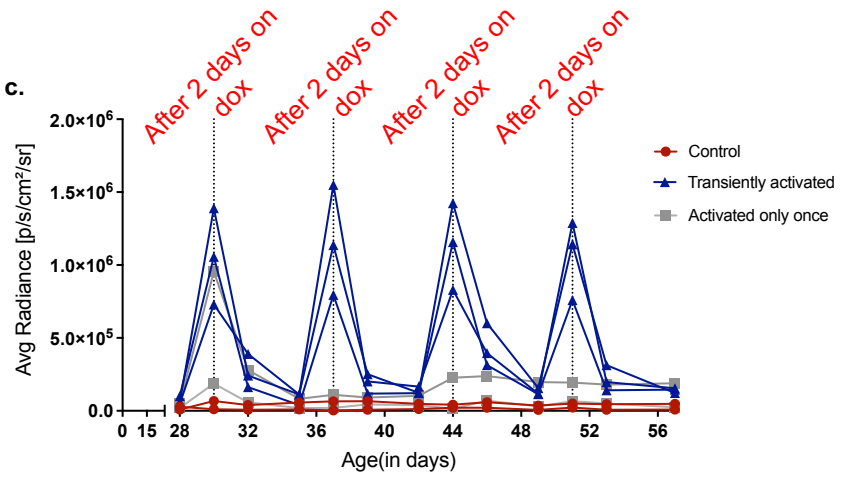
c.
After 2 days on dox
After 2 days on dox
After 2 days on dox
After 2 days on dox
Avg Radiance [p/s/cm²/sr]
2.0×10⁶
1.5×10⁶
1.0×10⁶
5.0×10⁵
0.0
0 15 28 32 36 40 44 48 52 56
Age(in days)
Control
Transiently activated
Activated only once

d.

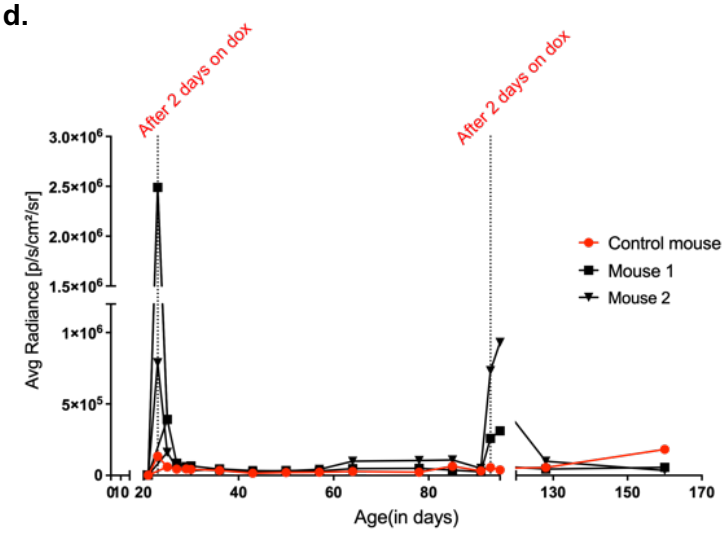

Fig 8. Transient expression of the developed AAV system can be achieved with high accuracy. A) Schematic representation of the *i.t.* injection, dox administration regimen, and IVIS imaging time points. **B)** Representative IVIS images of control mice (never administered with dox), transiently activated mice (dox administered for 2 days of each week) and activated once mice (Dox administered for 2 days only during the first week). Images are from day 2 and day 7 of each week during cyclic activation. IVIS images were normalized for a signal count ranging from 600 to 4500. **C)** Quantification of the signal (of mice from fig 7b) from the thorax (lung) region in control mice (in red), activated once (in grey), transiently activated mice (in blue). Data are represented as the mean radiance. **D)** Quantification of the IVIS images from the thorax (lung) region of mice injected *i.t.* with AAV-Luc and AAV-Tet vector that were either never administered with dox (Control: in red) or administered with dox on PND 21 and 91 (Mouse 1 and 2: in black). Data are represented as the mean radiance.

4.7 Transient overexpression of the OSK factors did not improve the lung structure and function after hyperoxia-induced injury.

Evidence suggests that BPD lungs lose their regenerative capacity and/or undergo premature aging resulting in emphysema and pulmonary vascular disease (Aukland et al., 2006; Meiners & Hilgendorff, 2016b; Wong et al., 2008). Cellular reprogramming can rejuvenate certain organs after an injury (Chen et al., 2021b; Cheng et al., 2022; Hishida et al., 2022a; Lu et al., 2020; Wang et al., 2021). Whether reprogramming the BPD lungs can improve lung structure and function is unknown. To answer this question, we used the 14-day hyperoxia exposure lung injury model in newborn mice as previously described. After 14 days of hyperoxia exposure, these mice receive 10^{11} vg of AAV-Tet and the AAV-OSK vectors through *i.t.* injections. The mice were given a week to recover after which transient activation of the OSK factors was performed for 4 weeks starting at PND21. Each cycle was composed of a period in which the OSK factors were activated (on dox), followed by a period of deactivation (off dox). Three durations of OSK activation per week were tested: 1) 2 days of OSK activation (short), 2) 3 days of OSK activation (medium), and 3) 4 days of OSK activation (long). Each of these OSK activation conditions was followed by 5, 4, or 3 days without OSK activation, respectively. FlexiVent analysis did not show any significant improvement in the PV loop of the 2, 3, or 4-day treated animals. However, the PV loop of the 3-day OSK-activated mice was improved compared to the untreated mice as well to the 2- and 4-day treated mice, but did not improve as much as the animals that were administered with just dox for 4 days per cycle and for 4 cycles (dox ctrl) (fig 9 a). Lung function parameters including the inspiratory capacity, residual volume, compliance, and elastance followed a similar trend (fig 9 b). Two- and 4-days OSK treated animals did not show any improvement in lung function, but although not significant, 3-day treated mice showed improvement in these parameters

when compared to the untreated control animals (fig 9b). Lung structure analysis also revealed a similar trend. There was no significant improvement in the lung structure in the 2, 3, or 4 day treated group (fig 9c). Similar to the lung function data, mice in the 3-day treated group had better lung structure as observed from MLI analysis (fig 9d).

In summary, 2, 3, or 4 days of OSK activation for 4 cycles did not improve lung function or structure.

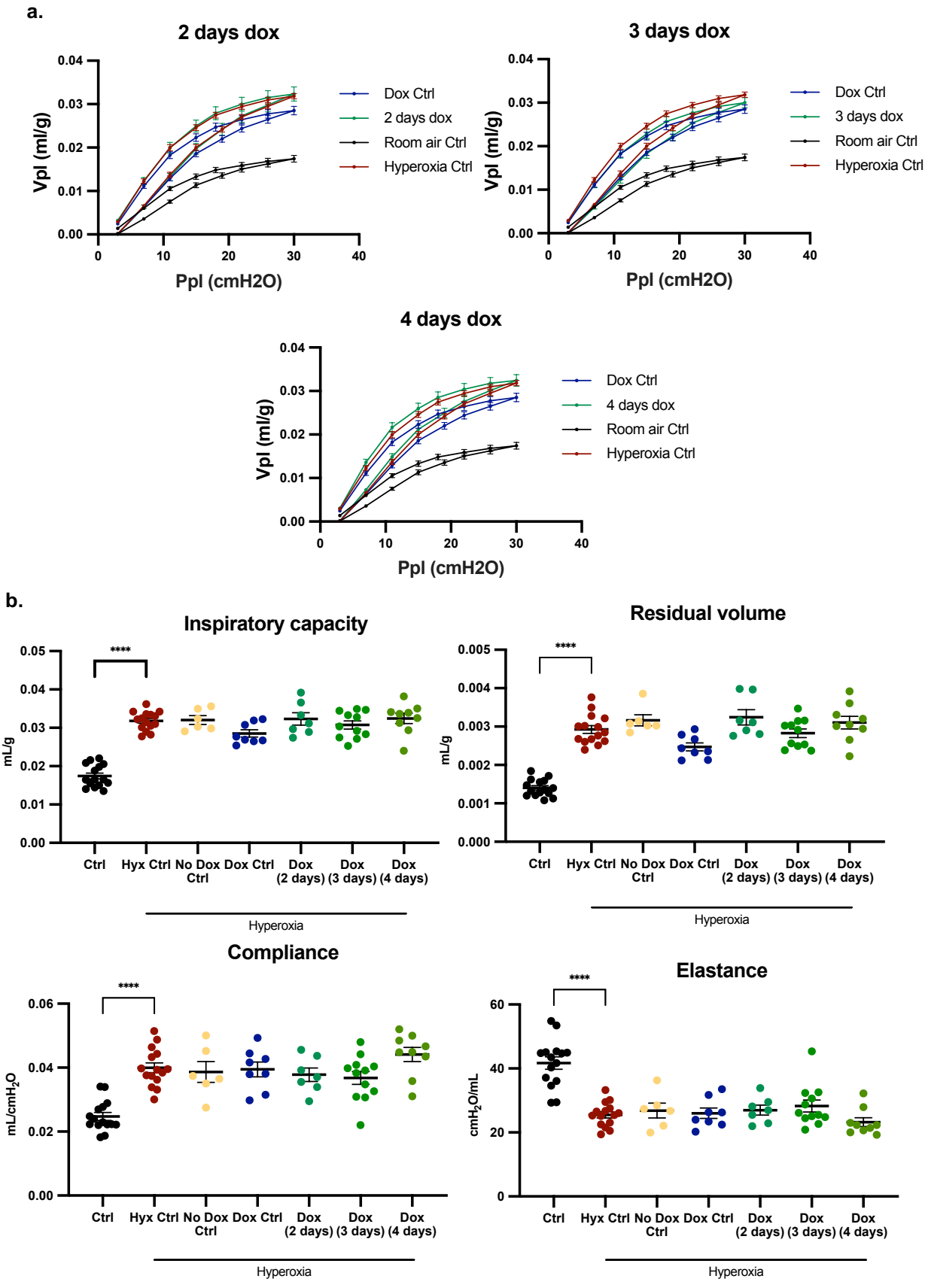
a.
2 days dox
Vpl (ml/g)
Ppl (cmH2O)
Dox Ctrl
2 days dox
Room air Ctrl
Hyperoxia Ctrl
3 days dox
3 days dox
4 days dox
4 days dox
b.
Inspiratory capacity
mL/g
****
Residual volume
Compliance
mL/cmH2O
Elastance
cmH2O/mL
Ctrl
Hyx Ctrl
No Dox Ctrl
Dox Ctrl
Dox (2 days)
Dox (3 days)
Dox (4 days)
Hyperoxia

c.

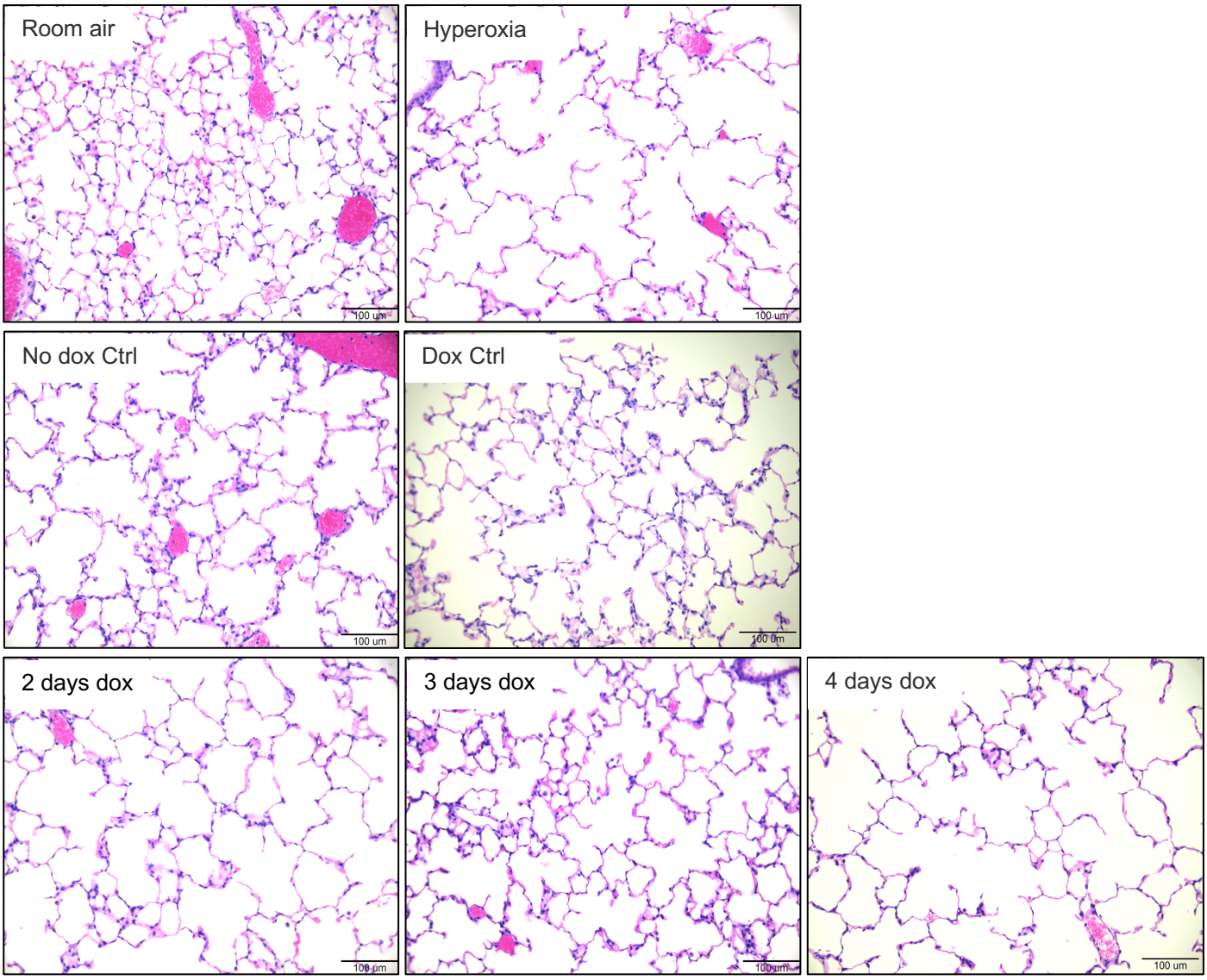
Room air
Hyperoxia
No dox Ctrl
Dox Ctrl
2 days dox
3 days dox
4 days dox
100 um

d.

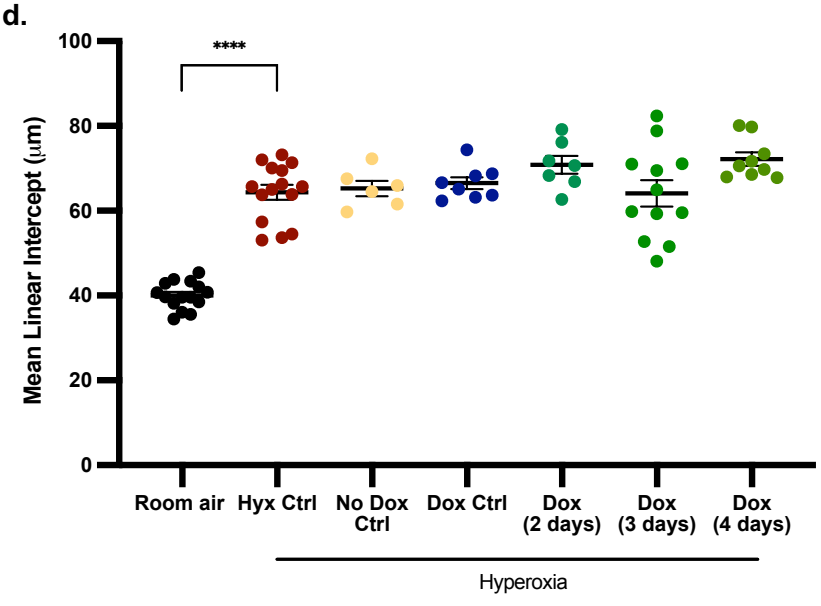
Mean Linear Intercept (μm)
100
80
60
40
20
0
****
Room air
Hyx Ctrl
No Dox Ctrl
Dox Ctrl
Dox (2 days)
Dox (3 days)
Dox (4 days)
Hyperoxia

Fig 9. Transient overexpression of the OSK factors did not improve the lung structure and function after hyperoxia-induced injury. A) Body weight adjusted PV-loops. PV-loops are shown as mean volumes of all mice in one group at each set pressure level. (Room air: n= 15; Hyperoxia: n=15; No dox ctrl: n= 6; Dox ctrl: n= 8; 2 days dox: n= 7; 3 days dox; n= 13; 4 days dox: n=9) **B)** Respiratory mechanics parameters extracted from PV-loop comparing controls vs treated groups. (Room air: n= 15; Hyperoxia: n=15; No dox ctrl: n= 6; Dox ctrl: n= 8; 2 days dox: n= 7; 3 days dox; n= 13; 4 days dox: n=9) **D)** Representative images of left lung histology stained with H&E from control and treated mice. **E)** Graph comparing the MLI of control mice vs treated mice. (Room air: n= 15; Hyperoxia: n=15; No dox ctrl: n= 6; Dox ctrl: n= 8; 2 days dox: n= 7; 3 days dox; n= 13; 4 days dox: n=9). Values are represented as mean ± SEM. P values were calculated using the two-way ANOVA with Tukey's multiple comparisons test for PV-loop and one-way ANOVA for the rest. Significant results are shown as *$P \leq 0.05$, **$P \leq 0.01$, ***$P \leq 0.001$, and ****$P \leq 0.0001$.

4.8 14-day hyperoxia exposure in neonatal i4f-b induces an arrest in lung development phenotype and doxycycline administration triggers expression of the OSK factors in the lungs.

Another strategy that we employed to test whether or not transient overexpression of the OSKM factors can rejuvenate hyperoxia-induced injury includes the use of i4f-b mice. I4f-b transgenic mice line developed by Dr. Manuel Serrano's group contained transcriptional activator (rtTA) within the Rosa26 locus and the Oct4, Sox2, Klf4, and cMyc factors in the form of a polycistronic cassette which is dox inducible (Abad et al., 2013). Continuous exposure to hyperoxia starting at PND0 for 14 days resulted in the arrested lung development phenotype similar to what we observe in wild type C57bl/ 6 mice exposed to hyperoxia. PV loops generated using the FlexiVent machine in 49-day-old mice showed an upward shift representing an emphysematous phenotype in the hyperoxia-exposed animals. (Fig 10a) The respiratory parameter profile also had a similar trend as with the hyperoxia exposed wild type C57Bl/6 mice. We observed a significant increase in the inspiratory capacity and residual volume. A significant increase in compliance and a significant decrease in elastance were also observed which further confirmed an emphysematous profile (Fig 10 b). We also observed larger and fewer alveoli in the hyperoxia-exposed mice compared to control mice as seen in the representative H&E-stained lung section images (Fig 10 c). This was confirmed from MLI analysis as we observed a significant increase in the MLI of hyperoxia exposed mice when compared to room air controls (Fig 10 d).

The expression of the OSK factors in the lungs of young i4f-b mice has never been characterized. As our rejuvenation strategy entails transient expression for 4 cycles, we studied the expression of the OSK factors using immunoblotting during the course of the 4 cycles starting at PND21 until PND49. We compared the levels of protein expression at every cycle between

hyperoxia-exposed animals that either received dox or never received dox, and room air control animals that either received dox or never received dox. We observed expression of the OSK factors was detected only in mice that received dox in both the normoxia and hyperoxia-exposed mice (Fig 10 e). Four cycles of transient OSK expression did not result in any adverse effects as the histological examination of the lungs showed no teratoma formation.

To sum up, i4f-b mice acquire the same lung damage phenotype as wild type mice when exposed to neonatal hyperoxia and 4 weeks of transient OSK overexpression starting PND21 is possible without being harmful.

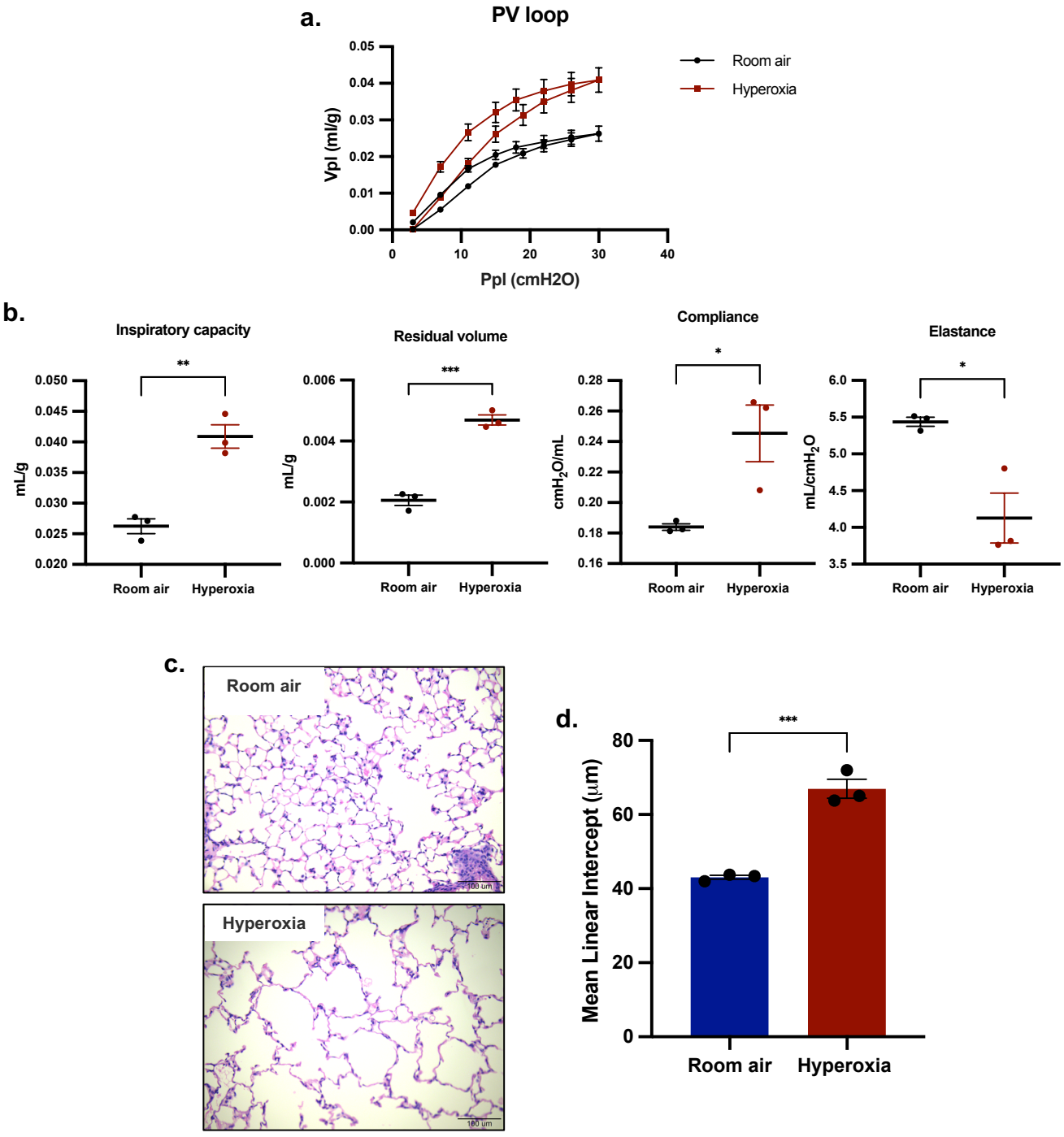
a.
PV loop
Vpl (ml/g)
Ppl (cmH2O)
Room air
Hyperoxia
b.
Inspiratory capacity
mL/g
Residual volume
mL/g
Compliance
cmH2O/mL
Elastance
mL/cmH2O
Room air
Hyperoxia
c.
Room air
Hyperoxia
d.
Mean Linear Intercept (μm)
Room air
Hyperoxia

e.

Week 1 (PND21 to PND28)

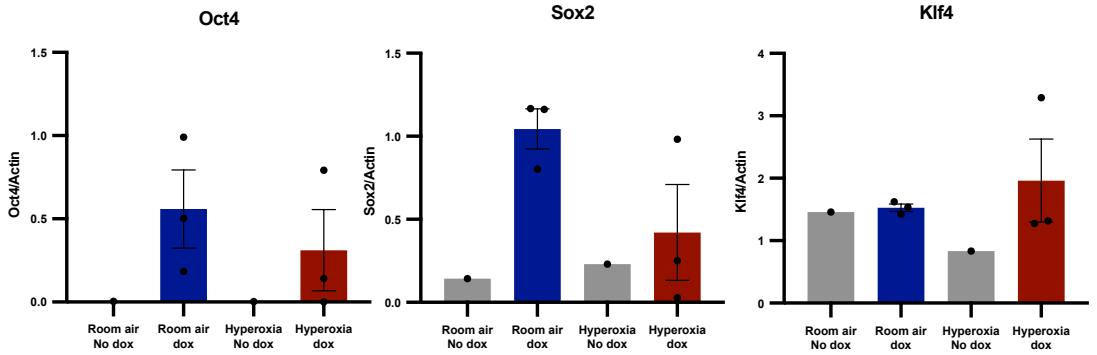

Week 2 (PND28 to PND35)

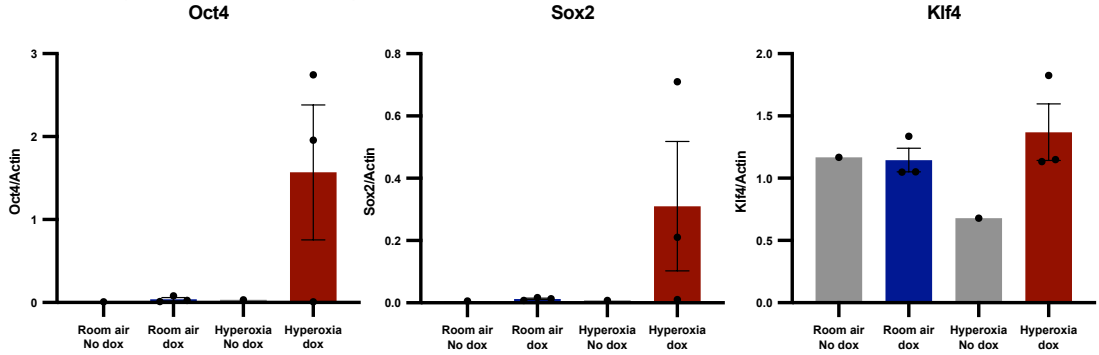

Week 3 (PND35 to PND42)

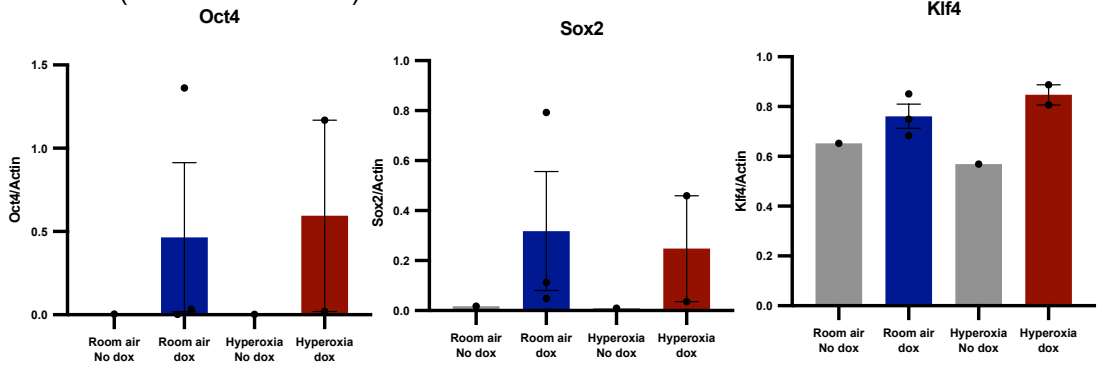

Week 4 (PND42 to PND49)

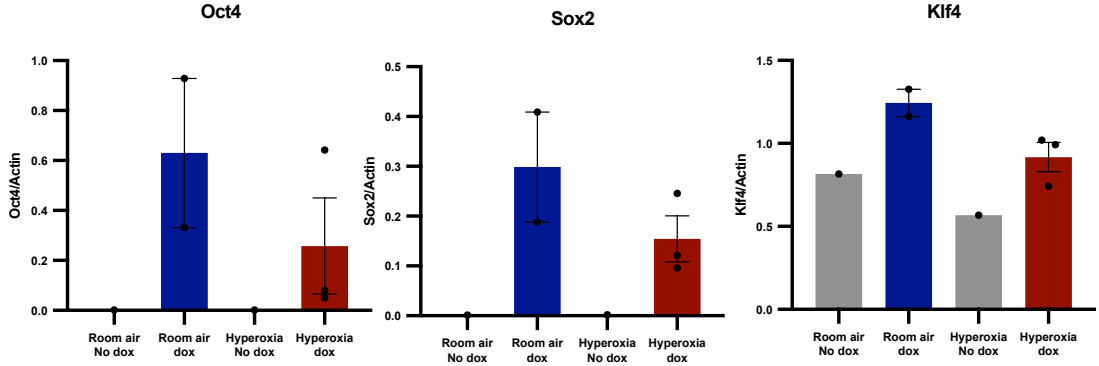

Fig 10. 14-day hyperoxia exposure in neonatal i4f-b induces an arrest in lung development phenotype and doxycycline administration triggers expression of the OSK factors in the lungs. **A)** Body weight adjusted PV-loop at PND49. PV-loops are shown as mean volumes of all mice in one group at each set pressure level. (Room air: n= 3; Hyperoxia: n=3) **B)** Respiratory mechanics parameters extracted from PV-loop comparing room air mice vs hyperoxia exposed mice. (Room air: n= 3; Hyperoxia: n=3) **C)** Representative images of left lung histology stained with H&E from room air and hyperoxia exposed animals. **D)** Graph comparing the MLI of room air control mice vs hyperoxia exposed mice. (Room air: n= 3; Hyperoxia: n=3) **E)** Quantification of the Oct4, Sox2, and Klf4 protein levels from i4f-b mouse lung from conditions: Room air without dox; Room air with 2 days dox administration; Hyperoxia exposed mice without dox administration; Hyperoxia exposed mice with 2 days dox administration. Oct4, Sox2, and Klf4 protein expression was normalized to ß-Actin. Values are represented as mean ± SEM. P values were calculated using the student's t-test except in PV loop where two-way ANOVA with Tukey's multiple comparisons test was used. Significant results are shown as *$P \leq 0.05$, **$P \leq 0.01$, ***$P \leq 0.001$, and ****$P \leq 0.0001$.

4.9 Transient expression of OSKM factors for 4 cycles in the i4f-b mice does not improve lung function after hyperoxia induced lung injury.

From our previous experiments, we have already shown that 1 mg/ml dox for a period of 2 days induced OSKM expression in the lungs and 4 cycles of OSKM activation was safe, we proceeded to test if 4 weeks of OSKM cyclical induction had any effect in rejuvenating the lung after hyperoxia induced injury. Newborn pups were exposed to 85% hyperoxia for 14 days. Cyclical OSKM induction was started at PND 21. Each cycle consisted of OSKM induction for 2 days followed by a 5-day recovery period.

After 4 weeks of OSKM induction, lung function analysis was performed. We observed no improvement in the PV-loop of mice that underwent cyclical OSKM induction (fig 11 a). Lung function parameters such as inspiratory capacity, residual volume, compliance, and elastance of the partially reprogrammed mice also did not show any improvement when compared to untreated controls (fig 11 b).

In summary, 2 days of OSKM activation for 4 cycles in i4f-b mice did not improve lung function after an injury.

a.

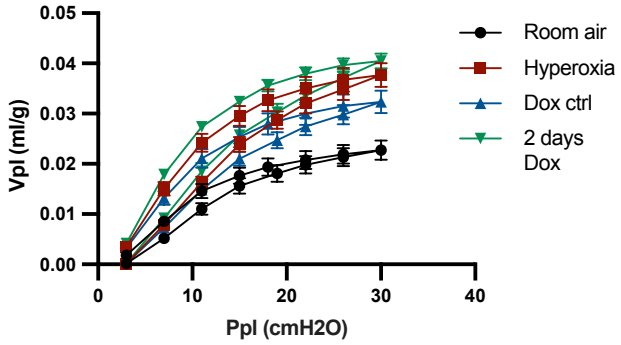
PV loop
Vpl (ml/g)
Ppl (cmH2O)
Room air
Hyperoxia
Dox ctrl
2 days Dox

b.

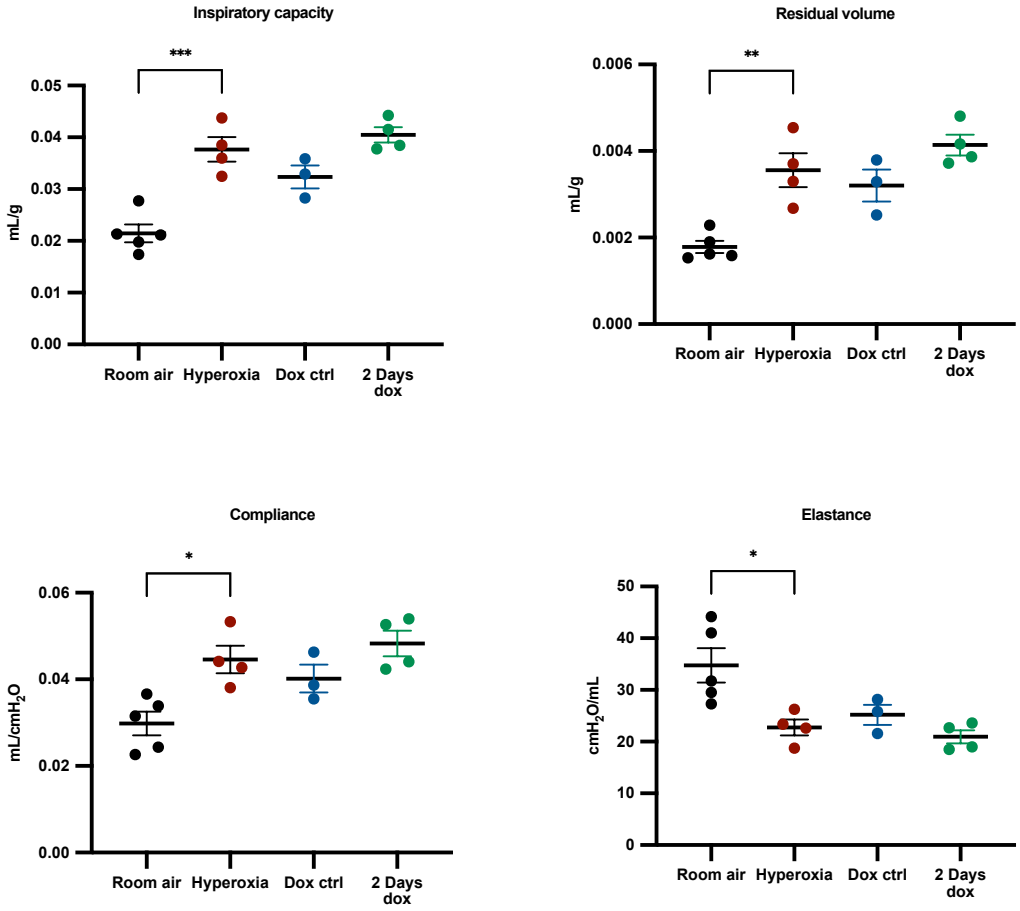
Inspiratory capacity
mL/g
Residual volume
mL/g
Compliance
mL/cmH2O
Elastance
cmH2O/mL
Room air
Hyperoxia
Dox ctrl
2 Days dox

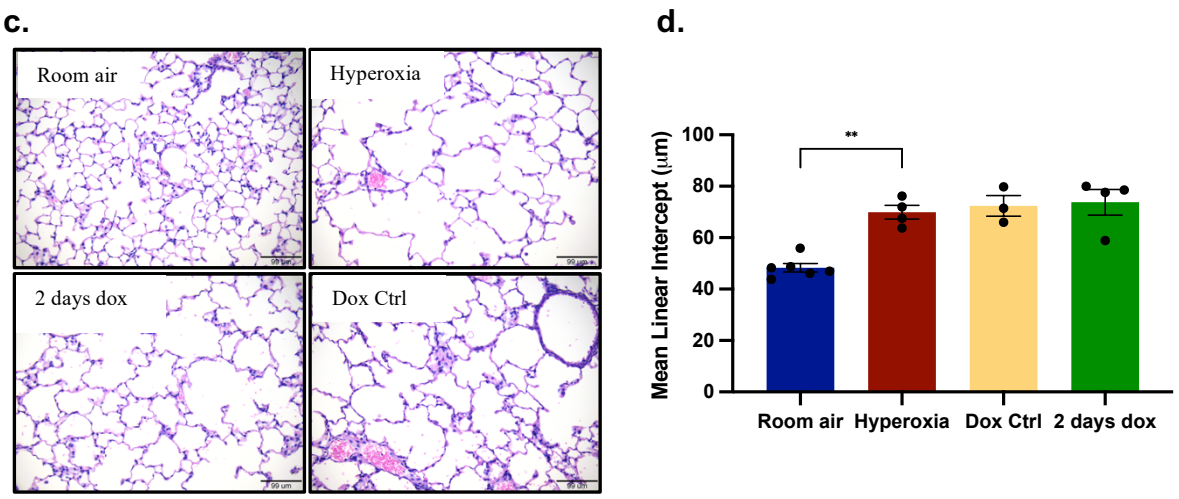

Fig 11. Transient expression of OSKM factors for 4 cycles in the i4f-b mice does not improve lung function after hyperoxia induced lung injury.

A) Body weight adjusted PV-loop at PND49. PV-loops are shown as mean volumes of all mice in one group at each set pressure level. (Room air: n= 5; Hyperoxia: n= 4; Dox Ctrl: n= 3; 2 Days dox: n= 4) **B)** Respiratory mechanics parameters extracted from PV-loop comparing room air mice vs hyperoxia exposed mice (Room air: n= 5; Hyperoxia: n= 4; Dox Ctrl: n= 3; 2 Days dox: n= 4). Values are represented as mean ± SEM. P values were calculated using the two-way ANOVA with Tukey's multiple comparisons test was used for the PV-loop and one-way ANOVA with multiple comparisons for respiratory parameters. **C)** Representative images of left lung histology stained with H&E from control and treated mice. **D)** Graph comparing the MLI of control mice vs treated mice. (Room air: n= 5; Hyperoxia: n= 4; Dox Ctrl: n= 3; 2 Days dox: n= 4). P values were calculated using the two-way ANOVA with Tukey's multiple comparisons test for PV-loop and one-way ANOVA for the rest. Significant results are shown as *P ≤ 0.05, **P ≤ 0.01, ***P ≤ 0.001, and ****P ≤ 0.0001.

5. Discussion and future directions

5.1 Discussion

In this body of work, we have shown that: (1) Neonatal exposure to hyperoxia induces a lasting lung injury similar to seen in BPD patients with signs of senescence in the lungs of hyperoxia exposed mice. (2) We have developed an inducible AAV vector system that is dox inducible with high sensitivity and capability to target type II alveolar epithelial cells. (3) Transient over expression of the OSK (with the AAV vectors) or OSKM (using the reprogrammable i4f-b mouse line) factors did not improve either lung function or structure under tested conditions.

Despite the advancement in neonatal care over the past years, the rate of BPD incidence has not decreased. More importantly, BPD-associated morbidities remain past childhood and even later in life resulting in a significant economic burden to health services. Currently, there is no treatment for BPD. As partial reprogramming was previously shown to regenerate injured tissues in the liver, heart, muscle, and the eye, it would be interesting to investigate the impact of partial reprogramming in regenerating the growth arrested BPD lung. For this, we used a hyperoxia-induced lung injury model in neonatal mice. Continuous exposure to 85% oxygen resulted in a phenotype that closely resembled the characteristics of human BPD. The lungs had significantly larger and fewer alveoli with compromised lung function. Very little catch-up growth was observed in our model. The alveolar stage of lung development in mice occurs postnatally up until early adulthood (PND36). Lung function and lung structure analysis at seven weeks of age confirmed that neonatal hyperoxia exposure (from PND0 to PND14) completely disrupts lung organogenesis without any signs of catch-up growth.

Accelerated aging in former preterm infants with BPD has been speculated to be the reason for arrested development as a result of mechanical ventilation and oxygen toxicity. In this study,

we show that 14 days of hyperoxia exposure gives rise to increased expression of established markers of senescence such as p21 and p16, and SASP factors including IL6 and MMP12. The increase in p21 expression suggests initiation of senescence in the lungs of hyperoxia-exposed mice. Moreover, in a recently published study, using single-cell transcriptomic analysis of the mouse lungs, our lab has previously shown that the increase in p21 expression due to hyperoxia exposure is specific to Col13a1^{+} fibroblasts, myofibroblasts and capillary cells (Hurskainen et al., 2021). In-depth analyses taking into account more timepoints (PND4, PND8, PND14, PND 21, and PND49) and an extended panel of markers are required to better understand the role of senescence in the BPD lung.

In brief, we generated a neonatal hyperoxia mouse model that closely resembles a BPD-like phenotype with an indication of initiation of senescence due to hyperoxia exposure which is a good injury model to study the therapeutic effects of partial reprogramming in the lungs.

Partial reprogramming *in vivo* can be induced by transient overexpression of the OSK or the OSKM factors. Proof of concept studies in the field of *in vivo* partial reprogramming have come either by using transgenic reprogrammable mice (Abad et al., 2013; Chen et al., 2021b; Hishida et al., 2022a) or by AAV mediated reprogramming (Lu et al., 2020). Our AAV mediated transient reprogramming approach made use of the AAV6.2FF capsid. Recently published work from our lab has shown that the AAV6.2FF vector has a high affinity in targeting alveolar type II cells among other cell types in the lungs (Kang et al., 2020). This is a key factor as alveolar type II cell (a progenitor cell population in the alveolar epithelium) injury due to hyperoxia exposure is one of the root causes of persistent epithelial injury in BPD (Roper et al., 2004).

With the developed AAV vector system, our first focus was to validate the tight control nature of the Tet-On promoter *in vitro* and *in vivo*. This is of high importance as long-term or

uncontrolled reprogramming can give rise to teratomas (Abad et al., 2013; Ohnishi et al., 2014). In our set-up, we observed a very tight control of transgene expression (with dox) in cells and in mice transfected with the AAVs. Also, with *i.t.* route of administration, the expression of transgenes was localized to the lungs which allow for site-specific reprogramming.

Formation of dysplastic lesions and teratomas is the most deleterious obstacle to reprogramming (Abad et al., 2013; Ohnishi et al., 2014) but this can be overcome by the process of transient reprogramming. (Ocampo et al., 2016) To address this issue, we used *in vivo* bioluminescent tracking to study the expression pattern of AAV vector system. By taking advantage of the AAV-luciferase construct, we have shown that transient expression can be achieved efficiently hence reducing the risk of tumor formation.

The specificity of the AAV6.2ff vector system and *i.t.* route of administration enables us to induce targeted reprogramming in the epithelial cell population of the lungs.

Site-specific reprogramming (Lu et al., 2020) and cell-type-specific partial reprogramming *in vivo* (Chen et al., 2021b; Hishida et al., 2022a) have been shown to have immense potential to rejuvenate an organ both structurally and functionally after an injury. Cells that undergo reprogramming were seen to go back to a younger state (in their developmental hierarchy). The induced youthful nature improves their proliferation capabilities which were otherwise absent in injured tissues. In the case of BPD lungs, partially reprogramming the developmentally arrested cells in the lungs can be exploited to reinstate the process of alveolarization. Moreover, the capability to specifically reprogram the alveolar type II cells to re-trigger their lost progenitor function might improve the chances of forming new alveoli. Reprogramming to rejuvenate tissues in the lungs has not been reported so far. We used a reprogramming approach that was described to be safe (without teratoma formation) and well-established in mice. This strategy was previously

shown to ameliorate aging hallmarks (Ocampo et al., 2016; Rodríguez-Matellán et al., 2020), improve muscle regeneration (Wang et al., 2021), and reverse intervertebral disc degeneration (Cheng et al., 2022). Our partial reprogramming approach consisted of cyclic activation of the OSK factors for 4 cycles. Although none of our OSK activation schemes showed significant improvement in either lung function or lung structure, the 3-day per week OSK-activated mouse fared better than other conditions. Further assessment of the optimal duration of the OSK factors is required to induce lung reprogramming is required to induce lung regeneration and is discussed briefly in the future directions section. No teratomas were noted in the current set-up during gross necroscopic analysis.

Another approach that we employed to test if partial reprogramming can regenerate hyperoxia-induced lung damage was the with the use of a reprogrammable transgenic mouse line (i4f-b). As the effects of neonatal hyperoxia exposure in this mouse line were unknown, we first characterized the model. A lung injury model similar to the wild-type mouse was observed at the lung function and lung structure level hence making it a good model to study the effects of partial reprogramming to regenerate the lungs. I4f-b mice have been used to study the effects of reprogramming in various tissues (Abad et al., 2013; Chiche et al., 2020; Mosteiro et al., 2016) but effects of reprogramming in young mice have never been described in previously published literature. In our study, we show that there were no deleterious effects from starting cyclical reprogramming as early as 3 weeks of age. As expected, only the dox-administered mice had the expression of the OSKM factors, and 4 cycles of transient expression did not result in the mortality of any mice. Four cycles of OSKM transient expression in the i4f-b mice after hyperoxia exposure also did not show any improvement in lung function although only one OSKM activation scheme (2 days on dox followed by 5 days off dox) was tested.

The major differences in the expression pattern of the Yamanaka factors between the i4f-b mice and the AAV mediated approach are: i) AAVs express only Oct4, Sox2, and Klf4 while all four factors (Oct4, Sox2, Klf4, and c-Myc) can be expressed in the i4f-b mice, ii) more specific expression of the OSK factors majorly in the type II cells can be achieved using the AAV approach, whereas tissue wide expression of the OSKM factors occurs in the i4f-b mice and iii) when administered with dox, OSKM activation is seen in all mice tissues, whereas with the AAV approach, OSK expression is localized to the lungs. These differences make these two approaches quite distinct from each other and the end result in terms of reprogramming might be very different. Nevertheless, both approaches, under the conditions tested, failed to provide any therapeutic effects in terms of lung function and structure improvement.

5.2 Future directions

The extent of reprogramming occurring after a period of OSKM activation is of high importance as it determines the extent of the therapeutic response. Different organs and tissues respond to partial reprogramming through different mechanisms hence making it difficult to determine the optimal period of OSK/OSKM activation required to induce a therapeutic effect in the lungs. One common phenomenon as a result of partial reprogramming is the increased proliferation and this can be targeted along with the detection of early markers of reprogramming such as SSEA-4. These experiments could help determine the number of cells that are being reprogrammed (SSEA-4^{+} cells) after OSK/OSKM activation and the amount of proliferation induced at the end of each cycle as a result of reprogramming. Addressing this aspect can help to better design an appropriate cyclic reprogramming strategy required to efficiently regenerate injured lungs.

The timing of initiation of rejuvenation could also be delayed to achieve efficient reprogramming in the lungs. All the published literature in the field of *in vivo* reprogramming thus far have been with adult or aged mice. Likewise, the length of the reprogramming periods to promote proliferation is equally important to avoid potential harmful rather than therapeutic effects of this approach. Delaying the start of reprogramming is possible with our model as there is no evidence of catch-up growth.

Following the establishment of the optimal reprogramming strategy of the lungs (enough to see a therapeutic effect in improving the lung function and structure after hyperoxia-induced injury), in-depth transcriptomic (using single-cell RNA sequencing) and epigenetic (ChIP and methylation sequencing with NGS) analysis could be done to discover the mechanism behind the above-mentioned rejuvenation strategy.

Another area for exploration would be to partially reprogram resident progenitor and stem cells *in vitro* and transplant them back into the lungs of injured mice. Reprogrammed AEC II cells have better clonogenic capacity and were previously shown to improve lung structure and function after bleomycin-induced injury (Guo et al., 2018). It would be interesting to know the effect of reprogrammed or "replenished" AEC II, and other resident lung progenitor cells including mesenchymal or endothelial cells in improving lung function and structure in hyperoxia-induced lung injury model. The i4f-b mice that we currently have in the lab are an excellent source of these cells as no external vectors carrying the OSKM factors will be required to induce reprogramming.

6. Conclusion

This thesis explores *in vivo* partial reprogramming as a new approach to rejuvenate BPD, the most common and severe complication of preterm birth. Here we made use of two strategies to induce reprogramming in a robust experimental neonatal lung injury model: i) Exogenous overexpression of the OSK factors using a lung tropic AAV. ii) Inducible OSKM overexpression in a transgenic mouse line. Alveolar regrowth if achieved will significantly improve the efficiency of gas exchange and improve the overall health of the mouse. We showed feasibility of this approach. The transient OSK and OSKM activation schemes tested here did not regenerate lungs after an injury.

We are currently working on a determining the optimal OSK/OSKM activation scheme which is safe and effective in regenerating lung alveolarization.

7. References

Abad, M., Mosteiro, L., Pantoja, C., Cañamero, M., Rayon, T., Ors, I., Graña, O., Megías, D., Domínguez, O., Martínez, D., Manzanares, M., Ortega, S., & Serrano, M. (2013). Reprogramming in vivo produces teratomas and iPS cells with totipotency features. *Nature*, *502*(7471), 340–345. https://doi.org/10.1038/nature12586

Abman, S. H. (2012). Bronchopulmonary Dysplasia. *Https://Doi.Org/10.1164/Ajrccm.164.10.2109111c*, *164*(10 I), 1755–1756. https://doi.org/10.1164/AJRCCM.164.10.2109111C

Amsellem, V., Gary-Bobo, G., Marcos, E., Maitre, B., Chaar, V., Validire, P., Stern, J. B., Noureddine, H., Sapin, E., Rideau, D., Hue, S., le Corvoisier, P., le Gouvello, S., Dubois-Randé, J. L., Boczkowski, J., & Adnot, S. (2012). Telomere Dysfunction Causes Sustained Inflammation in Chronic Obstructive Pulmonary Disease. *Https://Doi.Org/10.1164/Rccm.201105-0802OC*, *184*(12), 1358–1366. https://doi.org/10.1164/RCCM.201105-0802OC

Aukland, S. M., Halvorsen, T., Fosse, K. R., Daltveit, A. K., & Rosendahl, K. (2006). High-resolution CT of the chest in children and young adults who were born prematurely: findings in a population-based study. *AJR. American Journal of Roentgenology*, *187*(4), 1012–1018. https://doi.org/10.2214/AJR.05.0383

Baker, C. D., Abman, S. H., & Mourani, P. M. (2014). Pulmonary Hypertension in Preterm Infants with Bronchopulmonary Dysplasia. *Pediatric Allergy, Immunology, and Pulmonology*, *27*(1), 8–16. https://doi.org/10.1089/PED.2013.0323

Baker, D. J., Wijshake, T., Tchkonia, T., Lebrasseur, N. K., Childs, B. G., van de Sluis, B., Kirkland, J. L., & van Deursen, J. M. (2011). Clearance of p16Ink4a-positive senescent cells delays ageing-associated disorders. *Nature*, *479*(7372), 232–236. https://doi.org/10.1038/NATURE10600

Barker, G. F., Manzo, N. D., Cotich, K. L., Shone, R. K., & Waxman, A. B. (2006). DNA Damage Induced by Hyperoxia. *American Journal of Respiratory Cell and Molecular Biology*, *35*(3), 277–288. https://doi.org/10.1165/rcmb.2005-0340OC

Bertoli, C., Skotheim, J. M., & de Bruin, R. A. M. (2013). Control of cell cycle transcription during G1 and S phases. *Nature Reviews Molecular Cell Biology*, *14*(8), 518–528. https://doi.org/10.1038/nrm3629

Browder, K. C., Reddy, P., Yamamoto, M., Haghani, A., Guillen, I. G., Sahu, S., Wang, C., Luque, Y., Prieto, J., Shi, L., Shojima, K., Hishida, T., Lai, Z., Li, Q., Choudhury, F. K., Wong, W. R., Liang, Y., Sangaraju, D., Sandoval, W., … Izpisua Belmonte, J. C. (2022). In vivo partial reprogramming alters age-associated molecular changes during physiological aging in mice. *Nature Aging 2022 2:3*, *2*(3), 243–253. https://doi.org/10.1038/s43587-022-00183-2

Brown, L. M., Rannels, S. R., & Rannels, D. E. (2001). Implications of post-pneumonectomy compensatory lung growth in pulmonary physiology and disease. *Respiratory Research*, *2*(6), 340. https://doi.org/10.1186/RR84

Chang, J., Wang, Y., Shao, L., Laberge, R. M., Demaria, M., Campisi, J., Janakiraman, K., Sharpless, N. E., Ding, S., Feng, W., Luo, Y., Wang, X., Aykin-Burns, N., Krager, K., Ponnappan, U., Hauer-Jensen, M., Meng, A., & Zhou, D. (2016). Clearance of senescent cells

by ABT263 rejuvenates aged hematopoietic stem cells in mice. *Nature Medicine*, *22*(1), 78. https://doi.org/10.1038/NM.4010

Chen, Y., Lüttmann, F. F., Schoger, E., Schöler, H. R., Zelarayán, L. C., Kim, K. P., Haigh, J. J., Kim, J., & Braun, T. (2021a). Reversible reprogramming of cardiomyocytes to a fetal state drives heart regeneration in mice. *Science*, *373*(6562), 1537–1540. https://doi.org/10.1126/science.abg5159

Chen, Y., Lüttmann, F. F., Schoger, E., Schöler, H. R., Zelarayán, L. C., Kim, K. P., Haigh, J. J., Kim, J., & Braun, T. (2021b). Reversible reprogramming of cardiomyocytes to a fetal state drives heart regeneration in mice. *Science*, *373*(6562), 1537–1540. https://doi.org/10.1126/SCIENCE.ABG5159/SUPPL_FILE/SCIENCE.ABG5159_MOVIES_S1_TO_S8.ZIP

Cheng, F., Wang, C., Ji, Y., Yang, B., Shu, J., Shi, K., Wang, L., Wang, S., Zhang, Y., Huang, X., Zhou, X., Xia, K., Liang, C., Chen, Q., & Li, F. (2022). Partial reprogramming strategy for intervertebral disc rejuvenation by activating energy switch. *Aging Cell*, *21*(4), e13577. https://doi.org/10.1111/ACEL.13577

Chiche, A., Chen, C., & Li, H. (2020). The crosstalk between cellular reprogramming and senescence in aging and regeneration. *Exp Gerontol*, *138*, 111005. https://doi.org/10.1016/j.exger.2020.111005

Chiche, A., le Roux, I., von Joest, M., Sakai, H., Aguín, S. B., Cazin, C., Salam, R., Fiette, L., Alegria, O., Flamant, P., Tajbakhsh, S., & Li, H. (2017). Injury-Induced Senescence Enables In Vivo Reprogramming in Skeletal Muscle. *Cell Stem Cell*, *20*(3), 407-414.e4. https://doi.org/10.1016/j.stem.2016.11.020

Coalson, J. J. (2006). Pathology of Bronchopulmonary Dysplasia. *Seminars in Perinatology*, *30*(4), 179–184. https://doi.org/10.1053/J.SEMPERI.2006.05.004

Conboy, I. M., Conboy, M. J., Wagers, A. J., Girma, E. R., Weismann, I. L., & Rando, T. A. (2005). Rejuvenation of aged progenitor cells by exposure to a young systemic environment. *Nature*, *433*(7027), 760–764. https://doi.org/10.1038/NATURE03260

Dasgupta, C., Sakurai, R., Wang, Y., Guo, P., Ambalavanan, N., Torday, J. S., & Rehan, V. K. (2009). Hyperoxia-induced neonatal rat lung injury involves activation of TGF-{beta} and Wnt signaling and is protected by rosiglitazone. *American Journal of Physiology. Lung Cellular and Molecular Physiology*, *296*(6). https://doi.org/10.1152/AJPLUNG.90392.2008

Davis, R. L., Weintraub, H., & Lassar, A. B. (1987). Expression of a single transfected cDNA converts fibroblasts to myoblasts. *Cell*, *51*(6), 987–1000. https://doi.org/10.1016/0092-8674(87)90585-X

Doeser, M. C., Schöler, H. R., & Wu, G. (2018). Reduction of Fibrosis and Scar Formation by Partial Reprogramming In Vivo. *Stem Cells*, *36*(8), 1216–1225. https://doi.org/10.1002/STEM.2842

Doyle, L. W., Carse, E., Adams, A.-M., Ranganathan, S., Opie, G., & Cheong, J. L. Y. (2017). Ventilation in Extremely Preterm Infants and Respiratory Function at 8 Years. *The New England Journal of Medicine*, *377*(4), 329–337. https://doi.org/10.1056/NEJMOA1700827

Doyle, L. W., Faber, B., Callanan, C., Freezer, N., Ford, G. W., & Davis, N. M. (2006). Bronchopulmonary Dysplasia in Very Low Birth Weight Subjects and Lung Function in Late Adolescence. *Pediatrics*, *118*(1), 108–113. https://doi.org/10.1542/PEDS.2005-2522

Evans, M. J., & Kaufman, M. H. (1981). Establishment in culture of pluripotential cells from mouse embryos. *Nature*, *292*(5819), 154–156. https://doi.org/10.1038/292154a0

Fawke, J., Lum, S., Kirkby, J., Hennessy, E., Marlow, N., Rowell, V., Thomas, S., & Stocks, J. (2010). Lung Function and Respiratory Symptoms at 11 Years in Children Born Extremely Preterm: The EPICure Study. *American Journal of Respiratory and Critical Care Medicine*, *182*(2), 237. https://doi.org/10.1164/RCCM.200912-1806OC

Ghaedi, M., Calle, E. A., Mendez, J. J., Gard, A. L., Balestrini, J., Booth, A., Bove, P. F., Gui, L., White, E. S., & Niklason, L. E. (2013). Human iPS cellâ€"derived alveolar epithelium repopulates lung extracellular matrix. *Journal of Clinical Investigation*, *123*(11), 4950–4962. https://doi.org/10.1172/JCI68793

Gill, D., Parry, A., Santos, F., Okkenhaug, H., Todd, C. D., Hernando-Herraez, I., Stubbs, T. M., Milagre, I., & Reik, W. (2022). Multi-omic rejuvenation of human cells by maturation phase transient reprogramming. *ELife*, *11*. https://doi.org/10.7554/ELIFE.71624

Guo, L., Karoubi, G., Duchesneau, P., Aoki, F. G., Shutova, M. v., Rogers, I., Nagy, A., & Waddell, T. K. (2018). Interrupted reprogramming of alveolar type II cells induces progenitor-like cells that ameliorate pulmonary fibrosis. *Npj Regenerative Medicine*, *3*(1), 14. https://doi.org/10.1038/s41536-018-0052-5

Gurdon, J. B. (1962). *The developmental capacity of nuclei taken from intestinal epithelium cells of feeding tadpoles*. https://journals.biologists.com/dev/article-abstract/10/4/622/35650

Gurdon, J., Nature, V. U.-, & 1966, undefined. (n.d.). "Fertile" intestine nuclei. *Nature.Com*. Retrieved February 5, 2023, from https://www.nature.com/articles/2101240a0

Hishida, T., Yamamoto, M., Hishida-Nozaki, Y., Shao, C., Huang, L., Wang, C., Shojima, K., Xue, Y., Hang, Y., Shokhirev, M., Memczak, S., Sahu, S. K., Hatanaka, F., Ros, R. R., Maxwell, M. B., Chavez, J., Shao, Y., Liao, H. K., Martinez-Redondo, P., … Izpisua Belmonte, J. C. (2022a). In vivo partial cellular reprogramming enhances liver plasticity and regeneration. *Cell Reports*, *39*(4). https://doi.org/10.1016/J.CELREP.2022.110730

Hishida, T., Yamamoto, M., Hishida-Nozaki, Y., Shao, C., Huang, L., Wang, C., Shojima, K., Xue, Y., Hang, Y., Shokhirev, M., Memczak, S., Sahu, S. K., Hatanaka, F., Ros, R. R., Maxwell, M. B., Chavez, J., Shao, Y., Liao, H.-K., Martinez-Redondo, P., … Izpisua Belmonte, J. C. (2022b). In vivo partial cellular reprogramming enhances liver plasticity and regeneration. *Cell Reports*, *39*(4), 110730. https://doi.org/https://doi.org/10.1016/j.celrep.2022.110730

Hurskainen, M., Mižíková, I., Cook, D. P., Andersson, N., Cyr-Depauw, C., Lesage, F., Helle, E., Renesme, L., Jankov, R. P., Heikinheimo, M., Vanderhyden, B. C., & Thébaud, B. (2021a). Single cell transcriptomic analysis of murine lung development on hyperoxia-induced damage. *Nat Commun*, *12*(1), 1565. https://doi.org/10.1038/s41467-021-21865-2

Hurskainen, M., Mižíková, I., Cook, D. P., Andersson, N., Cyr-Depauw, C., Lesage, F., Helle, E., Renesme, L., Jankov, R. P., Heikinheimo, M., Vanderhyden, B. C., & Thébaud, B. (2021b). Single cell transcriptomic analysis of murine lung development on hyperoxia-induced damage. *Nature Communications*, *12*(1), 1565. https://doi.org/10.1038/s41467-021-21865-2

Jensen, E. A., & Schmidt, B. (2014). Epidemiology of Bronchopulmonary Dysplasia. *Birth Defects Research. Part A, Clinical and Molecular Teratology*, *100*(3), 145. https://doi.org/10.1002/BDRA.23235

JOBE, A. H., & BANCALARI, E. (2001). Bronchopulmonary Dysplasia. *American Journal of Respiratory and Critical Care Medicine*, *163*(7), 1723–1729. https://doi.org/10.1164/ajrccm.163.7.2011060

Jobe, A. J. (1999). The new BPD: an arrest of lung development. *Pediatric Research*, *46*(6), 641–643. https://doi.org/10.1203/00006450-199912000-00007

Justice, J. N., Nambiar, A. M., Tchkonia, T., LeBrasseur, N. K., Pascual, R., Hashmi, S. K., Prata, L., Masternak, M. M., Kritchevsky, S. B., Musi, N., & Kirkland, J. L. (2019). Senolytics in idiopathic pulmonary fibrosis: Results from a first-in-human, open-label, pilot study. *EBioMedicine*, *40*, 554–563. https://doi.org/10.1016/j.ebiom.2018.12.052

Kang, M. H., van Lieshout, L. P., Xu, L., Domm, J. M., Vadivel, A., Renesme, L., Mühlfeld, C., Hurskainen, M., Mižíková, I., Pei, Y., van Vloten, J. P., Thomas, S. P., Milazzo, C., Cyr-Depauw, C., Whitsett, J. A., Nogee, L. M., Wootton, S. K., & Thébaud, B. (2020). A lung tropic AAV vector improves survival in a mouse model of surfactant B deficiency. *Nat Commun*, *11*(1), 3929. https://doi.org/10.1038/s41467-020-17577-8

Kotecha, S. J., Edwards, M. O., Watkins, W. J., Henderson, A. J., Paranjothy, S., Dunstan, F. D., & Kotecha, S. (2013). Effect of preterm birth on later FEV1: a systematic review and meta-analysis. *Thorax*, *68*(8), 760–766. https://doi.org/10.1136/THORAXJNL-2012-203079

Kotton, D. N., & Morrisey, E. E. (2014). Lung regeneration: mechanisms, applications and emerging stem cell populations. *Nature Medicine*, *20*(8), 822. https://doi.org/10.1038/NM.3642

Lecarpentier, Y., Schussler, O., Hébert, J. L., & Vallée, A. (2019). Multiple Targets of the Canonical WNT/β-Catenin Signaling in Cancers. *Frontiers in Oncology*, *9*, 1248. https://doi.org/10.3389/FONC.2019.01248

Lehmann, M., Hu, Q., Hu, Y., Hafner, K., Costa, R., van den Berg, A., & Königshoff, M. (2020). Chronic WNT/β-catenin signaling induces cellular senescence in lung epithelial cells. *Cellular Signalling*, *70*, 109588. https://doi.org/10.1016/J.CELLSIG.2020.109588

Londhe, V. A., Sundar, I. K., Lopez, B., Maisonet, T. M., Yu, Y., Aghai, Z. H., & Rahman, I. (2011). Hyperoxia impairs alveolar formation and induces senescence through decreased histone deacetylase activity and up-regulation of p21 in neonatal mouse lung. *Pediatr Res*, *69*(5 Pt 1), 371–377. https://doi.org/10.1203/PDR.0b013e318211c917

López-Otín, C., Blasco, M. A., Partridge, L., Serrano, M., & Kroemer, G. (2013). The Hallmarks of Aging. *Cell*, *153*(6), 1194–1217. https://doi.org/10.1016/j.cell.2013.05.039

Lu, Y., Brommer, B., Tian, X., Krishnan, A., Meer, M., Wang, C., Vera, D. L., Zeng, Q., Yu, D., Bonkowski, M. S., Yang, J. H., Zhou, S., Hoffmann, E. M., Karg, M. M., Schultz, M. B., Kane, A. E., Davidsohn, N., Korobkina, E., Chwalek, K., … Sinclair, D. A. (2020). Reprogramming to recover youthful epigenetic information and restore vision. *Nature*, *588*(7836), 124–129. https://doi.org/10.1038/s41586-020-2975-4

Lum, S., Kirkby, J., Welsh, L., Marlow, N., Hennessy, E., & Stocks, J. (2011). Nature and severity of lung function abnormalities in extremely pre-term children at 11 years of age. *European Respiratory Journal*, *37*(5), 1199–1207. https://doi.org/10.1183/09031936.00071110

Mahmoudi, S., Xu, L., & Brunet, A. (2019). Turning back time with emerging rejuvenation strategies. *Nature Cell Biology*, *21*(1), 32. https://doi.org/10.1038/S41556-018-0206-0

Martin, G. R. (1981). Isolation of a pluripotent cell line from early mouse embryos cultured in medium conditioned by teratocarcinoma stem cells. *Proceedings of the National Academy of Sciences*, *78*(12), 7634–7638. https://doi.org/10.1073/pnas.78.12.7634

McGrath, S. A. (1998). Induction of p21WAF/CIP1 during hyperoxia. *Am J Respir Cell Mol Biol*, *18*(2), 179–187. https://doi.org/10.1165/ajrcmb.18.2.2964m

Meiners, S., & Hilgendorff, A. (2016a). Early injury of the neonatal lung contributes to premature lung aging: a hypothesis. *Mol Cell Pediatr*, *3*(1), 24. https://doi.org/10.1186/s40348-016-0052-8

Meiners, S., & Hilgendorff, A. (2016b). Early injury of the neonatal lung contributes to premature lung aging: a hypothesis. *Molecular and Cellular Pediatrics*, *3*(1), 24. https://doi.org/10.1186/s40348-016-0052-8

Mosteiro, L., Pantoja, C., Alcazar, N., Marión, R. M., Chondronasiou, D., Rovira, M., Fernandez-Marcos, P. J., Muñoz-Martin, M., Blanco-Aparicio, C., Pastor, J., Gómez-López, G., de Martino, A., Blasco, M. A., Abad, M., & Serrano, M. (2016). Tissue damage and senescence provide critical signals for cellular reprogramming in vivo. *Science*, *354*(6315). https://doi.org/10.1126/science.aaf4445

Mosteiro, L., Pantoja, C., de Martino, A., & Serrano, M. (2018). Senescence promotes in vivo reprogramming through p16(INK)(4a) and IL-6. *Aging Cell*, *17*(2). https://doi.org/10.1111/acel.12711

Mourani, P. M., & Abman, S. H. (2013). Pulmonary vascular disease in bronchopulmonary dysplasia: pulmonary hypertension and beyond. *Current Opinion in Pediatrics*, *25*(3), 329–337. https://doi.org/10.1097/MOP.0B013E328360A3F6

Mourani, P. M., & Abman, S. H. (2015). Pulmonary Hypertension and Vascular Abnormalities in Bronchopulmonary Dysplasia. *Clinics in Perinatology*, *42*(4), 839. https://doi.org/10.1016/J.CLP.2015.08.010

Narayanan, M., Beardsmore, C. S., Owers-Bradley, J., Dogaru, C. M., Mada, M., Ball, I., Garipov, R. R., Kuehni, C. E., Spycher, B. D., & Silverman, M. (2013). Catch-up alveolarization in ex-preterm children: Evidence from 3He magnetic resonance. *American Journal of Respiratory and Critical Care Medicine*, *187*(10), 1104–1109. https://doi.org/10.1164/RCCM.201210-1850OC/SUPPL_FILE/DISCLOSURES.PDF

Northway Jr., W. H., Rosan, R. C., & Porter, D. Y. (1967). Pulmonary disease following respirator therapy of hyaline-membrane disease. Bronchopulmonary dysplasia. *N Engl J Med*, *276*(7), 357–368. https://doi.org/10.1056/nejm196702162760701

Ocampo, A., Reddy, P., Martinez-Redondo, P., Platero-Luengo, A., Hatanaka, F., Hishida, T., Li, M., Lam, D., Kurita, M., Beyret, E., Araoka, T., Vazquez-Ferrer, E., Donoso, D., Roman, J. L., Xu, J., Rodriguez Esteban, C., Nuñez, G., Nuñez Delicado, E., Campistol, J. M., … Izpisua Belmonte, J. C. (2016). In Vivo Amelioration of Age-Associated Hallmarks by Partial Reprogramming. *Cell*, *167*(7), 1719-1733.e12. https://doi.org/10.1016/j.cell.2016.11.052

Ohnishi, K., Semi, K., Yamamoto, T., Shimizu, M., Tanaka, A., Mitsunaga, K., Okita, K., Osafune, K., Arioka, Y., Maeda, T., Soejima, H., Moriwaki, H., Yamanaka, S., Woltjen, K., & Yamada, Y. (2014). Premature termination of reprogramming in vivo leads to cancer development through altered epigenetic regulation. *Cell*, *156*(4), 663–677. https://doi.org/10.1016/j.cell.2014.01.005

O'Reilly, M. A. (2001). DNA damage and cell cycle checkpoints in hyperoxic lung injury: braking to facilitate repair. *American Journal of Physiology-Lung Cellular and Molecular Physiology*, *281*(2), L291–L305. https://doi.org/10.1152/ajplung.2001.281.2.L291

Pierro, M., Ionescu, L., Montemurro, T., Vadivel, A., Weissmann, G., Oudit, G., Emery, D., Bodiga, S., Eaton, F., Péault, B., Mosca, F., Lazzari, L., & Thébaud, B. (2013). Short-term, long-term and paracrine effect of human umbilical cord-derived stem cells in lung injury prevention and repair in experimental bronchopulmonary dysplasia. *Thorax*, *68*(5), 475–484. https://doi.org/10.1136/thoraxjnl-2012-202323

Qian, L., Huang, Y., Spencer, C. I., Foley, A., Vedantham, V., Liu, L., Conway, S. J., Fu, J., & Srivastava, D. (2012). In vivo reprogramming of murine cardiac fibroblasts into induced cardiomyocytes. *Nature*, *485*(7400), 593–598. https://doi.org/10.1038/nature11044

Rodríguez-Matellán, A., Alcazar, N., Hernández, F., Serrano, M., & Ávila, J. (2020). In Vivo Reprogramming Ameliorates Aging Features in Dentate Gyrus Cells and Improves Memory in Mice. *Stem Cell Reports*, *15*(5), 1056–1066. https://doi.org/10.1016/J.STEMCR.2020.09.010

Roper, J. M., Mazzatti, D. J., Watkins, R. H., Maniscalco, W. M., Keng, P. C., & O'Reilly, M. A. (2004). In vivo exposure to hyperoxia induces DNA damage in a population of alveolar type II epithelial cells. *American Journal of Physiology - Lung Cellular and Molecular Physiology*, *286*(5 30-5), 1045–1054. https://doi.org/10.1152/AJPLUNG.00376.2003/ASSET/IMAGES/LARGE/ZH5005041749 1008.JPEG

Schafer, M. J., White, T. A., Iijima, K., Haak, A. J., Ligresti, G., Atkinson, E. J., Oberg, A. L., Birch, J., Salmonowicz, H., Zhu, Y., Mazula, D. L., Brooks, R. W., Fuhrmann-Stroissnigg, H., Pirtskhalava, T., Prakash, Y. S., Tchkonia, T., Robbins, P. D., Aubry, M. C., Passos, J. F., … LeBrasseur, N. K. (2017). Cellular senescence mediates fibrotic pulmonary disease. *Nature Communications 2017 8:1*, *8*(1), 1–11. https://doi.org/10.1038/ncomms14532

Schittny, J. C. (2017). Development of the lung. *Cell and Tissue Research*, *367*(3), 427–444. https://doi.org/10.1007/s00441-016-2545-0

Song, K., Nam, Y.-J., Luo, X., Qi, X., Tan, W., Huang, G. N., Acharya, A., Smith, C. L., Tallquist, M. D., Neilson, E. G., Hill, J. A., Bassel-Duby, R., & Olson, E. N. (2012). Heart repair by reprogramming non-myocytes with cardiac transcription factors. *Nature*, *485*(7400), 599–604. https://doi.org/10.1038/nature11139

Stein, G. H., Drullinger, L. F., Soulard, A., & Dulić, V. (1999). Differential Roles for Cyclin-Dependent Kinase Inhibitors p21 and p16 in the Mechanisms of Senescence and Differentiation in Human Fibroblasts. *Molecular and Cellular Biology*, *19*(3), 2109. https://doi.org/10.1128/MCB.19.3.2109

Sucre, J., Haist, L., Bolton, C. E., & Hilgendorff, A. (2021). Early Changes and Indicators Characterizing Lung Aging in Neonatal Chronic Lung Disease. *Frontiers in Medicine*, *8*. https://doi.org/10.3389/fmed.2021.665152

Sucre, J. M. S., Deutsch, G. H., Jetter, C. S., Ambalavanan, N., Benjamin, J. T., Gleaves, L. A., Millis, B. A., Young, L. R., Blackwell, T. S., Kropski, J. A., & Guttentag, S. H. (2018). A Shared Pattern of β-Catenin Activation in Bronchopulmonary Dysplasia and Idiopathic

Pulmonary Fibrosis. *The American Journal of Pathology*, *188*(4), 853. https://doi.org/10.1016/J.AJPATH.2017.12.004

Takahashi, K., Tanabe, K., Ohnuki, M., Narita, M., Ichisaka, T., Tomoda, K., & Yamanaka, S. (2007). Induction of pluripotent stem cells from adult human fibroblasts by defined factors. *Cell*, *131*(5), 861–872. https://doi.org/10.1016/J.CELL.2007.11.019

Thébaud, B., Goss, K. N., Laughon, M., Whitsett, J. A., Abman, S. H., Steinhorn, R. H., Aschner, J. L., Davis, P. G., McGrath-Morrow, S. A., Soll, R. F., & Jobe, A. H. (2019). Bronchopulmonary dysplasia. *Nat Rev Dis Primers*, *5*(1), 78. https://doi.org/10.1038/s41572-019-0127-7

Torper, O., Pfisterer, U., Wolf, D. A., Pereira, M., Lau, S., Jakobsson, J., Björklund, A., Grealish, S., & Parmar, M. (2013). Generation of induced neurons via direct conversion in vivo. *Proceedings of the National Academy of Sciences*, *110*(17), 7038–7043. https://doi.org/10.1073/pnas.1303829110

Tsuji, T., Aoshiba, K., & Nagai, A. (2010). Alveolar cell senescence exacerbates pulmonary inflammation in patients with chronic obstructive pulmonary disease. *Respiration; International Review of Thoracic Diseases*, *80*(1), 59–70. https://doi.org/10.1159/000268287

Tsuji, T., Aoshiba, K., & Nagai, A. (2012). Alveolar Cell Senescence in Patients with Pulmonary Emphysema. *Https://Doi.Org/10.1164/Rccm.200509-1374OC*, *174*(8), 886–893. https://doi.org/10.1164/RCCM.200509-1374OC

van Deursen, J. M. (2014). The role of senescent cells in ageing. *Nature*, *509*(7501), 439–446. https://doi.org/10.1038/nature13193

vom Hove, M., Prenzel, F., Uhlig, H. H., & Robel-Tillig, E. (2014). Pulmonary outcome in former preterm, very low birth weight children with bronchopulmonary dysplasia: a case-control follow-up at school age. *The Journal of Pediatrics*, *164*(1). https://doi.org/10.1016/J.JPEDS.2013.07.045

Wang, C., Rabadan Ros, R., Martinez-Redondo, P., Ma, Z., Shi, L., Xue, Y., Guillen-Guillen, I., Huang, L., Hishida, T., Liao, H. K., Nuñez Delicado, E., Rodriguez Esteban, C., Guillen-Garcia, P., Reddy, P., & Izpisua Belmonte, J. C. (2021). In vivo partial reprogramming of myofibers promotes muscle regeneration by remodeling the stem cell niche. *Nature Communications 2021 12:1*, *12*(1), 1–15. https://doi.org/10.1038/s41467-021-23353-z

Wilmut, I., Schnieke, A. E., McWhir, J., Kind, A. J., & Campbell, K. H. S. (1997). Viable offspring derived from fetal and adult mammalian cells. *Nature 1997 385:6619*, *385*(6619), 810–813. https://doi.org/10.1038/385810a0

Wong, P. M., Lees, A. N., Louw, J., Lee, F. Y., French, N., Gain, K., Murray, C. P., Wilson, A., & Chambers, D. C. (2008). Emphysema in young adult survivors of moderate-to-severe bronchopulmonary dysplasia. *Eur Respir J*, *32*(2), 321–328. https://doi.org/10.1183/09031936.00127107

Yamanaka, S., & Takahashi, K. (2006). [Induction of pluripotent stem cells from mouse fibroblast cultures]. *Tanpakushitsu Kakusan Koso*, *51*(15), 2346–2351. https://www.ncbi.nlm.nih.gov/pubmed/17154061

Yao, H., Wallace, J., Peterson, A. L., Scaffa, A., Rizal, S., Hegarty, K., Maeda, H., Chang, J. L., Oulhen, N., Kreiling, J. A., Huntington, K. E., de Paepe, M. E., Barbosa, G., & Dennery, P. A. (2023). Timing and cell specificity of senescence drives postnatal lung development and

injury. *Nature Communications 2023 14:1*, *14*(1), 1–15. https://doi.org/10.1038/s41467-023-35985-4

You, K., Parikh, P., Khandalavala, K., Wicher, S. A., Manlove, L., Yang, B., Roesler, A., Roos, B. B., Teske, J. J., Britt Jr., R. D., Pabelick, C. M., & Prakash, Y. S. (2019). Moderate hyperoxia induces senescence in developing human lung fibroblasts. *Am J Physiol Lung Cell Mol Physiol*, *317*(5), L525-l536. https://doi.org/10.1152/ajplung.00067.2019

Zhou, Q., Brown, J., Kanarek, A., Rajagopal, J., & Melton, D. A. (2008). In vivo reprogramming of adult pancreatic exocrine cells to β-cells. *Nature*, *455*(7213), 627–632. https://doi.org/10.1038/nature07314

Abad, M., Mosteiro, L., Pantoja, C., Cañamero, M., Rayon, T., Ors, I., Graña, O., Megías, D., Domínguez, O., Martínez, D., Manzanares, M., Ortega, S., & Serrano, M. (2013). Reprogramming in vivo produces teratomas and iPS cells with totipotency features. *Nature*, *502*(7471), 340–345. https://doi.org/10.1038/nature12586

Abman, S. H. (2012). Bronchopulmonary Dysplasia. *Https://Doi.Org/10.1164/Ajrccm.164.10.2109111c*, *164*(10 I), 1755–1756. https://doi.org/10.1164/AJRCCM.164.10.2109111C

Amsellem, V., Gary-Bobo, G., Marcos, E., Maitre, B., Chaar, V., Validire, P., Stern, J. B., Noureddine, H., Sapin, E., Rideau, D., Hue, S., le Corvoisier, P., le Gouvello, S., Dubois-Randé, J. L., Boczkowski, J., & Adnot, S. (2012). Telomere Dysfunction Causes Sustained Inflammation in Chronic Obstructive Pulmonary Disease.

Https://Doi.Org/10.1164/Rccm.201105-0802OC, *184*(12), 1358–1366. https://doi.org/10.1164/RCCM.201105-0802OC

Aukland, S. M., Halvorsen, T., Fosse, K. R., Daltveit, A. K., & Rosendahl, K. (2006). High-resolution CT of the chest in children and young adults who were born prematurely: findings in a population-based study. *AJR. American Journal of Roentgenology*, *187*(4), 1012–1018. https://doi.org/10.2214/AJR.05.0383

Baker, C. D., Abman, S. H., & Mourani, P. M. (2014). Pulmonary Hypertension in Preterm Infants with Bronchopulmonary Dysplasia. *Pediatric Allergy, Immunology, and Pulmonology*, *27*(1), 8–16. https://doi.org/10.1089/PED.2013.0323

Baker, D. J., Wijshake, T., Tchkonia, T., Lebrasseur, N. K., Childs, B. G., van de Sluis, B., Kirkland, J. L., & van Deursen, J. M. (2011). Clearance of p16Ink4a-positive senescent cells delays ageing-associated disorders. *Nature*, *479*(7372), 232–236. https://doi.org/10.1038/NATURE10600

Barker, G. F., Manzo, N. D., Cotich, K. L., Shone, R. K., & Waxman, A. B. (2006). DNA Damage Induced by Hyperoxia. *American Journal of Respiratory Cell and Molecular Biology*, *35*(3), 277–288. https://doi.org/10.1165/rcmb.2005-0340OC

Bertoli, C., Skotheim, J. M., & de Bruin, R. A. M. (2013). Control of cell cycle transcription during G1 and S phases. *Nature Reviews Molecular Cell Biology*, *14*(8), 518–528. https://doi.org/10.1038/nrm3629

Browder, K. C., Reddy, P., Yamamoto, M., Haghani, A., Guillen, I. G., Sahu, S., Wang, C., Luque, Y., Prieto, J., Shi, L., Shojima, K., Hishida, T., Lai, Z., Li, Q., Choudhury, F. K., Wong, W. R., Liang, Y., Sangaraju, D., Sandoval, W., … Izpisua Belmonte, J. C. (2022). In vivo partial

reprogramming alters age-associated molecular changes during physiological aging in mice. *Nature Aging 2022 2:3*, *2*(3), 243–253. https://doi.org/10.1038/s43587-022-00183-2

Brown, L. M., Rannels, S. R., & Rannels, D. E. (2001). Implications of post-pneumonectomy compensatory lung growth in pulmonary physiology and disease. *Respiratory Research*, *2*(6), 340. https://doi.org/10.1186/RR84

Chang, J., Wang, Y., Shao, L., Laberge, R. M., Demaria, M., Campisi, J., Janakiraman, K., Sharpless, N. E., Ding, S., Feng, W., Luo, Y., Wang, X., Aykin-Burns, N., Krager, K., Ponnappan, U., Hauer-Jensen, M., Meng, A., & Zhou, D. (2016). Clearance of senescent cells by ABT263 rejuvenates aged hematopoietic stem cells in mice. *Nature Medicine*, *22*(1), 78. https://doi.org/10.1038/NM.4010

Chen, Y., Lüttmann, F. F., Schoger, E., Schöler, H. R., Zelarayán, L. C., Kim, K. P., Haigh, J. J., Kim, J., & Braun, T. (2021a). Reversible reprogramming of cardiomyocytes to a fetal state drives heart regeneration in mice. *Science*, *373*(6562), 1537–1540. https://doi.org/10.1126/science.abg5159

Chen, Y., Lüttmann, F. F., Schoger, E., Schöler, H. R., Zelarayán, L. C., Kim, K. P., Haigh, J. J., Kim, J., & Braun, T. (2021b). Reversible reprogramming of cardiomyocytes to a fetal state drives heart regeneration in mice. *Science*, *373*(6562), 1537–1540. https://doi.org/10.1126/SCIENCE.ABG5159/SUPPL_FILE/SCIENCE.ABG5159_MOVIES_S1_TO_S8.ZIP

Cheng, F., Wang, C., Ji, Y., Yang, B., Shu, J., Shi, K., Wang, L., Wang, S., Zhang, Y., Huang, X., Zhou, X., Xia, K., Liang, C., Chen, Q., & Li, F. (2022). Partial reprogramming strategy for

intervertebral disc rejuvenation by activating energy switch. *Aging Cell*, *21*(4), e13577. https://doi.org/10.1111/ACEL.13577

Chiche, A., Chen, C., & Li, H. (2020). The crosstalk between cellular reprogramming and senescence in aging and regeneration. *Exp Gerontol*, *138*, 111005. https://doi.org/10.1016/j.exger.2020.111005

Chiche, A., le Roux, I., von Joest, M., Sakai, H., Aguín, S. B., Cazin, C., Salam, R., Fiette, L., Alegria, O., Flamant, P., Tajbakhsh, S., & Li, H. (2017). Injury-Induced Senescence Enables In Vivo Reprogramming in Skeletal Muscle. *Cell Stem Cell*, *20*(3), 407-414.e4. https://doi.org/10.1016/j.stem.2016.11.020

Coalson, J. J. (2006). Pathology of Bronchopulmonary Dysplasia. *Seminars in Perinatology*, *30*(4), 179–184. https://doi.org/10.1053/J.SEMPERI.2006.05.004

Conboy, I. M., Conboy, M. J., Wagers, A. J., Girma, E. R., Weismann, I. L., & Rando, T. A. (2005). Rejuvenation of aged progenitor cells by exposure to a young systemic environment. *Nature*, *433*(7027), 760–764. https://doi.org/10.1038/NATURE03260

Dasgupta, C., Sakurai, R., Wang, Y., Guo, P., Ambalavanan, N., Torday, J. S., & Rehan, V. K. (2009). Hyperoxia-induced neonatal rat lung injury involves activation of TGF-{beta} and Wnt signaling and is protected by rosiglitazone. *American Journal of Physiology. Lung Cellular and Molecular Physiology*, *296*(6). https://doi.org/10.1152/AJPLUNG.90392.2008

Davis, R. L., Weintraub, H., & Lassar, A. B. (1987). Expression of a single transfected cDNA converts fibroblasts to myoblasts. *Cell*, *51*(6), 987–1000. https://doi.org/10.1016/0092-8674(87)90585-X

Doeser, M. C., Schöler, H. R., & Wu, G. (2018). Reduction of Fibrosis and Scar Formation by Partial Reprogramming In Vivo. *Stem Cells*, *36*(8), 1216–1225. https://doi.org/10.1002/STEM.2842

Doyle, L. W., Carse, E., Adams, A.-M., Ranganathan, S., Opie, G., & Cheong, J. L. Y. (2017). Ventilation in Extremely Preterm Infants and Respiratory Function at 8 Years. *The New England Journal of Medicine*, *377*(4), 329–337. https://doi.org/10.1056/NEJMOA1700827

Doyle, L. W., Faber, B., Callanan, C., Freezer, N., Ford, G. W., & Davis, N. M. (2006). Bronchopulmonary Dysplasia in Very Low Birth Weight Subjects and Lung Function in Late Adolescence. *Pediatrics*, *118*(1), 108–113. https://doi.org/10.1542/PEDS.2005-2522

Evans, M. J., & Kaufman, M. H. (1981). Establishment in culture of pluripotential cells from mouse embryos. *Nature*, *292*(5819), 154–156. https://doi.org/10.1038/292154a0

Fawke, J., Lum, S., Kirkby, J., Hennessy, E., Marlow, N., Rowell, V., Thomas, S., & Stocks, J. (2010). Lung Function and Respiratory Symptoms at 11 Years in Children Born Extremely Preterm: The EPICure Study. *American Journal of Respiratory and Critical Care Medicine*, *182*(2), 237. https://doi.org/10.1164/RCCM.200912-1806OC

Ghaedi, M., Calle, E. A., Mendez, J. J., Gard, A. L., Balestrini, J., Booth, A., Bove, P. F., Gui, L., White, E. S., & Niklason, L. E. (2013). Human iPS cellâ€"derived alveolar epithelium repopulates lung extracellular matrix. *Journal of Clinical Investigation*, *123*(11), 4950–4962. https://doi.org/10.1172/JCI68793

Gill, D., Parry, A., Santos, F., Okkenhaug, H., Todd, C. D., Hernando-Herraez, I., Stubbs, T. M., Milagre, I., & Reik, W. (2022). Multi-omic rejuvenation of human cells by maturation phase transient reprogramming. *ELife*, *11*. https://doi.org/10.7554/ELIFE.71624

Guo, L., Karoubi, G., Duchesneau, P., Aoki, F. G., Shutova, M. v., Rogers, I., Nagy, A., & Waddell, T. K. (2018). Interrupted reprogramming of alveolar type II cells induces progenitor-like cells that ameliorate pulmonary fibrosis. *Npj Regenerative Medicine*, *3*(1), 14. https://doi.org/10.1038/s41536-018-0052-5

Gurdon, J. B. (1962). *The developmental capacity of nuclei taken from intestinal epithelium cells of feeding tadpoles*. https://journals.biologists.com/dev/article-abstract/10/4/622/35650

Gurdon, J., Nature, V. U.-, & 1966, undefined. (n.d.). "Fertile" intestine nuclei. *Nature.Com*. Retrieved February 5, 2023, from https://www.nature.com/articles/2101240a0

Hishida, T., Yamamoto, M., Hishida-Nozaki, Y., Shao, C., Huang, L., Wang, C., Shojima, K., Xue, Y., Hang, Y., Shokhirev, M., Memczak, S., Sahu, S. K., Hatanaka, F., Ros, R. R., Maxwell, M. B., Chavez, J., Shao, Y., Liao, H. K., Martinez-Redondo, P., … Izpisua Belmonte, J. C. (2022a). In vivo partial cellular reprogramming enhances liver plasticity and regeneration. *Cell Reports*, *39*(4). https://doi.org/10.1016/J.CELREP.2022.110730

Hishida, T., Yamamoto, M., Hishida-Nozaki, Y., Shao, C., Huang, L., Wang, C., Shojima, K., Xue, Y., Hang, Y., Shokhirev, M., Memczak, S., Sahu, S. K., Hatanaka, F., Ros, R. R., Maxwell, M. B., Chavez, J., Shao, Y., Liao, H.-K., Martinez-Redondo, P., … Izpisua Belmonte, J. C. (2022b). In vivo partial cellular reprogramming enhances liver plasticity and regeneration. *Cell Reports*, *39*(4), 110730. https://doi.org/https://doi.org/10.1016/j.celrep.2022.110730

Hurskainen, M., Mižíková, I., Cook, D. P., Andersson, N., Cyr-Depauw, C., Lesage, F., Helle, E., Renesme, L., Jankov, R. P., Heikinheimo, M., Vanderhyden, B. C., & Thébaud, B. (2021a).

Single cell transcriptomic analysis of murine lung development on hyperoxia-induced damage. *Nat Commun*, *12*(1), 1565. https://doi.org/10.1038/s41467-021-21865-2

Hurskainen, M., Mižíková, I., Cook, D. P., Andersson, N., Cyr-Depauw, C., Lesage, F., Helle, E., Renesme, L., Jankov, R. P., Heikinheimo, M., Vanderhyden, B. C., & Thébaud, B. (2021b). Single cell transcriptomic analysis of murine lung development on hyperoxia-induced damage. *Nature Communications*, *12*(1), 1565. https://doi.org/10.1038/s41467-021-21865-2

Jensen, E. A., & Schmidt, B. (2014). Epidemiology of Bronchopulmonary Dysplasia. *Birth Defects Research. Part A, Clinical and Molecular Teratology*, *100*(3), 145. https://doi.org/10.1002/BDRA.23235

JOBE, A. H., & BANCALARI, E. (2001). Bronchopulmonary Dysplasia. *American Journal of Respiratory and Critical Care Medicine*, *163*(7), 1723–1729. https://doi.org/10.1164/ajrccm.163.7.2011060

Jobe, A. J. (1999). The new BPD: an arrest of lung development. *Pediatric Research*, *46*(6), 641–643. https://doi.org/10.1203/00006450-199912000-00007

Justice, J. N., Nambiar, A. M., Tchkonia, T., LeBrasseur, N. K., Pascual, R., Hashmi, S. K., Prata, L., Masternak, M. M., Kritchevsky, S. B., Musi, N., & Kirkland, J. L. (2019). Senolytics in idiopathic pulmonary fibrosis: Results from a first-in-human, open-label, pilot study. *EBioMedicine*, *40*, 554–563. https://doi.org/10.1016/j.ebiom.2018.12.052

Kang, M. H., van Lieshout, L. P., Xu, L., Domm, J. M., Vadivel, A., Renesme, L., Mühlfeld, C., Hurskainen, M., Mižíková, I., Pei, Y., van Vloten, J. P., Thomas, S. P., Milazzo, C., Cyr-Depauw, C., Whitsett, J. A., Nogee, L. M., Wootton, S. K., & Thébaud, B. (2020). A lung

tropic AAV vector improves survival in a mouse model of surfactant B deficiency. *Nat Commun*, *11*(1), 3929. https://doi.org/10.1038/s41467-020-17577-8

Kotecha, S. J., Edwards, M. O., Watkins, W. J., Henderson, A. J., Paranjothy, S., Dunstan, F. D., & Kotecha, S. (2013). Effect of preterm birth on later FEV1: a systematic review and meta-analysis. *Thorax*, *68*(8), 760–766. https://doi.org/10.1136/THORAXJNL-2012-203079

Kotton, D. N., & Morrisey, E. E. (2014). Lung regeneration: mechanisms, applications and emerging stem cell populations. *Nature Medicine*, *20*(8), 822. https://doi.org/10.1038/NM.3642

Lecarpentier, Y., Schussler, O., Hébert, J. L., & Vallée, A. (2019). Multiple Targets of the Canonical WNT/β-Catenin Signaling in Cancers. *Frontiers in Oncology*, *9*, 1248. https://doi.org/10.3389/FONC.2019.01248

Lehmann, M., Hu, Q., Hu, Y., Hafner, K., Costa, R., van den Berg, A., & Königshoff, M. (2020). Chronic WNT/β-catenin signaling induces cellular senescence in lung epithelial cells. *Cellular Signalling*, *70*, 109588. https://doi.org/10.1016/J.CELLSIG.2020.109588

Londhe, V. A., Sundar, I. K., Lopez, B., Maisonet, T. M., Yu, Y., Aghai, Z. H., & Rahman, I. (2011). Hyperoxia impairs alveolar formation and induces senescence through decreased histone deacetylase activity and up-regulation of p21 in neonatal mouse lung. *Pediatr Res*, *69*(5 Pt 1), 371–377. https://doi.org/10.1203/PDR.0b013e318211c917

López-Otín, C., Blasco, M. A., Partridge, L., Serrano, M., & Kroemer, G. (2013). The Hallmarks of Aging. *Cell*, *153*(6), 1194–1217. https://doi.org/10.1016/j.cell.2013.05.039

Lu, Y., Brommer, B., Tian, X., Krishnan, A., Meer, M., Wang, C., Vera, D. L., Zeng, Q., Yu, D., Bonkowski, M. S., Yang, J. H., Zhou, S., Hoffmann, E. M., Karg, M. M., Schultz, M. B., Kane, A. E., Davidsohn, N., Korobkina, E., Chwalek, K., … Sinclair, D. A. (2020). Reprogramming to recover youthful epigenetic information and restore vision. *Nature*, *588*(7836), 124–129. https://doi.org/10.1038/s41586-020-2975-4

Lum, S., Kirkby, J., Welsh, L., Marlow, N., Hennessy, E., & Stocks, J. (2011). Nature and severity of lung function abnormalities in extremely pre-term children at 11 years of age. *European Respiratory Journal*, *37*(5), 1199–1207. https://doi.org/10.1183/09031936.00071110

Mahmoudi, S., Xu, L., & Brunet, A. (2019). Turning back time with emerging rejuvenation strategies. *Nature Cell Biology*, *21*(1), 32. https://doi.org/10.1038/S41556-018-0206-0

Martin, G. R. (1981). Isolation of a pluripotent cell line from early mouse embryos cultured in medium conditioned by teratocarcinoma stem cells. *Proceedings of the National Academy of Sciences*, *78*(12), 7634–7638. https://doi.org/10.1073/pnas.78.12.7634

McGrath, S. A. (1998). Induction of p21WAF/CIP1 during hyperoxia. *Am J Respir Cell Mol Biol*, *18*(2), 179–187. https://doi.org/10.1165/ajrcmb.18.2.2964m

Meiners, S., & Hilgendorff, A. (2016a). Early injury of the neonatal lung contributes to premature lung aging: a hypothesis. *Mol Cell Pediatr*, *3*(1), 24. https://doi.org/10.1186/s40348-016-0052-8

Meiners, S., & Hilgendorff, A. (2016b). Early injury of the neonatal lung contributes to premature lung aging: a hypothesis. *Molecular and Cellular Pediatrics*, *3*(1), 24. https://doi.org/10.1186/s40348-016-0052-8

Mosteiro, L., Pantoja, C., Alcazar, N., Marión, R. M., Chondronasiou, D., Rovira, M., Fernandez-Marcos, P. J., Muñoz-Martin, M., Blanco-Aparicio, C., Pastor, J., Gómez-López, G., de Martino, A., Blasco, M. A., Abad, M., & Serrano, M. (2016). Tissue damage and senescence provide critical signals for cellular reprogramming in vivo. *Science*, *354*(6315). https://doi.org/10.1126/science.aaf4445

Mosteiro, L., Pantoja, C., de Martino, A., & Serrano, M. (2018). Senescence promotes in vivo reprogramming through p16(INK)(4a) and IL-6. *Aging Cell*, *17*(2). https://doi.org/10.1111/acel.12711

Mourani, P. M., & Abman, S. H. (2013). Pulmonary vascular disease in bronchopulmonary dysplasia: pulmonary hypertension and beyond. *Current Opinion in Pediatrics*, *25*(3), 329–337. https://doi.org/10.1097/MOP.0B013E328360A3F6

Mourani, P. M., & Abman, S. H. (2015). Pulmonary Hypertension and Vascular Abnormalities in Bronchopulmonary Dysplasia. *Clinics in Perinatology*, *42*(4), 839. https://doi.org/10.1016/J.CLP.2015.08.010

Narayanan, M., Beardsmore, C. S., Owers-Bradley, J., Dogaru, C. M., Mada, M., Ball, I., Garipov, R. R., Kuehni, C. E., Spycher, B. D., & Silverman, M. (2013). Catch-up alveolarization in ex-preterm children: Evidence from 3He magnetic resonance. *American Journal of Respiratory and Critical Care Medicine*, *187*(10), 1104–1109. https://doi.org/10.1164/RCCM.201210-1850OC/SUPPL_FILE/DISCLOSURES.PDF

Northway Jr., W. H., Rosan, R. C., & Porter, D. Y. (1967). Pulmonary disease following respirator therapy of hyaline-membrane disease. Bronchopulmonary dysplasia. *N Engl J Med*, *276*(7), 357–368. https://doi.org/10.1056/nejm196702162760701

Ocampo, A., Reddy, P., Martinez-Redondo, P., Platero-Luengo, A., Hatanaka, F., Hishida, T., Li, M., Lam, D., Kurita, M., Beyret, E., Araoka, T., Vazquez-Ferrer, E., Donoso, D., Roman, J. L., Xu, J., Rodriguez Esteban, C., Nuñez, G., Nuñez Delicado, E., Campistol, J. M., … Izpisua Belmonte, J. C. (2016). In Vivo Amelioration of Age-Associated Hallmarks by Partial Reprogramming. *Cell*, *167*(7), 1719-1733.e12. https://doi.org/10.1016/j.cell.2016.11.052

Ohnishi, K., Semi, K., Yamamoto, T., Shimizu, M., Tanaka, A., Mitsunaga, K., Okita, K., Osafune, K., Arioka, Y., Maeda, T., Soejima, H., Moriwaki, H., Yamanaka, S., Woltjen, K., & Yamada, Y. (2014). Premature termination of reprogramming in vivo leads to cancer development through altered epigenetic regulation. *Cell*, *156*(4), 663–677. https://doi.org/10.1016/j.cell.2014.01.005

O'Reilly, M. A. (2001). DNA damage and cell cycle checkpoints in hyperoxic lung injury: braking to facilitate repair. *American Journal of Physiology-Lung Cellular and Molecular Physiology*, *281*(2), L291–L305. https://doi.org/10.1152/ajplung.2001.281.2.L291

Pierro, M., Ionescu, L., Montemurro, T., Vadivel, A., Weissmann, G., Oudit, G., Emery, D., Bodiga, S., Eaton, F., Péault, B., Mosca, F., Lazzari, L., & Thébaud, B. (2013). Short-term, long-term and paracrine effect of human umbilical cord-derived stem cells in lung injury prevention and repair in experimental bronchopulmonary dysplasia. *Thorax*, *68*(5), 475–484. https://doi.org/10.1136/thoraxjnl-2012-202323

Qian, L., Huang, Y., Spencer, C. I., Foley, A., Vedantham, V., Liu, L., Conway, S. J., Fu, J., & Srivastava, D. (2012). In vivo reprogramming of murine cardiac fibroblasts into induced cardiomyocytes. *Nature*, *485*(7400), 593–598. https://doi.org/10.1038/nature11044

Rodríguez-Matellán, A., Alcazar, N., Hernández, F., Serrano, M., & Ávila, J. (2020). In Vivo Reprogramming Ameliorates Aging Features in Dentate Gyrus Cells and Improves Memory in Mice. *Stem Cell Reports*, *15*(5), 1056–1066. https://doi.org/10.1016/J.STEMCR.2020.09.010

Roper, J. M., Mazzatti, D. J., Watkins, R. H., Maniscalco, W. M., Keng, P. C., & O'Reilly, M. A. (2004). In vivo exposure to hyperoxia induces DNA damage in a population of alveolar type II epithelial cells. *American Journal of Physiology - Lung Cellular and Molecular Physiology*, *286*(5 30-5), 1045–1054. https://doi.org/10.1152/AJPLUNG.00376.2003/ASSET/IMAGES/LARGE/ZH5005041749 1008.JPEG

Schafer, M. J., White, T. A., Iijima, K., Haak, A. J., Ligresti, G., Atkinson, E. J., Oberg, A. L., Birch, J., Salmonowicz, H., Zhu, Y., Mazula, D. L., Brooks, R. W., Fuhrmann-Stroissnigg, H., Pirtskhalava, T., Prakash, Y. S., Tchkonia, T., Robbins, P. D., Aubry, M. C., Passos, J. F., … LeBrasseur, N. K. (2017). Cellular senescence mediates fibrotic pulmonary disease. *Nature Communications 2017 8:1*, *8*(1), 1–11. https://doi.org/10.1038/ncomms14532

Schittny, J. C. (2017). Development of the lung. *Cell and Tissue Research*, *367*(3), 427–444. https://doi.org/10.1007/s00441-016-2545-0

Song, K., Nam, Y.-J., Luo, X., Qi, X., Tan, W., Huang, G. N., Acharya, A., Smith, C. L., Tallquist, M. D., Neilson, E. G., Hill, J. A., Bassel-Duby, R., & Olson, E. N. (2012). Heart repair by reprogramming non-myocytes with cardiac transcription factors. *Nature*, *485*(7400), 599–604. https://doi.org/10.1038/nature11139

Stein, G. H., Drullinger, L. F., Soulard, A., & Dulić, V. (1999). Differential Roles for Cyclin-Dependent Kinase Inhibitors p21 and p16 in the Mechanisms of Senescence and Differentiation in Human Fibroblasts. *Molecular and Cellular Biology*, *19*(3), 2109. https://doi.org/10.1128/MCB.19.3.2109

Sucre, J., Haist, L., Bolton, C. E., & Hilgendorff, A. (2021). Early Changes and Indicators Characterizing Lung Aging in Neonatal Chronic Lung Disease. *Frontiers in Medicine*, *8*. https://doi.org/10.3389/fmed.2021.665152

Sucre, J. M. S., Deutsch, G. H., Jetter, C. S., Ambalavanan, N., Benjamin, J. T., Gleaves, L. A., Millis, B. A., Young, L. R., Blackwell, T. S., Kropski, J. A., & Guttentag, S. H. (2018). A Shared Pattern of β-Catenin Activation in Bronchopulmonary Dysplasia and Idiopathic Pulmonary Fibrosis. *The American Journal of Pathology*, *188*(4), 853. https://doi.org/10.1016/J.AJPATH.2017.12.004

Takahashi, K., Tanabe, K., Ohnuki, M., Narita, M., Ichisaka, T., Tomoda, K., & Yamanaka, S. (2007). Induction of pluripotent stem cells from adult human fibroblasts by defined factors. *Cell*, *131*(5), 861–872. https://doi.org/10.1016/J.CELL.2007.11.019

Thébaud, B., Goss, K. N., Laughon, M., Whitsett, J. A., Abman, S. H., Steinhorn, R. H., Aschner, J. L., Davis, P. G., McGrath-Morrow, S. A., Soll, R. F., & Jobe, A. H. (2019). Bronchopulmonary dysplasia. *Nat Rev Dis Primers*, *5*(1), 78. https://doi.org/10.1038/s41572-019-0127-7

Torper, O., Pfisterer, U., Wolf, D. A., Pereira, M., Lau, S., Jakobsson, J., Björklund, A., Grealish, S., & Parmar, M. (2013). Generation of induced neurons via direct conversion in vivo.

Proceedings of the National Academy of Sciences, *110*(17), 7038–7043. https://doi.org/10.1073/pnas.1303829110

Tsuji, T., Aoshiba, K., & Nagai, A. (2010). Alveolar cell senescence exacerbates pulmonary inflammation in patients with chronic obstructive pulmonary disease. *Respiration; International Review of Thoracic Diseases*, *80*(1), 59–70. https://doi.org/10.1159/000268287

Tsuji, T., Aoshiba, K., & Nagai, A. (2012). Alveolar Cell Senescence in Patients with Pulmonary Emphysema. *Https://Doi.Org/10.1164/Rccm.200509-1374OC*, *174*(8), 886–893. https://doi.org/10.1164/RCCM.200509-1374OC

van Deursen, J. M. (2014). The role of senescent cells in ageing. *Nature*, *509*(7501), 439–446. https://doi.org/10.1038/nature13193

vom Hove, M., Prenzel, F., Uhlig, H. H., & Robel-Tillig, E. (2014). Pulmonary outcome in former preterm, very low birth weight children with bronchopulmonary dysplasia: a case-control follow-up at school age. *The Journal of Pediatrics*, *164*(1). https://doi.org/10.1016/J.JPEDS.2013.07.045

Wang, C., Rabadan Ros, R., Martinez-Redondo, P., Ma, Z., Shi, L., Xue, Y., Guillen-Guillen, I., Huang, L., Hishida, T., Liao, H. K., Nuñez Delicado, E., Rodriguez Esteban, C., Guillen-Garcia, P., Reddy, P., & Izpisua Belmonte, J. C. (2021). In vivo partial reprogramming of myofibers promotes muscle regeneration by remodeling the stem cell niche. *Nature Communications 2021 12:1*, *12*(1), 1–15. https://doi.org/10.1038/s41467-021-23353-z

Wilmut, I., Schnieke, A. E., McWhir, J., Kind, A. J., & Campbell, K. H. S. (1997). Viable offspring derived from fetal and adult mammalian cells. *Nature 1997 385:6619*, *385*(6619), 810–813. https://doi.org/10.1038/385810a0

Wong, P. M., Lees, A. N., Louw, J., Lee, F. Y., French, N., Gain, K., Murray, C. P., Wilson, A., & Chambers, D. C. (2008). Emphysema in young adult survivors of moderate-to-severe bronchopulmonary dysplasia. *Eur Respir J*, *32*(2), 321–328. https://doi.org/10.1183/09031936.00127107

Yamanaka, S., & Takahashi, K. (2006). [Induction of pluripotent stem cells from mouse fibroblast cultures]. *Tanpakushitsu Kakusan Koso*, *51*(15), 2346–2351. https://www.ncbi.nlm.nih.gov/pubmed/17154061

Yao, H., Wallace, J., Peterson, A. L., Scaffa, A., Rizal, S., Hegarty, K., Maeda, H., Chang, J. L., Oulhen, N., Kreiling, J. A., Huntington, K. E., de Paepe, M. E., Barbosa, G., & Dennery, P. A. (2023). Timing and cell specificity of senescence drives postnatal lung development and injury. *Nature Communications 2023 14:1*, *14*(1), 1–15. https://doi.org/10.1038/s41467-023-35985-4

You, K., Parikh, P., Khandalavala, K., Wicher, S. A., Manlove, L., Yang, B., Roesler, A., Roos, B. B., Teske, J. J., Britt Jr., R. D., Pabelick, C. M., & Prakash, Y. S. (2019). Moderate hyperoxia induces senescence in developing human lung fibroblasts. *Am J Physiol Lung Cell Mol Physiol*, *317*(5), L525-l536. https://doi.org/10.1152/ajplung.00067.2019

Zhou, Q., Brown, J., Kanarek, A., Rajagopal, J., & Melton, D. A. (2008). In vivo reprogramming of adult pancreatic exocrine cells to β-cells. *Nature*, *455*(7213), 627–632. https://doi.org/10.1038/nature07314